CHAPTER I

INTRODUCTION

The rapid expansion of biotechnology made the biological macromolecules such as peptides and proteins possible to use as therapeutic agents in pharmaceutical. Calcitonin is a 32 amino acids cyclic polypeptide (molecular weight of approximately 3450 Da), it appears to play a significant physiological role in calcium homeostasis and is a potential blocking effect on osteoclastic bone resorption (Azria et al., 1995). Calcitonin has been found in ultimobranchial gland of birds, fishs, pigs, reptiles and mammals. Salmon calcitonin (sCT) available as a high potency therapeutic agent for treat osteoporosis in women who are at least 5 years past menopause, hypercalcemia, Paget's disease, and potentially in the treatment of osteoarthritis (Schneyer, 1991). sCT is available as a sterile solution has been commercialized in the form of subcutaneous (SC), intramuscular injections and nasal spray formulations (Torres-Lugo and Peppas, 2000; Physicans' Desk Reference, 2011). The currently limitations of injectable dosage form were causing of facial flushes and nausea (Harvey and Withrow, 1985). Moreover, the infection at site of injection, pain and poor patient compliance were the problems of IM injection. The nasal delivery was established for simple patient administration, however the limitation of nasal formulations were irritate nasal mucosa and cause side effects such as rhinitis, rhinorrhea, and allergic rhinitis (Ugwoke et al., 2001). However, the best known of side effects have been difficult to extinguish because nasal formulations generally use absorption enhancers that promote transmucosal sCT delivery. Consistent to the use of absorption enhancers, approximately 3% for clinically used nasal sprays, showing sCT bioavailability is much lower than IM and SC injection (Lee et al., 1994). Despite the most sCT formulated in solution dosage form, the restriction of its therapeutic application is aqeous instability. To anticipate the instability problem of protein drugs in aqueous forms, the solid formulations has frequently been improved.

The systemic effect of calcitonin delivery via the lungs is an ensure substitute (Patton, 2000). The distinction to other mucosal barriers, the pulmonary route is more absorptive to protein drugs and macromolecules because it has low enzymatic action (Patton, 1996). The satisfied barriers still concession the systemic absorption of protein and peptide drugs. These barriers are composed of pulmonary mucus membrane, basement membrane, lung epithelium, macrophages, mucociliary clearance and pulmonary enzymes (Agu et al., 2001). By the last two decades, various procedure were assessed for increased the proteins absorption by intrapulmonary delivery (Agu et al., 2001; Siekmeier and Scheuch, 2009). Instantly, there is an accessed attract in nanocarriers system for pulmonary delivery. In comparison to nanoparticles and microparticles have the probable to diffuse pass the pulmonary mucus membrane and translocate via alveolar epithelium by the endocytosis mechanism (Yang et al., 2008). In further, it is notify that the particles smaller than 0.26 μm can leave from phagocytosis in the alveoli (Lauweryns and Baert, 1977). To increase the retention of the nanocarrier in the lung and avoid fast elimination by ciliary movement, much involve is also provide to mucoadhesive formulations.

The formulation of polymeric nanoparticles have been an interesting concept for pulmonary delivery through their capacity for penetrate to intracellular compartments and avoidance the phagocytosis of macrophages. Additionally, they support the attainable of acquiring high drug loading capacity, promoted the absorption of drug, stability and sustained release, differently targeted deposition (Azarmi et al., 2008). Chitosan (CS) is susceptible for drug delivery via transmucosal route, e.g. pulmonary delivery, approving to its revealed low toxicity, biocompatibility, biodegradability and mucoadhesive property (Grenha et al., 2007), including improvment of macromolecules permeation (Issa et al., 2005), thus being effectively operated in the promotion of micro- and nanocarriers system. In addition to, it has also been used as a dispersing agent for dry powders (Li and Birchall, 2006). There has been establish CS based nanoparticles (NPs), using an ionotropic gelation method (Calvo et al., 1997), that display a great feasible for macromoleculars transmucosal delivery (Fernández-Urrusuno et al., 1999). Despite, NPs are inflexible for pulmonary delivery whereas the truth that their direct delivery affect many

challenges, including instable formulation as particle–particle interactions and poor delivery ability due to exhalation of low-inertia NPs (Yang et al., 2008). Thereby, the microencapsulation of NPs by spray drying technique and using a sugar, with regard to receive a dry powder (Grenha et al., 2005). Moreover, dry powder formulation of drug advise the accessible for increased stability in storage. The microencapsulation able to improved NPs aerosolization performance and handling, obtained by stability enhancement and aerodynamic properties achievement which value determinately in accomplished pulmonary delivery (Grenha et al., 2005 and Sham et al., 2004). Arrestingly, these new powders have been displayed to be biocompatible with pulmonary (Grenha et al., 2007). Considering deep lung deposition, dry powders are markedly order to form adequate aerodynamic properties, e.g. aerodynamic diameter which less than 5 μm (Glover et al., 2008). Futher, the microparticles and nanoparticles established delivery can distribute compose overhead the cellular levels, target tissue and drug released profile. In the exsistent study, we assess in vivo the promising of peptide loaded CS NPs microencapsulation for aerosol delivery, and that are in the form of dry powders. It attend to powder that prepared by spray drying technique is appropriate to the NPs delivery whichever, then, estimate the absorption of macromolecules, following in a systemic effect.

In this study, the spray dried powders of protein loaded chitosan/tripolyphosphate (CS/TPP) nanoparticles were prepared with aerosol excipients. For these objective, salmon calcitonin was loaded to nanoparticles by the method of ionic gelation anywhere the CS which compose of positively charged of amino groups interact with anionic TPP which show negatively charged. The spray dried powder of protein loaded CS/TPP nanoparticles were prepared, mannitol and lactose selected as excipients; their aerodynamic achievement were evaluated and the capable of nanoparticles delivery and finally, the in vivo study of dry powder were investigated.

More specifically, the objectives of this study are:

1. To study the effect of chitosan concentration and CS/TPP ratio on preparation and physicochemical properties of salmon calcitonin loaded chitosan nanoparticles.
2. To study the effect of aerosol excipients (lactose and mannitol) and amount of excipients on physicochemical properties of salmon calcitonin loaded chitosan nanoparticles spray dried powder.
3. To study the aerodynamic properties of salmon calcitonin loaded chitosan nanoparticles spray dried powder.
4. To evaluate the efficiency of salmon calcitonin loaded chitosan nanoparticles spray dried powder.

CHAPTER II

LITERATURE REVIEW

The pharmaceutical macromolecular such as peptide and protein substances are likely to enzymatic degradation in the intestine and illustrate low capacity of membrane permeation as a result of their hydrophilic properties and molecular sizes. This is the interpretation for current administration of them as injection form, which generate painful and distress. Hence, peptide and protein molecules are good possibilities for noninvasive applications via the pulmonary route. Pulmonary are gracefully satisfy for this objective as they are described by expansive absorption surface area, the great vascularization and thin layer of the alveolar barrier whichever, compose, promote macromolecule transport into the blood circulation system. Approach to the oral route, pulmonary have become more challenge for drug delivery whereas the deserted of first pass metabolism and low activity of enzyme (Patton, 1996). Otherwise, the targeted drug delivery to the lungs is an interesting therapeutic advace that may event in the reducing dose of administration, moreover diminished drug side effects (Azarmi, 2008). Individual peptides and proteins have been effectively analyzed for pulmonary delivery, such as insulin (Bi et al., 2009; Grainger et al., 2004), rhDNase (Geller et al., 2003), calcitonin (Kobayashi et al., 1996), interferon-alpha and human growth hormone (Jalaliour et al., 2008). Including, aerosolization inhaler offer noticeable feasible for pulmonary delivery of macromolecular for systemic and local response (Grainger et al., 2004; Lee et al., 2009). About, the formulations possible for inhalation, dry powders are often presented, since they have exhibited the most reasonable performance of active ingredient stability and bioavailability, verified to the liquid supplements.

Calcitonin (CT) is a 32 amino acids cyclic polypeptide hormone, which is secreted from the parafollicular cells of the thyroid gland inmammals. The amino

acid sequences of these peptide has Cys-Ser-Asn-Leu-Ser-Thr-Cys-Val-Leu-Gly-Lys-Leu-Ser-Gln-Glu-Leu-His-Lys-Leu-Gln-Thr-Tyr-Pro-Arg-Thr-Asn-Thr-Gly-Ser-Gly-Thr-Pro-NH_2. The calcitonin maintain to modulate the body calcium homeostasis and preserve the osteoclastic bone resorption regulation (Sigurjonsdottir et al., 1999; Song et al., 2005; Lamprecht et al., 2004). Calcitonin is discovered in human and pig and regulate in ultimobranchial gland of birds and fishes. Despite, salmon calcitonin has been used as an alternative as a therapeutic agent by means of its higher potency than any other species (Sigurjonsdottir et al., 1999; Sinswat et al., 2003; Chang et al., 2000).

Calcitonin is a cyclic polypeptide with hypophosphatemic and hypocalcemic operations which perform a fundamental role in calcium homeostasis by preventing through the regulation of both the functioning and numeral of osteoclasts (Hattersley and Chambers, 1989) and by expanding the excretion of urinary calcium. Nonmammalian vertebrates calcitonin, in several those of fish such as eel and salmon, have been described to spend a higher hypocalcemic effect than calcitonin in mammalian. The molecular capacity to prohibit the resorption of osteoclast mediated bone is the stand of its use in the regimen of bone disorders, such as hypercalcemia, Paget's disease and osteoporosis. Between the derivertives of human and animal calcitonins, salmon calcitonin (sCT) has the most active biological activity.

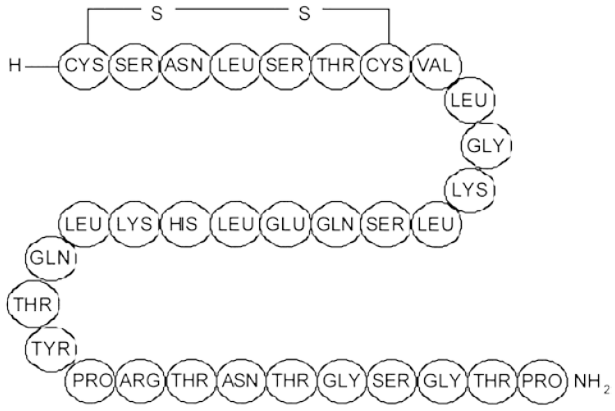

Figure 1. Amino acid sequences of salmon calcitonin

Salmon calcitonin

Salmon calcitonin (sCT) is the most effective molecular in humans and is the most normally used for therapeutic reasons. sCT express its antiresorptive effect by represent on calcitonin receptor (CTR) that observed on bone resorbing osteoclast cells (Naot and Cornish, 2008). sCT, whichever molecular weight of approximately 3500 Da polypeptide with low permeable membrane and sensitive in gastrointestinal tract, has a physiological action in the application of calcium homeostasis and is a potent inhibitor of osteoclastic bone resorption. The major physiological role of the sCT is to control the calcium concentration as well as its metabolism in the body.

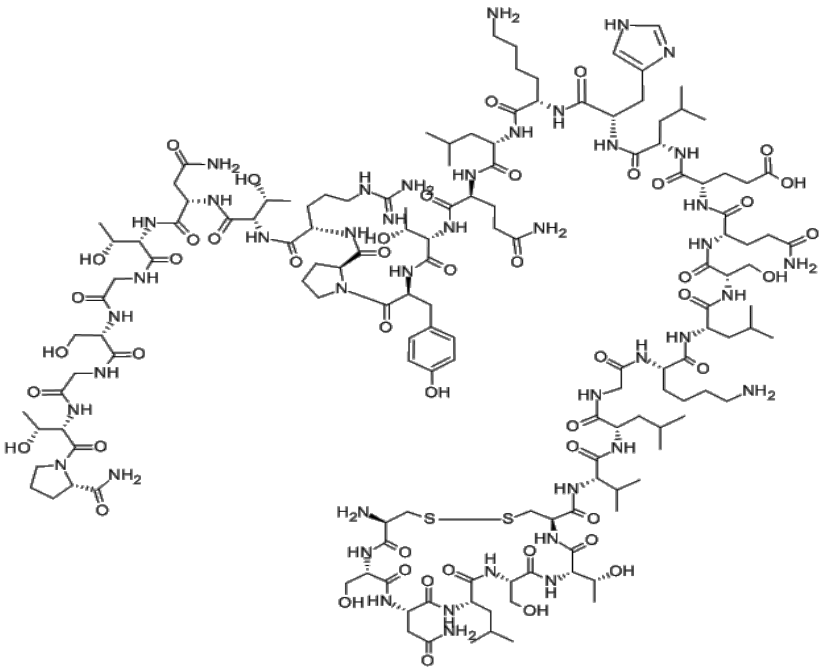

Figure 2. Chemical structure of salmon calcitonin

It is currently indicated and used in the treatment of Paget's disease of bone, osteolytic bone cancers (Lee and Sinko, 2000; Torres-Lugo and Peppas, 2000) and osteoporosis, a disease of low bone mass and the micro-architectural deterioration of bone structure, which in combination, predispose the patient to enhanced bone fragility and fracture risk (Raisz, 2005; Chambers and Magnus, 1982; Chambers, 1982). Calcitonin therapy inhibits or slows osteoclast mediated resorptive bone loss and positively influences osteogenesis and bone formation (Okubo et al., 2000; Farley et al., 2000). It has also recently been shown to attenuate cartilage degradation and stimulate new cartilage formation in osteoarthritis (Karsdal et al., 2007). Salmon calcitonin has been reported to slow the progression of osteoarthritis (OA) and to improve the clinical signs and symptoms of rheumatoid arthritis (Aida et al., 1994). However, the therapeutic use of exogenously administered, calcitonin is severely hampered by its rapid elimination from the body and short half-life (~43 min), which in combination contribute to its poor and variable systemic bioavailability (Lee et al., 2003; Shin et al., 2004; Youn et al., 2006). Currently, the most common delivery route to administer sCT is through intramuscular or intravenous injections. Various researchers have studied different systems to deliver sCT through various delivery routes. The most common include nasal, rectal, oral, and vaginal systems as well as implants. In the case of vaginal and intrauterine systems it has been demonstrated that sCT can be successfully delivered (Golomb and Avramoff, 1993; Golomb et al., 1995; Richardson et al., 1995; Richardson et al., 1996). However, this route restricts

the type of patients that could benefit from the treatment. It is well known that bone diseases do not affect exclusively women. Men are also in risk of suffering these diseases. Therefore, additional efforts have been put into biodegradable, nasal, and oral systems. The only such system that has successfully reached the market is the nasal formulation for sCT. This formulation is currently used in Europe and has been recently approved for clinical use in the United States by the FDA. The currently available treatment is limited to either intramuscular or subcutaneous administration, which compromises patient comfort (Tanko et al., 2004). A nasal spray is also available, but has limited use due to low bioavailability. It has been reported that the bioavailability of sCT solution was less than 0.1% following intra-duodenal, -colonic and -ileac administration in rats and dogs (Hee Lee et al., 2000; Lee et al., 2000; Sinko et al., 1995).

These properties of sCT are drawbacks to long term therapy as they limit patient compliance, especially when a daily injection regimen is required. Therefore, development of new drug delivery systems, alternate routes of administration or analogs for sustained biological activity and increased stability are strongly desired. sCT has been commercialized as injection and nasal spray formulations so far. The main limitations of injection formulation are nausea and especially low patient compliance such as needle phobia and pain (Nakamura et al., 2001). The nasal formulations are thought to be useful for its simple usage. However, this formulation is inconvenient because it induces irritations to nasal mucosa and causes side effects such as rhinitis, rhinorrhea, and allergic rhinitis. These side effects are unavoidable since the nasal formulations inevitably contain absorption enhancers to increase trans-mucosal calcitonin delivery (Chaturvedula et al., 2005). Drug delivery systems based on biodegradable polymers are preferred in many biomedical applications because such systems are broken down either by hydrolysis or by enzymatic reaction into non-toxic molecules. The rate of degradation is controlled by manipulating the composition of the biodegradable polymer matrix. These types of systems are used for the long-term release of therapeutic agents. They are usually designed to act directly in the bloodstream, while protecting the agent from the harmful environment.

Biodegradable polymers such as poly (glycolic acid) (PGA), poly- (lactic acid) (PLA), and poly (D,L-lactic-co-glycolic acid) (PLGA), have received considerable attention as possible drug delivery carriers, since the degradation products of these polymers have been found to have low toxicity. During the normal metabolic function of the body these polymers degrade into carbon dioxide and water (Mehta et al., 1994). These polymers have also exhibited excellent biocompatibility.

Lee et al. studied an injectable biodegradable system based on PGA microspheres for the sustained release of sCT. This system was evaluated by sCT release in rats, and its e$ciency was compared to that of injectable sCT without any controlled delivery carrier. A sustained hypocalcemic e!ect (reduced calcium serum concentration) was obtained. Mehta et al. studied a system of PLGA for the sustained release of sCT. Different preparation parameters for PLGA microspheres were considered and their effect on the in vivo release behavior of sCT was studied. PLGA microspheres were prepared by different solvent extraction techniques. sCT was incorporated both during microsphere preparation and after the formation of the microspheres by adsorption. Adsorbed sCT was found to form multiple layers in the polymer surface. Moreover, it was observed that sCT was capable of binding to the polymer matrix by hydrophobic as well as ionic forces. In vivo release studies indicated that polymer matrices with entrapped sCT were able to induce a hypocalcemic e!ect for an average of six days, while those with adsorbed sCT had an effect for only four days. Natural biodegradable polymers have also received attention as possible carriers for peptides and proteins. Aydin and Akbuga reported the use of chitosan, for sCT delivery. They were able to successfully incorporate and release the protein in vitro for a period of 27 days using high sCT concentrations. The release profiles of sCT from chitosan microspheres were shown to be non-Fickian in nature.

Therapeutic macromolecules (i.e. peptides and proteins) are prone to intestinal enzymatic degradation and exhibit poor membrane permeability due to their hydrophilicity and large size. This is the explanation for their usual administration as

injectable formulations, which causes patient's pain and discomfort. Thus, these molecules are good candidates for non-invasive administration through mucosal routes, such as the pulmonary. Lungs are ideally suited for this purpose as they are characterized by large absorptive surface area, high vascularization and thin blood–alveolar barrier which, together, facilitate macromolecule transport into systemic circulation. When compared to the oral route, lungs have become more enticing for drug delivery due to the absence of hepatic first pass-effect and low enzymatic activity (Patton, 1996). Besides, the possible targeted drug delivery to the lungs is an attractive therapeutic approach that may result in reduced administered dose, as well as reduced drug side effects (Azarmi et al., 2008). Different peptides and proteins have been successfully explored for pulmonary administration, such as insulin (Bi et al., 2009; Grainger et al., 2004), calcitonin (Kobayashi et al., 1996), human growth hormone (Jalaliour et al., 2008), rhDNase (Geller et al., 2003) and interferon-alpha. Moreover, inhalation aerosols offer significant potential for pulmonary administration of macromolecules for either local or systemic effect (Grainger et al., 2004). From the formulations available for inhalation, dry powders are usually preferred, as they have demonstrated the most suitable behavior in terms of stability and bioavailability of active ingredient, compared to the liquid counterparts.

Despite the advantages mentioned above, the lungs present several challenges to drug delivery which include airway geometry and humidity, pulmonary epithelium and the specific defensemechanisms, including the mucociliary escalator, as well as the macrophagic and enzymatic activities (James et al., 2008). In addition, the presence of lung disease might also affect therapeutic outcomes. These physiological barriers are known to interfere with inhalation therapy and, therefore, adequate drug carriers are required to overcome the imposed limitations, enhancing aerosolization properties and delivery and, consequently, drug bioavailability. To this end, many formulation strategies have been pursued, such as the use of protease inhibitors, macrophage activity suppressors, surfactants, as well as mucoadhesive and permeation enhancing polymers (Kobayashi et al., 1996; Jalaliour et al., 2008; Rooijen and Sanders, 1998; Hussain et al., 2004)

Pulmonary drug delivery

Pulmonary drug delivery represents another promising non-invasive administration route for peptide and protein drugs because of the large and highly absorptive surface area of the lung (80–120 m^2), its extensive vascularization, and low thickness of the alveolar epithelium. This method of delivery provides a more rapid onset of drug action compared to oral administration, as the drug is immediately absorbed into the bloodstream and is not compromised by gastrointestinal degradation, and also avoids hepatic first-pass metabolism. On the other hand, in the lung, different absorption barriers (alveolar lining fluid layer, macrophages and other cells, and alveolar epithelium) play an important role in impeding drug permeation into the circulation, and in affecting its cellular uptake and/or proteolytic degradation. Hence, peptide and protein stabilizers, protease inhibitors, as well as penetration enhancers might also be used to increase the pulmonary absorption after alveolar deposition.

Despite the advantages mentioned above, the lungs present several challenges to drug delivery which include airway geometry and humidity, pulmonary epithelium and the specific defense mechanisms, including the mucociliary escalator, as well as the macrophagic and enzymatic activities (James et al., 2008). In addition, the presence of lung disease might also affect therapeutic outcomes. These physiological barriers are known to interfere with inhalation therapy and, therefore, adequate drug carriers are required to overcome the imposed limitations, enhancing aerosolization properties and delivery and, consequently, drug bioavailability. To this end, many formulation strategies have been pursued, such as the use of protease inhibitors, macrophage activity suppressors, surfactants, as well as mucoadhesive and permeation enhancing polymers (Kobayashi et al., 1996; Jalaliour et al., 2008; Rooijen and Sanders, 1998). Pulmonary drug delivery may be employed for therapeutic agents having local or systemic activity. It provides advantages over other delivery routes as it is non-invasive, avoid first-pass metabolism and the lung offers a highly vascularized, large surface area for drug absorption. Pressurized metered dose inhalers (pMDIs) are widely used inhalation devices, being convenient to use and offering a sealed environment, providing protection from air, light, moisture and

microbial degradation. These medical devices comprise a therapeutic agent either suspended or dissolved in a hydrofluoroalkane (HFA) propellant. To achieve deep lung deposition of particles, one successful approach has been to formulate low density hollow particles, which have relatively large physical diameters, corresponding to a much smaller aerodynamic diameter (Dellamary et al., 2000). An alternative approach is the use of nanoparticles that are particularly attractive for pulmonary delivery, as their size not only permits access to the peripheral airways but also ensures that they escape both phagocytic and mucociliary clearance mechanisms. Incorporating drugs into, or onto, nanoparticles potentially cprovides protection against intracellular and extracellular barriers. degradation and may overcome formulation challenges, such as delivery of poorly aqueous soluble and unstable drugs without compromising the native conformation of these molecules. The small size of dry nanoparticles leads to high inter-particle cohesive forces that negatively impact on their aggregation behaviour, which is particularly problematic for dry powder inhaler (DPI) formulation. However, in a pMDI formulation, the presence of propellants such as HFAs offers potential for deaggregating the nanoparticles, though other excipients may be necessary. A number of groups have studied pMDI nanoparticle delivery, though adequate dispersion of such small particles in liquefied aerosol propellants is a major formulation challenge (Nyambura et al., 2009; Williams et al., 1998).

Polymeric nanoparticles (NPs) have been an exciting approach for lung delivery due to their ability to enter intracellular compartments and escape macrophages phagocytosis. Furthermore, they provide the possibility of achieving high drug loading capacity, sustained release, enhanced drug stability and absorption, as well as targeted deposition (Azarmi et al., 2008). Protein and peptides encapsulation or adsorption on nanocarriers have been achieved by various methods like emulsion polymerization, interfacial polymerization, solvent evaporation, salting out, coacervation, combination of sonication and layer by layer technology, solvent displacement/solvent diffusion etc. Each methods of protein encapsulation have their own advantage and disadvantage. Since each protein and peptides requires its own specific condition for stability, solubilization, control releases immune elimination.

The method of encapsulation is entirely based on the physicochemical activity of protein and its application.

Nanocarriers for peptide and protein delivery

Nanocarriers are one of the useful tools for achieving the main objective of protein therapeutics and its targeted delivery. A variety of nanocarriers have received much attention for the delivery of peptides, proteins, and genes due to their ability to protect protein and peptides from degradation in the gastrointestinal track and also in blood circulation. These protein encapsulated carriers have many advantages, such as a potential for selective targeting, controlled release and increase persistence of proteins therapeutics in the body. The protein therapeutic agents have short half-life due to proteolysis, rapid clearance from the blood stream and repeated administration. Encapsulation of protein drugs on nanoparticles provides sustained release and protects the non-released protein from degradation. The therapeutic protein molecules interact with nanocarriers by forming a coat or adsorption on the surface, or by bioconjugation (direct or using cross linkers). Various methods and nanocarriers systems are used to overcome the problems associated with functional native protein encapsulation on nanoparticles.

The choices of encapsulation methods and nanocarriers system entirely depends on the application and nature of protein encapsulate. The major advantage of colloidal drug carrier system in protein and peptide therapeutics are the controlled drug targeting, modified body distribution and enhancement of cellular uptake. The polymeric nanocarriers are very promising since they are biodegradable, non-antigenic, relatively easy to prepare and full control on size distribution. A variety of polymeric nanoparticles (natural and synthetic) can be synthesized in laboratory and

are also commercially available. Polymeric materials used for the formulation of nanoparticles include synthetic (poly(lactic acids) (PLA), poly(lactic-coglycolic acids) (PLGA), poly(ε-caprolactone) (PCL), poly(methyl methacrylates), and poly(alkyl cyanoacrylates)) or natural polymers (albumin, gelatin, alginate, collagen or chitosan). Polymeric nanoparticles have been synthesized using various methods (Pinto et al., 2006) according to needs of its application and type of drugs to be encapsulated. These nanoparticles are extensively used for the nanoencapsulation of various useful bioactive molecules and medicinal drugs to develop nanomedicine. Biodegradable polymeric nanoparticles are highly preferred because they show promise in drug delivery system. Such nanoparticles provide controlled/sustained release property, subcellular size and biocompatibility with tissue and cells (Panyam et al., 2003). Apart from this, these nanomedicines are stable in blood, non-toxic, nonthrombogenic, nonimmunogenic, noninflammatory, do not activate neutrophils, biodegradable, avoid reticuloendothelial system and applicable to various molecules such as drugs, proteins, peptides, or nucleic acids. The general synthesis and encapsulation of biodegradable nanomedicines are represented in Fig. 3. The drug molecules either bound to surface as nanosphere or encapsulated inside as nanocapsules.

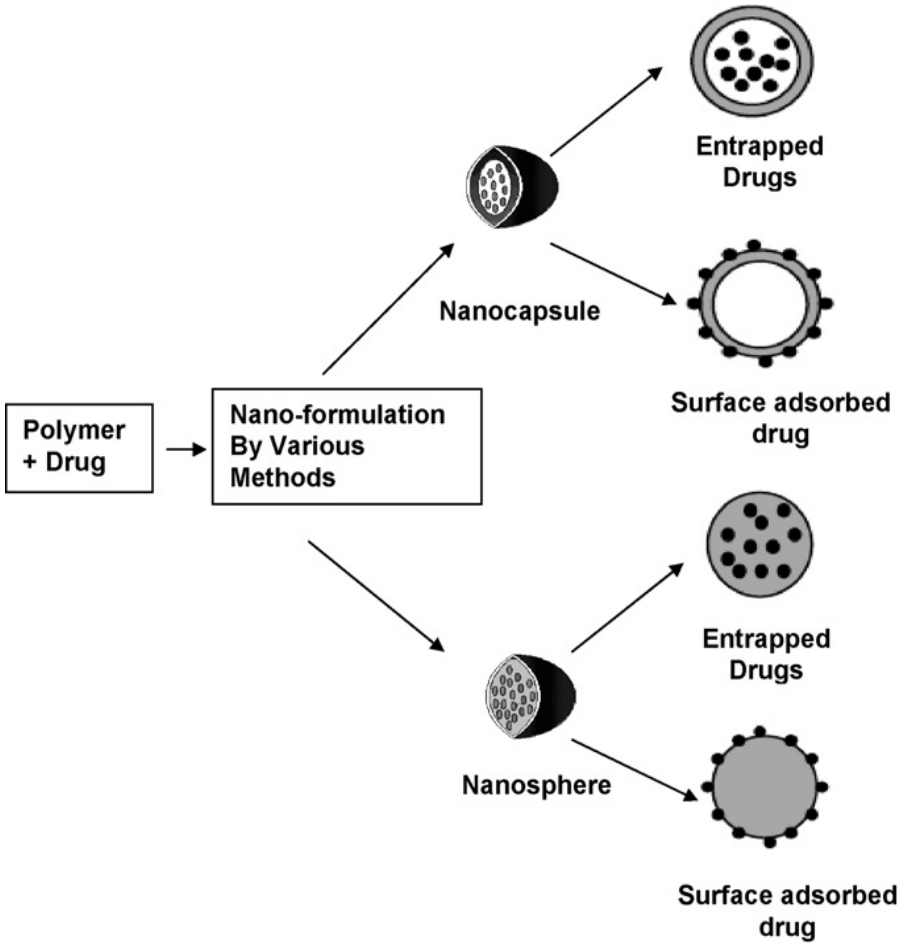

Figure 3. Type of biodegradable nanoparticles: According to the structural organization biodegradable nanoparticles are classified as nanocapsule, and nanosphere. The drug molecules are either entrapped inside or adsorbed on the surface. (Originally adapted from (Tiyaboonchai, 2003))

Learning from environmental toxicology studies, nano-sized air pollutants, especially the spherical solid materials, easily enter the lungs and reach the alveoli, and subsequently are cleared from the lungs by different clearance mechanisms. However, due to their small size, nano-sized particles are not likely to be detected around the lung epithelial barriers. They will translocate into systemic circulation and target other organs. Since the definition for the cut-off size of airborne nanoparticles is the same as that of engineered nanoparticles (100 nm), they should share the same

biokinetics upon inhalation into the lungs. Furthermore, the high surface-to-volume ratio of natural airborne and engineered nanomaterials renders them more reactive, even though they are inert as larger particles. Therefore, any possible effects of the nanomaterials may be amplified once entering the body via inhalation. On the other

hand, the extrapulmonary toxicity induced by inhaled nano-sized air pollutants may also provide evidence for systemic delivery of nano-sized pharmaceutical agents by inhalation, for the medicines not suitable for oral or parenteral administration to improve bioavailability and patient compliance. Due to rapid advances in nanotechnology and biotechnology, nanoparticles have been considered as an effective form for delivery, and have been studied extensively to deliver the newgeneration of protein, gene-based macromolecular therapeutic agents into the body, since many of the components of living cells are constructed at the nano-level, such as ribosomes, membrane transporters, receptors and cell signaling systems (Labhasetwar, 2005). Nanoparticles fall in the same size range of the biological entities; therefore they can readily interact with molecules on both the cell surface and within the cell (Rao et al., 2004; Moore, 2002). Furthermore, drugs that are deposited within the lungs in nanoparticulate form have a greater chance to escape from the clearance mechanisms by the lung defense systems, compared to microparticulate form (Chono et al., 2006; Schurch et al., 1990). Thus, drug-bearing nanoparticles have the potential to deliver drugs efficiently to the epithelium, while avoiding unwanted mucociliary clearance.

In the pharmaceutical area, most nanoparticles described in the literature for drug delivery are between 50 and 500 nm in diameter (Yokoyama, 2005). Nanoparticles are useful to deliver water-insoluble drugs. Despite high potency, the effectiveness of water-insoluble drugs can be severely limited because the solubility is too low to reach therapeutic systemic concentrations. However, when their size is reduced to nano-level, the increased particle surface-to-volume ratio helps to enhance solubility and dissolution rate in an aqueous environment. Nanoparticulate forms of drug could have an enormous benefit by significantly improving systemic bioavailability (defined as the rate and extent of therapeutically active drugs reaching the systemic circulation) and allowing a more rapid onset of therapeutic action (Shargel and Yu, 1999). The route of administration is as important as the drug itself for therapeutic success. Nano-based approaches to drug delivery are focused on crossing a particular physical barrier, such as the gastro-intestinal epithelium for

absorption of macromolecules, blood–brain barrier; or on finding alternative and acceptable routes for the delivery of drugs expensive and vulnerable to the gastro-intestinal environment. Nanoparticles have gained increasing attention for pulmonary drug delivery, due to their advantages for targeted deposition, bioadhesion, sustained release and reduced dosing frequency for improving convenience to the patient (Sung et al., 2007). Some incentives for using nanoparticles for the controlled delivery of drugs, peptides, proteins, genes, siRNA and vaccines in the lung include having an appropriate size for avoiding alveolar macrophage clearance and promoting transepithelial transport.

Nanocarriers used for pulmonary applications also include liposomes, solid lipid nanoparticles, nanotubes and polymeric nanocarriers (Vyas and Khatri, 2007; Jaspart et al., 2007). Recent years have seen increasing interest in polymeric nanoparticles as carriers for hydrophilic macromolecules such as proteins, vaccines, and polynucleotides (Panyam and Labhasetwar, 2003; Soppimath et al., 2001). Numerous investigations have shown that nanoparticles can not only improve the stability of therapeutic agents against enzymatic degradation and control the release of therapeutic agents, but they can also be delivered to distant target sites either by localized delivery using a catheter based approach with a minimal invasive procedure, or they can be conjugated to a biospecific ligand which could direct them to the target tissue or organ (Panyam and Labhasetwar, 2003; Brunner et al., 1999). For an effective nanoparticulate delivery system, the nanoparticle size and loading must be adjusted carefully, and protein stability during preparation and release must be ensured. Depending on the preparation method, drugs or antigens can either be entrapped in the polymer matrix, encapsulated in a liquid core, surrounded by a shell-like polymer membrane, or bound to the particle surface by adsorption (Jung et al., 2000). Chitosan (CS) is attractive for transmucosal drug delivery, e.g. pulmonary administration, owing to its reported low toxicity, biodegradability, biocompatibility (Grenha et al., 2007) and mucoadhesivity, as well as enhancement of macromolecules permeation (Issa et al., 2005), thus being extensively employed in the development of

micro- and nanocarriers. Furthermore, it has also been used as a dispersibility enhancer for dry powders (Li et al., 2006).

Chitosan

Chitosan (CS) is a polysaccharide, similar in structure to cellulose. Both are made by linear β-(1→4)-linked monosaccharides (Fig. 4). Chitosan is obtained from the deacetylation of chitin, a naturally occurring and abundantly available (in marine crustaceans) biocompatible polysaccharide. Chitosan is relatively reactive and can be produced in various forms such as powder, paste, film, fiber, etc. Commercially available CS has an average molecular weight ranging between 3800 and 20,000 Daltons and is 66% to 95% deacetylated. Chitosan, being a cationic polysaccharide in neutral or basic pH conditions, contains free amino groups and hence, is insoluble in water. In acidic pH, amino groups can undergo protonation thus, making it soluble in water.

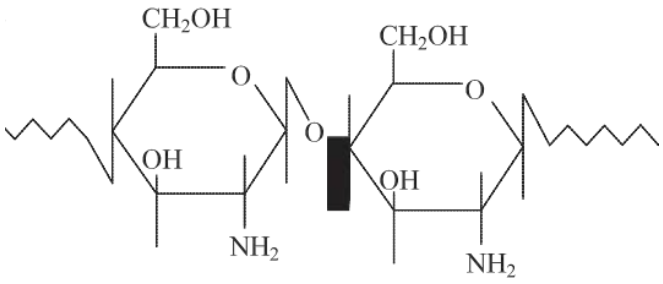

Figure 4. Structure of chitosan

Solubility of CS depends upon the distribution of free amino and N-acetyl groups. Usually 1–3% aqueous acetic acid solutions are used to solubilize CS. Chitosan is biocompatible with living tissues since it does not cause allergic reactions and rejection. It breaks down slowly to harmless products (amino sugars), which are completely absorbed by the human body. Chitosan degrades under the action of ferments, it is nontoxic; LD_{50} of CS in laboratory mice is 16 g/kg body weight, which is close to sugar or salt and easily removable from the organism without causing concurrent side reactions.

Chitosan has gained considerable interest as a polymer for preparing nanoparticles because of its biodegradable, biocompatible, non-toxic and mucoadhesive properties (Illum, 1998; Fel et al., 1998). Chitosan has been reported to increase the uptake of macromolecules through opening of tight junctions of epithelial cells and has also been formulated as nanoparticles designed to improve the delivery of therapeutically active molecules across mucosal surfaces (Fernandez-Urrusuno et al., 1999). The successful application of chitosan for in vitro and in vivo gene delivery has demonstrated its potential for pharmaceutical and biomedical applications (Chae et al., 2005). The potential for pulmonary delivery has been recognized, and chitosan nanoparticles encapsulated in mannitol microspheres have been demonstrated to be biocompatible with Calu-3 and A549 human respiratory epithelial cell lines for up to 48 h (Grenha et al., 2007). Crosslinked chitosan microparticulates containing the bronchodilator, salbutamol sulphate prepared using spray drying, were able to achieve controlled release of the drug (Corrigan et al., 2006) and could be formulated into DPIs, with good aerosolization properties. Chitosan has not been extensively studied as a carrier for delivery from pMDI systems, the formulation and characterization of crosslinked chitosan nanoparticles for delivery using pMDIs are explored. Chitosan has been recognized as a promising material for delivery of drugs and labile macromolecular compounds, attributed to its excellent physicochemical and biological properties. It is regarded as a biocompatible and biodegradable polymer of low toxicity (Illum, 1998; Mi et al., 2002). Furthermore, it is extremely important to

note that chitosan is soluble in aqueous mild acidic solution, which is an obvious advantage over other biodegradable polymers.

CS is extensively used in developing drug delivery systems. Particularly, CS has been used in the preparation of mucoadhesive formulations (Lehr et al., 1992; Luehen et al., 1994; llum et al., 1994), improving the dissolution rate of the poorly soluble drugs (Sawayanagi et al., 1983), drug targeting (Hassan et al., 1992) and enhancement of peptide absorption (Luehen et al., 1994; llum et al., 1994; Artursson et al., 1994). Different methods have been used to prepare CS particulate systems. Selection of any of the methods depends upon factors such as particle size requirement, thermal and chemical stability of the active agent, reproducibility of the release kinetic profiles, stability of the final product and residual toxicity associated with the final product. Chitosan is a modified natural carbohydrate polymer prepared by the partial N-deacetylation of crustacean derived natural biopolymer chitin. It is the second most abundant polysaccharide in nature, and has attracted particular interest as a biodegradable material for mucosal delivery systems. There are at least four methods reported (Tiyaboonchai, 2003) for the preparation of chitosan nanoparticles as ionotropic gelation, microemulsion, emulsification solvent diffusion and polyelectrolyte complex formation. Chitosan nanoparticles have low toxicity and high susceptibility to biodegradation, mucoadhesive properties and has an important capacity to enhance protein drug permeability/absorption at mucosal sites (Tiyaboonchai, 2003).

More importantly, chitosan micro/nanoparticles can be spontaneously formed through ionic gelation using tripolyphosphate as the precipitating agent. This reduces the use of harmful organic solvents during preparation and loading of protein therapeutics (van der Lubben et al., 2001). Chitosan solubility is poor above pH 6.0 which is a major drawback of this system. At physiological pH, chitosan is known to lose its capacity to enhance drug permeability and absorption, which can only be achieved in its protonated form in acidic environments. In contrast, quaternized

chitosan derivative, N-trimethyl chitosan chloride (TMC) shows perfect solubility in water over awide range of pH. In addition, these chitosan derivatized nanoparticles have bio-adhesive properties. Thus, it is used for enhancement of permeability and absorption of diverse protein drugs in neutral and basic-pH condition. N-trimethyl chitosan chloride (TMC) nanoparticles to carry proteins were prepared by ionic cross linking of TMC with tripolyphosphate (TPP) (Hamman et al., 2002). The results indicate that different degree of quaternization of TMC has influenced the physicochemical properties, release profile and degree of loading of different proteins. Thus, the particle size may depend upon the nature and concentration of the loading proteins (Hamman et al., 2002). Insulin was observed to be directly internalized by enterocytes in contact with intestine and retention of drugs at their absorptive sites by mucoadhesive carriers (Sarmento et al., 2007). Insulin loaded chitosan nanoparticles markedly enhanced intestinal absorption of insulin following oral administration. The hypoglycemia effect and insulinemia levels were significantly higher than that obtained from insulin solution and physical mixture of oral insulin and empty nanoparticles. The mechanism of insulin absorption seems to be a combination of both insulin internalization, probably through vesicular structures in enterocytes and insulin loaded nanoparticles uptake by Payers patches cells (Sarmento et al., 2007).

Chitosan nanoparticles are also explored for their efficacy to increase systemic absorption of hydrophobic peptides such as cyclosporin A (El-Shabouri et al., 2002). The relative bioavailability of cyclosporin A encapsulated chitosan nanoparticles was increased by about 73%. This formulation provides the highest C_{max} (2762.8 ng/ml) of Cy-A after 2.17 h. Chitosan nanoparticles administered orally to beagle dogs provide an improved absorption compared to the currently available cyclosporin A microemulsion (Neoral®) (Sarmento et al., 2007). It has been shown that ovalbumin loaded chitosan microparticles are taken up by the Peyer's patches of the gut associated lymphoid tissue (GALT). Additionally, after co-administering chitosan with antigens in nasal vaccination studies, a strong enhancement of both mucosal and systemic immune responses was observed (Van der Lubben et al., 2001). Van der Lubben et al. have demonstrated that large amounts of bovine serum albumin (BSA)

or tetanus toxoid (TT) vaccine were easily encapsulated in chitosan nanoparticles. Recently, Alonso's group has developed chitosan nanoparticles as carrier systems for transmucosal delivery. They have shown the enhanced mucosal absorption of chitosan NPs on rats and rabbits (Vila et al., 2004). The nanoparticles were in the 350 nm size range, and exhibited a positive electrical charge (+40mV) and high loading efficiency (50–60%). They have reported important capacity of chitosan nanoparticles for the association of peptides such as insulin, salmon calcitonin and tetanus toxoid. Their mechanism of interaction with epithelia was caused a concentration-dependent reduction in the transepithelial resistance of the cell monolayer (Vila et al., 2004).

Chitosan NP showed to be prospective drug delivery carriers as they offer many advantages. First, chitosan is considered as a safe material as it is natural polymer that possesses biocompatible and biodegradable properties. Second, it is water-soluble polymers which is an ideal property for drug delivery carriers, therefore, simple and mild preparation methods can be applied. This renders chitosan NP as promising drug delivery carriers that are suitable for a broad category of drugs including macromolecules and labile drugs. Third, chitosan is available in a wide range of molecular weights and is easily chemically modified by coupling with ligands providing flexibility in formulation development. Forth, chitosan provides absorption promoting effect that prolongs the contact time between substrate and cell membrane. In addition, their nano-sized facilitates the drug uptake through the cell membrane. Together, the absorption enhancing effect and nano-sized particles exhibited ability to improve drug bioavailability. Fifth, chitosan NP offer versatile routes of administration, especially non-invasive routes, i.e. peroral, nasal, pulmonary and ocular mucosa, which are preferable routes administration.

However, NPs are impractical for pulmonary administration due to the fact that their direct delivery poses many challenges, including formulation instability due to particle–particle interactions and poor delivery efficiency due to exhalation of low-inertia NPs (Yang et al., 2008). The microencapsulation of these NPs through a spray

drying technique and using a sugar, in order to obtain a dry powder (Grenha et al., 2005). Microencapsulation improved NPs handling and aerosolization performance, achieved by enhanced stability and acquisition of aerodynamic properties which result definitively in efficient lung delivery (Grenha et al., 2005; Sham et al., 2004). Interestingly, these new powders have been shown to be biocompatible with pulmonary cell lines (Grenha et al., 2007). For deep lung deposition, dry powders are mainly required to bear adequate aerodynamic characteristics, e.g. the aerodynamic diameter which must be less than 5 μm (Glover et al., 2008). Besides, micro- and nano-particles based delivery can provide control over drug release profile and targeting at the tissue and cellular levels. Accordingly, there have been increasing needs for development of efficient formulations of such labile therapeutics, which seem to have greater stability in the solid forms than in the liquid forms. One approach is to incorporate them into polymeric biodegradable micro-/nanoparticles. This could help simplify product storage and subsequently improve product stability. Several methods have been employed for micro-/nanoparticle productions, including spray drying (Blanco-Prieto et al., 2004; Mumenthaler et al., 1994; Tzannis and Prestrelski, 1999; Youan, 2004), spray freeze-drying (Costantino et al., 2004), emulsion-solvent evaporation method (Blanco and Alonso, 1997; Cegnar et al., 2004; Kim and Bae, 2004; Tobio et al., 1998), and precipitation in supercritical antisolvents (Winters et al., 1996). Of these, spray drying appears to be one of the most promising methods, because of its capacity to produce particles with controlled characteristics and narrow particle size distribution. Furthermore, it is considered as a fast, simple and energy-efficient process.

Spray dry powder

Spray drying is a useful and widely applied technique to prepare powders for inhalation. Supercritical fluids have recently been applied for producing powders for inhalation. In this section, we briefly review these techniques, stability of the produced dry powder peptides and proteins, and aerodynamic diameter being one of the most critical factors to determine the success of inhalation therapy. Spray drying is

a useful and widely applied technique for one-step preparation of powders for inhalation with a drug solution or suspension. The independent variables of spray drying processes are liquid feed rate, atomizing air flow rate, drying air flow rate, and inlet air temperature. Outlet temperature linearly depends on each of these variables ,suggesting that it can be estimated if the regression lines between outlet temperature and the independent variables are available for a spray drier. The inlet temperature is usually several tens of degrees higher than the outlet temperature. For pulmonary delivery of drug formulations in solid form, micron-sized powder particles containing the drug-bearing nanoparticles were designed for deep lung delivery by using MDIs and DPIs. Sham et al. (2004) developed a platform for aerosol delivery of nanoparticles by preparing carbohydrate (e.g., lactose, mannitol) carrier particles containing nanoparticle clusters using spray-drying technique.

Carrier particles can be made with an appropriate MMAD to optimize alveolar deposition. Dispersion of the lactose carrier containing either gelatin or polybutylcyanoacrylate nanoparticles by a DPI showed a fine particle fraction (FPF) of about 40% and MMAD of 3μm. Upon reaching the deep lung and contacting with the aqueous lining fluid of the lung epithelium, the carrier particles dissolved and released the nanoparticles. A novel type of effervescent carrier particle containing nanoparticles, with a MMAD suitable for deep lung delivery, was reported by Ely et al. (2007). Incorporation of effervescent technology into carrier particles adds an active release mechanism for the nanoparticles after pulmonary administration using DPI. The optimal size for deposition in the deep lung for systemic delivery is approximately 1 – 3 μm (Shoyele and Cawthorne, 2006). Particles larger than 5 – 10 μm result in oropharyngeal deposition, and are more likely to be swallowed than to reach the lung. Particles smaller than 1 μm will likely be exhaled. For particles between 1 and 5 μm, the smaller particles generally reach the deeper parts of the lung, and the larger particles land in the upper airways (Sakagami et al., 2006). The particles smaller than 150 nm encounter delayed lung clearance, increased protein interactions and more transepithelial transport compared to larger particles (Chow et al., 2007). Particle size may also affect particle degradation and drug release rates.

Surface charge is another important property to consider in particle design. Low surface energy is needed to avoid particle agglomeration (Shoyele and Cawthorne, 2006; Chow et al., 2007). Electrostatic interactions are also possible between the alveolar wall and oppositely charged particles, but this depends on hydrophobicity and humidity (Chow et al., 2007). The efficacy of many drugs is often limited by their potential to reach the site of therapeutic action. In most cases (conventional dosage forms), only a small amount of administered dose reaches the target site, while the majority of the drug distributes throughout the rest of the body in accordance with its physicochemical and biochemical properties. Therefore, developing a drug delivery system that optimizes the pharmaceutical action of a drug while reducing its toxic side effects *in vivo* is a challenging task.

Particle size characteristics have a crucial role in pulmonary delivery to avoid physiological barriers of the lung, as well as to target the drug to the appropriate lung region. Large particles (>10 μm) do not penetrate the lung because they are deposited by impaction in the upper respiratory tract. Small particles (0.1–1 μm) are inhaled into the alveoli but are exhaled subsequently from there without being deposited to a significant extent. Particles with diameters in the range of 2–4 μm show an optimal pulmonary deposition, and these are able to transport most pharmaceuticals into the lung. For any drug to be delivered to the lungs by inhalation, it has to be formulated as an aerosol, which involves three commonly used technologies: jet or ultrasonic nebulizers, metered dose inhalers and dry powder inhalers (Byron, 1990). The low efficiency of commercially available inhalation systems has led to the requirement for high doses compared to the parenteral administration route, and this has been the major problem with pulmonary delivery for many years. However, recently, new inhalation devices have been developed that allow the delivery of large drug doses to the airways, and that achieve significantly greater deposition efficiency of >50% lung deposition compared to <20% with older devices. Two distinct applications for systemic pulmonary delivery routes have emerged recently, i.e. in situations in which rapid absorption of the drug is crucial, and for administration of drugs that have shown low bioavailability by other non-invasive routes (Scheuch and Siekmeier,

2007). Such drugs include insulin and its analogues, growth hormone and growth hormone-releasing peptides (Wall, 1997), erythropoietin, and interferons (Zandwijk, 1997).

Dry powder inhalers (DPIs)

DPIs are devices through which a dry powder formulation of an active drug is delivered for local or systemic effect via the pulmonary route. DPIs have a number of advantages over other methods of pulmonary drug delivery, for example, direct delivery of drug into the deep lungs utilizing the patient's respiration and are increasingly being explored as a mechanism for the delivery of systemic drugs. Successful delivery of drugs into the deep lungs depends on the integration between powder formulations and the device performance (Peart and Clarke, 2001). Licensing and marketing approval requires that current DPIs demonstrate *in vitro* performance and *in vivo* efficacy and reliability. However, questions remain about the ability to interchange DPIs and the effects of different clinical states and patient characteristics.

Dry powders for inhalation are formulated either as loose agglomerates of micronised drug particles with aerodynamic particle sizes of less than 5μm or as carrier-based interactive mixtures with micronised drug particles adhered onto the surface of large lactose carriers (Hersey, 1975). For topical respiratory drug delivery, a particle size of 2–5μm yields optimal benefit, whereas for systemic effects particle size of less than 2μm is needed for drug deposition in the small peripheral airways. Particles greater than 5μm may also result in systemic effects due to impaction in the throat (i.e., oropharyngeal delivery) and oral absorption (Newman and Clarke, 1983; Byron, 1986; Hickey, 1992; Bisgaard, 1996). The powder formulation is aerosolized through a DPI device, where the drug particles are separated from the carrier (from drug–carrier mixtures) or deagglomerates drug particles, and the dose is delivered into the patient's deep lungs. In these systems, particle size and flow property,

formulation, drug–carrier adhesion, respiratory flow rate and design of DPI devices extensively influence the performance (Hickey and Concessio, 1997).

The inhalation device is important in achieving adequate delivery of inhaled drug to lungs. The device should be easy to use, inexpensive and portable. The device must provide an environment where the drug can maintain its physicochemical stability and produce reproducible drug dosing. The device should be designed to deliver high fine particle fraction (FPF) of drugs from the formulations (Srichana et al., 1998). However, devices with higher resistance, need a higher inspiratory force by the patients to achieve the desired air flow. This could be difficult for patients with severe asthma and for children and infants. Therefore, a balance between these two factors is necessary to achieve the desired therapeutic effect from DPI formulations. As previously mentioned most of the recent research has focused on inhaler devices rather than powder formulations. Furthermore, the concept of powder interaction with the device as well as the influence on powder dispersion has generally been poorly understood. Recently, computational fluid dynamics has enhanced understanding of the impact of inhaler design on powder dispersion and deposition and has demonstrated that small variations in the device design can produce significant variations in performance (Coates et al., 2004; Chan, 2006).

For example, active DPIs have been designed specifically for patients, or for clinical situations in which patients cannot generate sufficient inspiratory effort, and are being explored for systemic drug delivery. Variability in drug delivery due to insufficient inspiratory flow is often not a major problem for asthma drugs but it would probably be unsatisfactory for novel drugs such as inhaled proteins and macromolecules. Efficient delivery of drugs from DPIs depends not only on the device, but also on drug formulation and the formulation of a DPI involves the production of suitable powders for effective respiratory deposition as well as formulation of powders with or without excipients (Dolovich, 1992; Byron and Patton, 1994). Historically, drug particles for inhalation have been produced by

milling (micronisation) process and are then blended with a carrier (e.g., lactose) to improve flow properties and dose uniformity (Timsina et al., 1994; French et al., 1996). Other carriers such as mannitol and trehalose (Stahl et al., 2002; Mao and Blair, 2004) have also been reported to use in the DPI formulations. The properties of such blends are a function of the principal adhesive forces that exist between the particles and the surface tension of the adsorbed moisture layers (Ibrahim et al., 2000). In carrier-mediated formulations, drug–carrier adhesion is likely to affect the dispersion of drugs aerosolised via inhaler devices (Podczeck, 1997; Louey and Stewart, 2002; Young et al., 2002; Islam et al., 2005); however, this review article deals with the DPI devices only. Insufficiency of traditional methods of powder production has lead to the development of alternative techniques which produce powders of specific size, density and morphology and with less cohesion and adhesion (Hickey and Concessio, 1997). The dispersion of powder aerosols is also influenced by the geometric diameters of the particles which are generally at odds with the efficiency of deposition in the lungs (Hickey and Concessio, 1997).

A number of alternative techniques, including specialised spray drying, ultrasound-assisted crystallisation and supercritical fluid technology, in situ method have also been demonstrated (York and Hanna, 1996; Steckel et al., 2003; Shekunov et al., 2003; Chowet al., 2007). Development of sustained released spray dried recombinant human insulin with hyaluronic acid is an exciting example of the formulation of proteins for DPIs (Surendrakumar et al., 2003). The underlying principle has been described as enhanced performance through particle engineering and recent particle engineering has seen the development of highly porous particles with large geometric diameters but small aerodynamic diameters which by improving powder dispersion can improve efficacy of DPIs (Edwards et al., 1997, 1998). Recently, respiratory delivery of proteins (Edwards et al., 1997; Chan, 2003), interleukins and oligonucleotides (Nyce et al., 2000), gene therapy and vaccination was reported elsewhere (Laube, 2005; Yvonne et al., 2006; Erin and James, 2006; de Swart et al., 2007; Dilraj et al., 2007). Inhalation of insulin from DPI formulation showed to increase systemic level of insulin and suppressed systemic glucose levels

(Edwards et al., 1997; Patton et al., 1999; Graham and Ronald, 2006; Hussain et al., 2006; Thomas, 2006). Another study demonstrated that the bioavailability (66%) of inhaled calcitonin was more than double compared to that of the bioavailability (28%) of injected calcitonin (Banga, 2003). Pulmonary delivery of DPI for gentamicin (Crowther et al., 1999), colistin sulphate (Le Brun et al., 2002), and tobramycin sulphate (Newhouse et al., 2003) has been successfully investigated and inhaled delivery showed higher plasma concentrations compared to those achieved by nebulisation. These studies reveal the promising future of DPIs in drug delivery and the application of DPI is expanding from pulmonary diseases to other disorders. Local and systemic delivery of different drugs for systemic chronic diseases needs to be focused more on using DPI formulations, which have a lot of potential. The DPI delivery systems are likely to contribute to successful drug delivery into the lungs not only to treat asthma, but also to deliver a wide range of therapeutic agents for pulmonary delivery. In future, very small amount of potent drugs like products of biotechnology will require smart devices that deliver drugs efficiently into the lower airway of lungs. Many devices mentioned in this review have yet to be commercialised; however, some of them will come to market in near future.

Therefore, in combination with the increasing knowledge of DPI formulations and design of new devices, a step needs to be taken to develop more effective delivery system. The current trend in pulmonary drug delivery and potential benefits of this route, development of smart but reliable device will be continued to enhance deposition of drugs into deep lungs with a better patient compliance. From the discussion it seems that neither is more important than the other, i.e., device reliability or innovation. Rather, the comparative importance of device reliability and innovation differs depending on specific circumstances. For example, one could argue strongly that for local delivery of drugs for conditions such as asthma, our continuing efforts are better placed in optimizing existing devices and drug formulations rather than spending the considerable time and effort required to produce an innovative DPI. Alternatively, for systemic drug delivery via DPIs for conditions such as diabetes, cancer, CNS disorders and cystic fibrosis, there is considerably more demand and a

stronger rational for innovative DPIs designed to optimise powder delivery and systemic therapeutic effects. The recent focus on the regulatory requirements means that it is essential for the inhalers to have minimal dependence on the patients inspiratory flow rates, reproducible aerosol performance to attain optimal performance. The future development of DPI products may focus both on the inhaler device as well as the powder formulations for optimum therapeutic benefits. The delivery device may develop into a disposable device that will overcome the need for cleaning the device, concerns over product stability, and less expensive with improved patient compliance. Therefore, to realise the full potential of DPIs, at the lowest cost to both pharmaceutical companies and patients, innovation of new device with enhanced lung deposition and device reliability will play important roles in the future. With the development of the biomaterial science, some polymeric materials with good biocompatibility have been adopted in the field of pharmaceutics. In fact, polymeric nanoparticles have been considered to be a superior pulmonary delivery system for proteins and peptides, because they can overcome some disadvantages associated with liposomes and solid lipid nanoparticles, such as low encapsulation efficiency and poor stability during storage. In addition, polymeric nanoparticles can be prepared or modified with bioadhesive materials to prolong the retention of polymeric nanoparticles in vivo, and in return an improved bioavail-ability would be obtained. They have potential for delaying phagocytic clearance and improving the epithelial penetration. Although pulmonary drug delivery based on nanoparticles is gaining interests, relatively few studies on peptides and proteins have been published, because the practical utilities of nanoparticles are restricted by their low inertia properties. Pulmonary delivery based on nanoparticulate systems usually utilizes the nebulizer for administration, whilst the stability of peptides and proteins during and after nebulization is still a concern.

CHAPTER III

MATERIALS AND METHODS

1. Materials

The following materials obtained from commercial sources were used:

1.1 Chemicals

- Calcitonin (salmon I) (Lot no. 4033011.0005, Bachem, Swizerland)
- Chitosan, low molecular weight (Lot no. 10124AB, Sigma Aldrich)
- Sodium tripolyphosphate (TPP) (Lot no. 7758-29-4, Sigma Aldrich)
- D-Lactose monohydrate (Lot no. 3768231, Sigma Aldrich, Saint Louis, USA)
- D-mannitol (Lot no. 1721898, Sigma Aldrich, Saint Louis, USA)
- Potassium phosphate, monobasic (Lot No.AF705005, Ajax Finechem, NSW, Australia)
- Di-Sodium hydrogen orthophosphate dodeccahydrate (Lot No.0903241, Ajax Finechem, NSW, Australia)
- Potassium chloride (Lot no. AF501338, Ajax Finechem, NSW, Australia)
- Sodium chloride (Lot no. 0811292, Ajax Finechem, NSW, Australia)
- di-Sodium hydrogen orthophosphate dodeccahydrate (Lot no. 0903241, Ajax Finechem, NSW, Australia)
- Sodium hydroxide (Lot no. B131198 214, Merck KGaA, Damstadt, Germany)
- Acrylamide/Bis-acrylamide (Lot no. MFCD00080848, Sigma Aldrich)
- Ammonium persulfate (Lot no. 7727-54-0, Sigma Aldrich)
- 2-mercaptoethanol (Lot no. 773648, Sigma Aldrich, Saint Louis, USA)
- Trizma® Base (Tris Base) (Lot no. 741883, Sigma Aldrich, Saint Louis, USA)
- Glycine (Lot no. 24895355, Sigma Aldrich)

- Tris-Tricine-SDS running buffer (Lot no. 1165201, Sigma Aldrich, Saint Louis, USA)
- Urethane (Lot no. 635810, Sigma Aldrich)

1.2 Reagents

- Acetonitrile HPLC grade (Lot no.KBRA1H, Honeywell Berdick & Jackson, Ulsan, Korea)
- Methanol HPLC grade (Lot no.K33G2H, Honeywell Berdick & Jackson, Ulsan, Korea)
- Trifluoroacetic acid (Product no. 29953, Sigma-Aldrich, Singapore)
- EZBlue TM Gel Staining Reagent (Lot. No.G1041, Sigma, Saint Louis, USA)
- ELISA Kit for Salmon Calcitonin (Lot. No. E0152Ge, Uscn Life Science Inc. Wuhan)

2. Equipments

- Analytical Balance (Model PB3002, Mettler Toledo, Schwerzenbach, Switzerland and Model A200s, Sartorius Gbh, Goettingen, Germany)
- Büchi B-290 spray dryer (Büchi Labortechnik AG, Postfash, Switzerland)
- Andersen Cascade Impactor (ACI; Copley Scientific Ltd., Nottingham,UK)
- Scanning electron microscopy (SEM, JSM-6610LV, JEOL Ltd., Tokyo, Japan)
- Transmission Electron Microscope (TEM, JEM-2100, JEOL Ltd., Japan).
- Zetasizer® Nano-ZS (Malvern instruments, Malvern, UK)
- Freeze Dryer (Labconco, USA)
- Spectropolarimeter (Jasco model J-715, Jasco, Japan)

- High performance liquid chromatograph (Shimadzu, Kyoto, Japan) assembled with
    - Liquid chromatograph pump (Model LC-20AB, Shimadzu, Japan)
    - Auto injector (Model SIL-20A, Shimadzu, Japan)
    - UV-VIS detector (Model SPD-20A UV, Shimadzu, Japan)
    - Inertsil ODS-3, 5 µm, C18, 4.6 mm x 250 mm i.d.(GL Sciences Inc., Japan)(C/N 5020-01732, S/N 7HT86018)
    - Alltima Guard column, 5 µm, C18 (Lot no. 50277378, Serial no. 609100731)
- Liquid chromatograph pump (Model LC-10AB, Shimadzu, Japan)
- Laser diffraction (Malvern Mastersizer S, Malvern, UK)
- FTIR spectrometer (Perkin-Elmer, model Spectrum One)
- Ultracentrifuged (Beckmann Avanti 30, Beckman, USA)
- pH meter (Model 210A+, Thermo orion, Germany)
- Dry powder insufflators (Model DP-4, Penn Century Inc)
- Microplate Reader (VICTOR™ *X* , PerkinElmer)
- Helium pycnometer (Ultrapycnometer 1000, Quantachrome instruments, Florida, USA)
- Electrophoresis (Bio-Rad model Mini-PROTEAN III, Bio-Rad Laboratories, Hercules CA, USA)

Methods

Preparation of chitosan nanoparticles

The ionic gelation of chitosan (CS) and tripolyphosphate (TPP) that using as a cross linking polyanion was applied to preparing nanoparticles (NPs). Low molecular weight chitosan was dissolved in 1% (w/v) acetic acid solution to represent chitosan concentrations at 0.10, 0.20 and 0.30% (w/v). The chitosan solutions was mixed with TPP aqueous solution that acquire solution of 0.42-0.69 mg/ml (w/v). The CS/TPP nanoparticles formation become spontaneously through the initiated ionic crosslink mechanism of TPP. The nanoparticles were make up at decided chitosan to TPP weight ratios of 3:1, 5:1 and 7:1 respectively. The nanoparticles suspensions were gently stirred at room temperature for 60 min.

Nanoparticles drug loading, salmon calcitonin (sCT) was premixed with TPP solution to generate the ultimate 1 mg/ml nanoparticles dispersion concentration. The solution of sCT-TPP was added to CS solution to attain last hypothetic CS to TPP weight ratios of 3:1, 5:1 and 7:1 (w/w) respectively and using 0.1 N sodium hydroxide solution for pH adjustment to 4.5. The nanoparticles suspensions were lightly stirred for 60 min at room temperature. Ultracentrifugation on a 10 µl glycerol bed (45,000 rpm, 45 min, 4°C; Beckmann Avanti 30, Beckmann, USA) used for concentrate the nanoparticles and resuspended the particles in purified water after removing the supernatants before being subjected to advance characterize and operations.

Physicochemical characterization of chitosan nanoparticles

The morphological of nanoparticles were characterized by high resolution Transmission Electron Microscope (TEM) with EDX Attachment and Specimen Heating Holder (up to 800°C) (JEM-2100, JEOL Ltd., Japan). The nanoparticles samples were stained with 2% (w/v) phosphotungstic acid and placed on copper grids with Formvar® films for TEM observation.

Using Zetasizer® Nano-ZS (Malvern instruments, Malvern, UK) for evaluation the particles sizes, zeta potentials and polydispersity index (PDI) of freshly prepared chitosan nanoparticles by photon correlation spectroscopy and laser Doppler anemometry, respectively. For particle size and electrophoretic mobility analysis, each sample was diluted to the suitable concentration with ultrapure water and placed in the electrophoretic cell. Each determination was performed at 25 °C and each formulation were determined in triplicate (n = 3).

Determination of nanoparticles process yield

The production yield of nanoparticles was calculated by gravimetry. The fixing volume of nanoparticle suspensions was ultracentrifuged (45,000 rpm, 45min, 4 °C) and sediments of NPs were freeze-dried over 48 h (24 h set at −34 °C and gradual ascent until 20 °C), using a Labconco Freeze Dryer (Labconco, USA) (n=3). Calculate the percentage of process yield (% P.Y.) as following:

$$\text{P.Y. (\%)} = \frac{\text{Nanoparticles weight}}{\text{Total solids (CS + TPP + sCT)weight}} \times 100 \quad \text{.....(1)}$$

Determination of protein association efficiency (A.E.) and protein loading capacity (L.C.) of nanoparticles

The association efficiency indicate to the extent of associated protein in nanoparticles, the total amount of protein in the process was exhibit as the percentage; whereas, loading capacity is describe as the percentage by weight of the associated protein in the practical nanoparticles. To analyze these parameters, nanoparticles were isolated by ultracentrifugation (45,000 rpm, 45min, 4 °C) from the aqueous solution containing of non-associated protein. The free form of sCT amount was detected in the supernatant was determined by reversed phase high performance liquid

chromatography (RP-HPLC) method. The chromatographic condition was applied from Yang et al., 2007. The gradient elution was achieved with 0.1% trifluoroacetic acid in water (A) and 0.1% trifluoroacetic acid (TFA) in acetonitrile (B) and the amount of phase B increased from 25% to 75% over 45 minutes at flow rate 1.0 ml/min. Each sample was determined in triplicate. The association efficiency and NPs loading capacity of protein were calculated as follows:

Association Efficiency; (AE%)

$$\frac{\text{Total sCT amount - Free sCT amount}}{\text{Total sCT amount}} \times 100 \text{……..(2)}$$

Loading Capacity; (LC%)

$$\frac{\text{Total sCT amount - Free sCT amount}}{\text{NPs weight}} \times 100 \text{…..……(3)}$$

HPLC analysis

HPLC chromatographic conditions:

Column	: Inertsil ODS-3, C18, 250 x 4.6 mm, 5 µm
Mobile phase	: 0.1% TFA in water (A)
	: 0.1% TFA in acetonitrile (B)
	: mobile A: mobile B = 75:25
Flow rate	: 1.0 ml/min
Injection volume	: 50 µl
Detector	: UV 220 nm
Retention times	: Salmon calcitonin ~32 min

Validation of the HPLC method

The typical analytical characteristics used in method validation which were specificity, accuracy, precision and linearity (*USP 33/NF 28*, 2010) were shown in Appendix A.

Stability test of nanoparticles

The nanoparticles sample were kept for 3 month at the condition places of 4 °C, 25 °C or 40°C. The particle size and the polydispersity index of the nanoparticles were estimated after 0, 2, 5, 10, 15, 20, 30, 60 and 90 days, while salmon calcitonin was characterized monthly, using HPLC technique as previously reported.

Dry powders containing sCT loaded chitosan nanoparticles preparation

sCT loaded CS-NPs (CS/TPP=3:1) sedimented, accomplished following ultracentrifugation of nanoparticles suspensions, were resuspended in two excipients aqueous medium (mannitol and lactose) and the final suspension of nanoparticles in mannitol and lactose were spray dried. Mannitol and lactose solutions were prepared with such concentrations that provided result excipient/NPs to be attained at ratios of 90/10, 80/20, 70/30 (w/w) and suspensions with a solid content of 1%. Dry powders were collected in a one step process by spray drying either excipient aqueous solutions or nanoparticles suspensions in excipient using a laboratory scale spray dryer [Buchi® Mini Spray Dryer, B-290, Switzerland]. The liquid feed was pumped peristaltically and fed through a two-fluid nozzle (0.5 mm internal diameter) where it was atomized into fine droplets. Cooling water was circulated through the jacket around the nozzle throughout the process. The standard processing parameters comprised an atomizing air volumetric flow rate of 600 Nl/h and an aspirator vacuum of 80 mbar. The liquid feed rate was 5 ml/min. The inlet drying air temperature was varied at 110, 130 and 150°C. Since it was not possible to control the outlet air

temperature, it was thus only investigated. The final product of spray dried powders were collected and stored in a dessicator at room temperature until used.

Determination of spray-drying process yield

The spray-drying production yield (P.Y.) was calculated by gravimetry, comparing the total solids amount with the resultant powder (microspheres) amount collected after spray drying as follows (n = 3):

$$\text{P.Y. (\%)} = \frac{\text{Microspheres weight}}{\text{Total solids (CS + TPP + aerosol excipient) weight}} \times 100 \quad \text{.....(4)}$$

Microspheres morphological characterization

Microspheres were viewed using a scanning electron microscope (SEM, JSM-6610LV, **JEOL Ltd., Tokyo, Japan**). The dry powders were placed onto metal plates and a 200 nm thick gold palladium film was sputter-coated on the samples before viewing.

Particle size determination

Particle size distributions based on volume were determined by laser diffraction (Malvern Mastersizer S, Malvern, UK) using a 100 mm lens at an obscuration between 0.19 and 0.21. Samples of sCT loaded CS-NPs spray dried powder were prepared by suspending the particles in ethanol with the aid of sonication in a water bath for 2 min. Measurements were repeated 5–10 min apart to ensure that no dissolution or agglomeration of the powders obtained. Each sample was determined in triplicate. The size distribution was represented by the volume median diameter (VMD) and span. Span is a measure of the width of the size distribution.

$$\text{Span} = \frac{D(v,90)-D(v,10)}{D(v,50)} \quad \text{……..……..(5)}$$

where D(*v*, 90), D(*v*, 10) and D(*v*, 50) are the equivalent volume diameters at 90, 10 and 50% cumulative volume, respectively.

Determination of powder density

Helium pycnometer (Ultrapycnometer 1000, Quantachrome instruments, Florida, USA) using for determined the true density. Approximately 1 g of each powder sample was used after calibration of the instrument using standard stainless steel spheres supplied by the manufacturer. The mean value of triplicate determinations is reported. Apparent tap density was obtained by measuring the volume of a known weight of powder in a 10 ml measuring cylinder after tapping. After registration of the initial volume, the cylinder was submitted to tapping until constant volume was achieved (n = 3). Bulk and tapped density values allow the determination of Carr's compressibility index and aerodynamic diameter (d_{aer}) of dry powder using the formula:

$$\text{Carr's Index (\%)} = \frac{\rho_t - \rho_b}{\rho_t} \times 100 \quad \text{……..(6)}$$

Where ρ_t is the tapped density and ρ_b is the bulk density.

$$d_{aer} = D_{(v,\,50)} \times \sqrt{\rho_t / \rho_0} \quad \text{……(7)}$$

where $D_{(v, 50)}$ is geometrical particle diameter, ρ_t is the tapped density and ρ_0 is true density (g/cm^3)

Nanoparticles recovery from dry powders in aqueous medium

To recover the nanoparticles from dry powders, 50 mg of the spray-dried powders were incubated in 3ml of PBS pH 7.4 for 90 min, under mild magnetic stirring at room temperature. The nanoparticles morphology and physicochemical properties (size and zeta potential) were analyzed by TEM, photon correlation spectroscopy and laser Doppler anemometry, respectively (n = 3).

Evaluation of nanoparticles stability in the presence of lysozyme

The stability of fresh and recovered nanoparticles of a representative dry powder was analyzed following their incubation in a solution of lysozyme in PBS pH 7.4 (0.2 and 0.8 mg/ml) at 37 °C under mild horizontal shaking for 90 min. At appropriate time intervals (5, 15, 30, 45, 60 and 90 min), the mean particle size was analyzed using the Zetasizer® (n = 3)

Protein integrity

Sodium dodecyl sulfate-polyacrylamide gel electrophoresis (SDS-PAGE)

sCT in spray dried powder was recovered by dissolving microparticles in acetate buffer pH 4.4. One part of the samples was mixed with one part of reducing sample buffer (5% β-mercaptoethanol in Tris-HCl SDS sample buffer, Sigma, Saint Louis, USA) and heated at 100 ^{o}C for one minute. The mixture equivalent to 0.5 µg of sCT was loaded onto a pH 8.8 of 20% Bis-Tris polyacrylamide gel and subjected to electrophoresis (Bio-Rad model Mini-PROTEAN III, Bio-Rad Laboratories, Hercules CA, USA) in Tris-Tricine-SDS running buffer (Sigma, Saint Louis, USA) at 200 V for about 45 mins. The gel was stained with EZBlue™ Gel Staining Reagent (Sigma, Saint Louis, USA) for one hour and destained several times with distilled water until the protein bands were visualized.

Conformational changes assay

Circular dichroism (CD)

The secondary structures of salmon calcitonin in nanoparticles and nanoparticles spray dried powder were analysed by spectropolarimeter (JASCO model J-715, Jasco, Tokyo, Japan) with a quartz cell (0.1 cm of path length). The nanoparticles and nanoparticles spray dried powder were diluted with ultrapure water to obtain about 50 μg/ml of sCT in solution. This study were achieved for pure sCT, sCT loaded CS-NPs and sCT loaded CS-NPs spray dried powder. Data were collected at bandwidth of 1.0 nm, response of 4 s and scanning speed of 100 nm/min. Each measurement was repeated at least three times and the average value was plotted. Molar ellipticity ([θ], deg cm^2 d mol^{-1}) was calculated by the following equation:

$$[\theta] = \frac{\theta \cdot Mp}{10,000 \cdot n \cdot C \cdot l} \quad \text{.....(8)}$$

where Mp is the molecular weight of salmon calcitonin, n is the number of amino acid residues of salmon calcitonin , C is the concentration of salmon calcitonin solution and l is the path length of the cell (0.1cm). Spectra were displayed as the plot of molar ellipticity to wavelength.

Fourier transform infrared (FTIR) spectroscopy

The interactions between the different components of the nanoparticulate and nanoparticulate spray dried powder systems were determined by FTIR. Infrared spectra of the sCTs nanoparticles and sCT loaded CS-NPs powders obtained using a Perkin-Elmer FTIR spectrometer, model Spectrum One. In order to collect the spectra, a small amount of freeze-dried nanoparticles was mixed with KBr (1 wt% nanoparticles) and compressed to form tablets. The IR spectra of these tablets, in absorbance mode, were obtained in the spectral region of 400–4000 cm^{-1} region at room temperature using a resolution of 4 cm^{-1} and 64 co-added scans.

In vitro release studies of sCT from nanoparticles and dry powders

The release of sCT was evaluated by incubating the nanoparticles or the nanoparticle-loaded spray dried powder in 5ml of phosphate buffer pH 7.4 with horizontal shaking at 100 rpm and 37±1°C. At appropriate time intervals (5, 10, 15, 30, 45, 60 and 90 min), individual samples 100 µl were passed through a syringe filter (pore size 0.22 µm, low protein binding, Millipore, USA) and the amount of protein released in the supernatants was evaluated by HPLC (Shimadzu, Kyoto, Japan) at 220 nm (n = 3).

Dry powder aerosolisation evaluation

The aerosolisation properties of the spray-dried powders were initially investigated using an Andersen Cascade Impactor (ACI; Copley Scientific Ltd., Nottingham,UK). All parts of the ACI were washed and provided to dry. The collection plates were consequently immersed in a 1% glycerol in acetone solution and the solvent allowed to evaporate to leave a thin film of glycerol on the surface of the plates to avoid particle bounce. The ACI was then assembled and the flow rate through the impactor adjusted to 60 L/min. At a flow rate of 60 L/min, the effective cut-off diameters of the modified ACI are:

- Stage -1, 8.6 µm
- Stage 0, 6.5 µm
- Stage 1, 4.4 µm
- Stage 2, 3.2 µm
- Stage 3, 1.9 µm
- Stage 4, 1.2 µm
- Stage 5, 0.55 µm
- Stage 6, 0.26 µm

Glass device were loaded and aerosolised as above, with each deposition experiment involving the aerosolisation of five divice (20 mg of sample/device). Each experiment was repeated in triplicate. Each stage of the ACI was rinsed with HPLC mobile phase, and made up to 10 mL final volume. The mass of sCT deposited on each stage of the ACI was determined using HPLC. The fine particle dose (FPD), defined as the mass of drug less than 5 μm, was calculated by interpolation from a plot of cumulative mass vs. effective cut-off diameter of the respective stages. The fine particle fraction (FPF) was calculated as the ratio of FPD to total loaded dose, expressed as a percentage and corrected for actual sCT content in each powder. The mass median aerodynamic diameter (MMAD) of the powders was also derived, defined as the particle size at the 50% mark of a plot of cumulative fraction vs. effective cut-off diameter.

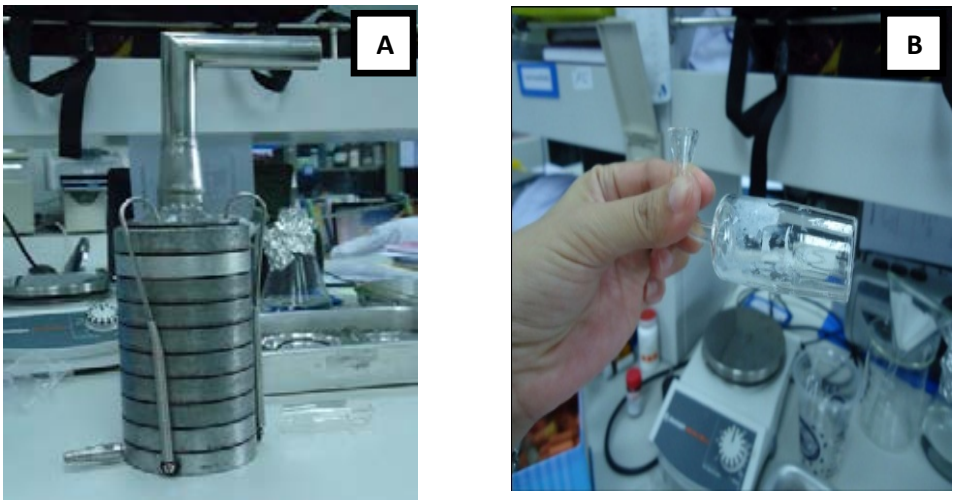

Figure 5. A). Andersen Cascade Impactor (ACI).

B). Glass device.

In vivo absorption of sCT loaded CS-NPs spray dried powder

The animal studies were observed using male Sprague–Dawley (SD) rats weighing 200–250 g (7–8 weeks bred). The SD rats were randomly divided into four groups (six each) and fasted for 24 h prior to the study but allowed free access to water. The rat were anesthetized by intraperitoneal injection of urethane (1.5g/kg), and restrained in a supine position. Anesthetisia was maintained with additional dose of sodium pentobarbital as needed throughout the experiment. The trachea was exposed and a PE-240 polyethylene tubing was inserted through a tracheal incision according to the method of Enna and Schanker, 1972 and Kobayashi et al., 1994. Dry powder of treatments were administered to rat pulmonary using dry powder insufflators (Penn Century Inc). The powder administration was made by insufflations of 3 ml of air contained in the syringe, the insufflators was weighed before and after powder filling and after administration to determine the actual amount of sample emitted and aerosolized into the lung. The PE-10 polyethylene tubing were cannulated to right jugular vein of the rats for blood sampling.

Figure 6. Dry Powder Insufflators.

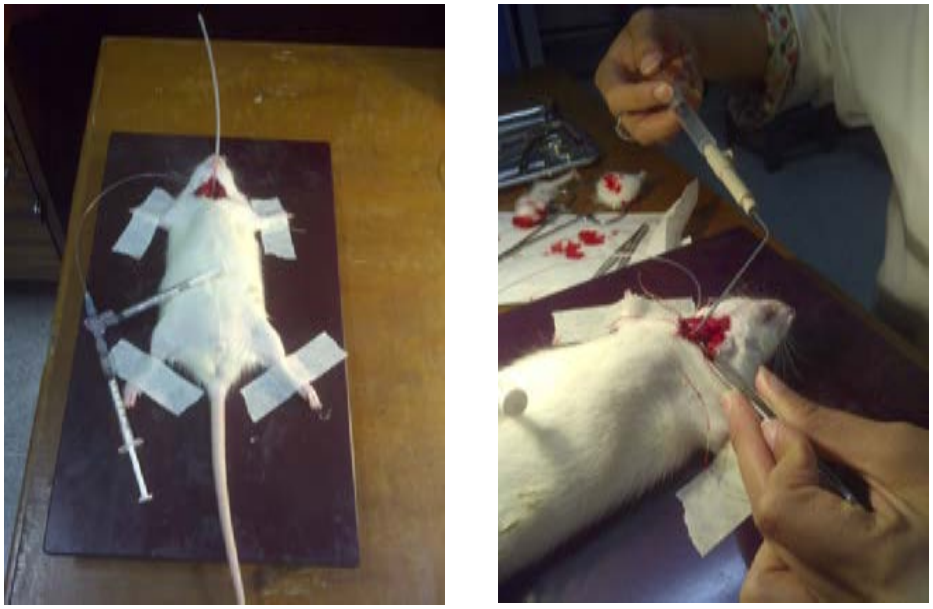

Figure 7. The intratracheal (i.t.) administration of the powder by insufflations.

Rat were randomly divided into groups and were receive 20 IU/kg of different treatments. Group1: rats administered a single intratracheal dose of sCT powder; group2: rats administered a single intratracheal dose of sCT loaded CS-NPs spray dried powder; group3: rats administered a single intratracheal dose of unloaded sCT CS-NPs spray dried powder and group4: rats administered a single dose of intravenous injection. Blood samples 200 µl were collected at predetermined time intervals after the administration and heparin solution (1000 unit/body) was injected from the PE-10 tubing in advance as an anticoagulant. The blood samples were centrifuged at 8,000 rpm for 15 min and kept at−20 °C until analysis. sCT levels were determined using ELISA Kit, and calibrations were made.

Statistical analysis

All experiments and analyses were performed in triplicate and the data were compared by one-way analysis of variance (ANOVA) and Scheffe's method tests all using the SPSS 17 software **(SPSS ID : 5068054)**. A p-value< 0.05 was considered statistically significant in all cases.

CHAPTER IV

RESULTS AND DISCUSSION

The sCT loaded chitosan nanoparticles formed instantaneously when readily mixed sCT-TPP is added to chitosan solutions. As a crosslink and condensing agent, TPP form further hydrogen bonds with free amine groups on both protein and chitosan molecules, resulting in more compact sCT–chitosan nanoparticles. Additional adsorption of protein molecules on the surface of the formed particles may occur in sequence, leading to additional protein loading on the particles. In these investigation, chitosan was dissolved in an aqueous solution of acetic acid to form a chitosan solution. The chitosan solution was stirred at room temperature using a magnetic stirrer. The pH of the resulting solution was around 2.5 and this was adjusted to 4.5 using 20% (w/w) sodium hydroxide solution.

The effect of the mass ratio of chitosan to TPP on the particle size and zeta potential was determined. The optimum TPP concentration was from 0.42 to 0.69 mg/ml, the increasing TPP concentration to 0.8 mg/ml would lead to a flocculent precipitate. The large positive charge density due to the high degree of deacetylation and protonation makes chitosan molecules have a large number of potential cross-linking sites. When TPP concentration was below 0.42 mg/ml, the reaction solution would be a clear solution without visible opalescence, indicating that the TPP concentration was inadequate to lead to the formation of a cross-linked structure of chitosan. As TPP increased from 0.42 to 0.69 mg/ml, the particle size decreased due to increased cross-linking density between chitosan and TPP. As TPP concentration continued to increase, it can be inferred that chitosan molecules were almost fully cross-linked and the excess TPP would lead to more chitosan molecules involved in the formation of a single nanoparticle, resulting in larger particle size. When TPP concentration was below 0.42 mg/ml, the low surface charge density of the particles was no longer able to maintain the stability of these large particles during stirring, resulting in the precipitation of particles.

Physicochemical characterization of sCT loaded chitosan nanoparticles

The morphology of nanoparticles consisting of sCT and chitosan–TPP with a different chitosan concentration (w/v) and CS/TPP ratio (w/w) were investigated by TEM and presented in Fig. 8. It was shown that the nanoparticles had a size range of about 200 nm. Generally nanoparticles had different shapes and the observed size by TEM was smaller than the size determined by Zetasizer®. This is in agreement with a previous study that reported that swelling of chitosan in aqueous medium caused the size of nanoparticles determined by Zetasizer® to increase with respect to TEM analysis which was performed in dry samples (Aktas et al., 2005). TEM yields a number average size while Zetasizer® measures the hydrodynamic diameter which reflects how a particle diffuses within a fluid. The hydrodynamic diameter depends not only on the size of the particle core, but also on its surface structure, as well as the concentration and type of ions in the medium. Therefore, the size determined by a Zetasizer® can be larger than that measured by TEM. Generally nanoparticles had different shapes look round, spherical or oval with relatively smooth surfaces and compact structure. No visual difference was evident among the appearance of the nanoparticles produced by various preparation condition.

Table 1 and 2 show particle size and zeta potential of blank CS/TPP nanoparticle and sCT loaded chitosan nanoparticles. As shown in Table 1, the incorporation of increasing concentraton of chitosan led to a significant decrese in the process yield ($P < 0.05$) from 47 to 25%, the maximum yield being achieved for the 3:1 CS/TPP ratio, which can be explained by the nanoparticles formation mechanism, as previously reported (Fern´andez-Urrusuno et al., 1999). Blank (without associated sCT) nanoparticles displayed a particle size in the range of approximately 155–238 nm and a positive zeta potential from +36.2 to +48.6 mV, with the lowest size and zeta potential also being obtained for the highest TPP concentration (CS/TPP = 3:1) ($P < 0.05$).

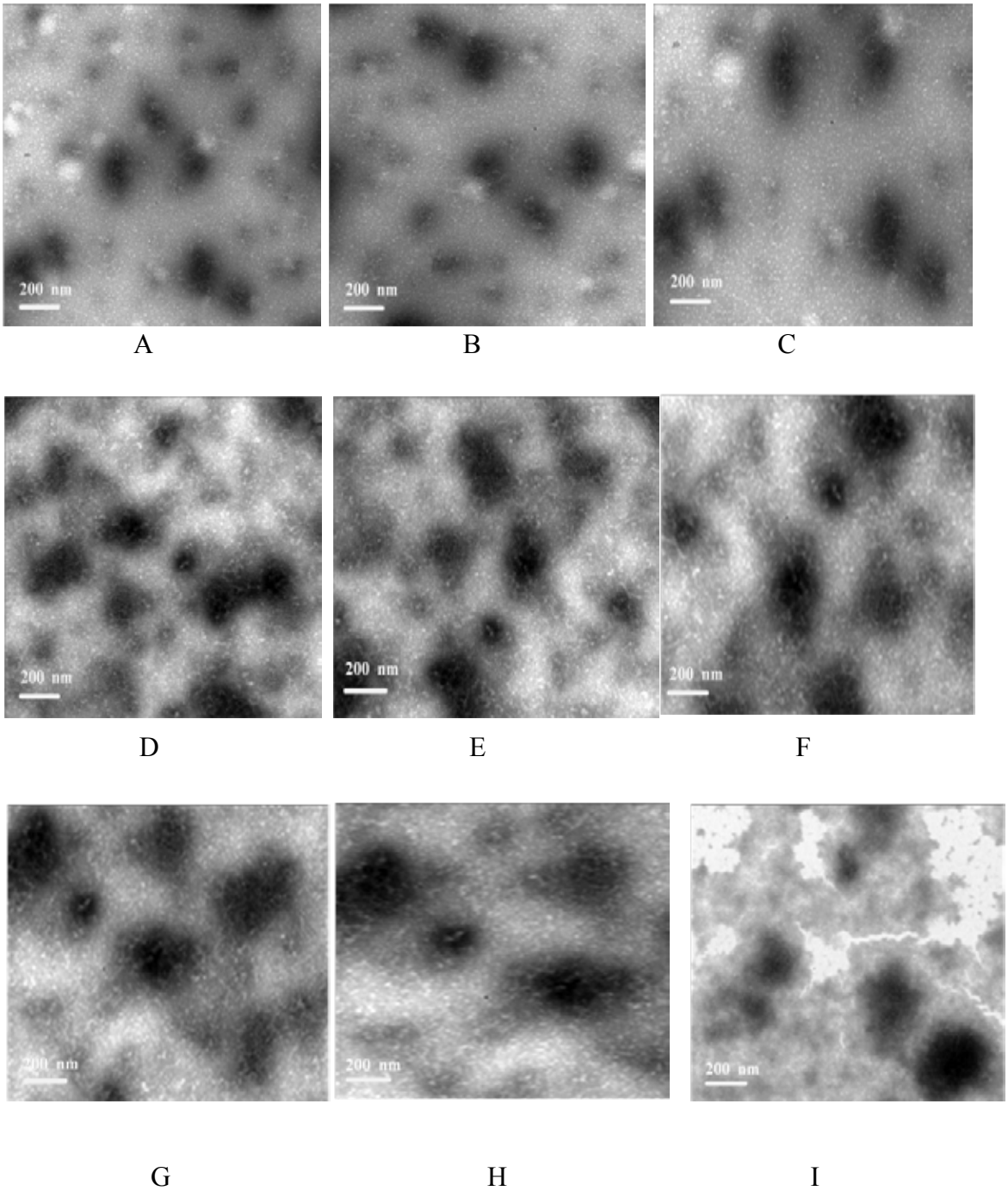

Figure 8. Transmission electron microphotographs of salmon calcitonin loaded CS/TPP nanoparticles: A.) CS/TPP=3:1, B.) CS/TPP=5:1 and C.) CS/TPP=7:1 prepared at 0.1% (w/v) chitosan concentration**;** D.) CS/TPP=3:1, E.) CS/TPP=5:1 and F.) CS/TPP=7:1 prepared at 0.2% (w/v) chitosan concentration**;** G.) CS/TPP=3:1, H.) CS/TPP=5:1 and I.) CS/TPP=7:1 prepared at 0.3% (w/v) chitosan concentration

Zeta potential of the sCT loaded chitosan nanoparticles can greatly influence their physical stability in suspension through electrostatic repulsion between the particles. The effect of sCT loading only slightly decreased zeta potential of the particles. This was unexpected as sCT entrapment in and adsorption on the particle would have significantly reduced the positive surface charge of cationic chitosan molecules. Chitosan molecules may spread conformation in solution because of electrostatic repulsion force existing between amine groups along the molecular chain. The carboxyl groups on the surface of a protein molecule may form hydrogen bond with amine groups at certain sites at the spread chitosan chain, but still maintaining a compact structure without spreading at the solution pH condition (pH 4.5) so as to keep an inner hydrophobic core. Therefore, protein molecule attachment did not sufficiently suppress the positive surface charge of chitosan molecules. There could still be a high proportion of free amine group on the chitosan chain which remains unoccupied.

As displayed in Table 2, the resultant sCT loaded chitosan nanoparticles were in the mean size of 153 to 240 nm and exhibit positive zeta potential from +32.7to +41.2 mV, which is an indicator of nanoparticles surface charge, as well as system stability. The positive charge of the particle surface is crucial for the interaction with the negatively charged mucosa, increasing the residence time of the delivery system at the absorption site. Regarding the nanoparticles formulations made of 0.1% CS solution, those consisting of CS/TPP = 3:1 (w/w), which have higher TPP content, registered increased production yield (50%), sCT association efficiency (63%) and loading capacity (55%) compared to the other ratio (CS/TPP = 5:1 and 7:1 w/w). The zeta potential increased from +32.7 mV to +37.3 mV due to the large positive charge density of protonation makes chitosan molecules have a large number of potential cross-linking sites. On the other hand, the nanoparticles made of 0.2 and 0.3% CS solution showed a lower production yield, association efficiency and loading capacity, but larger size than the nanoparticles made of 0.1% CS solution. The comparison of the blank nanoparticles results (data in Table 1.) and those of sCT loaded nanoparticles reveal that the incorporation of sCT in the nanoparticles led to a significantly higher production yield and to a significant decrease on zeta potential.

Table 1. Process yields and physicochemical properties of blank (without sCT) nanoparticles prepared with different chitosan/tripolyphosphate (CS/TPP) theoretical ratios (mean±S.D., n=3)

Chitosan concentration (%w/v)	CS/TPP (w/w)	Process yield (%)	Size (nm)	Zeta potential (mV)
0.1	3:1	47 ± 4	155 ± 09	+36.2 ± 1.7
	5:1	43 ± 3	168 ± 12	+38.7 ± 2.5
	7:1	38± 5	171 ± 15	+41.6 ± 4.1
0.2	3:1	42 ± 2	162 ± 17	+39.6 ± 1.5
	5:1	39 ± 6	175 ± 21	+41.2 ± 1.9
	7:1	32± 4	187 ± 25	+43.6 ± 5.3
0.3	3:1	36 ± 7	170 ± 10	+42.8 ± 2.3
	5:1	30± 4	186 ± 14	+45.3 ± 2.1
	7:1	25 ±6	238 ± 22	+48.6 ± 4.7

Table 2. Process yields and physicochemical properties of salmon calcitonin loaded chitosan nanoparticles (sCT loaded CS-NPs) prepared with different chitosan/tripolyphosphate (CS/TPP) theoretical ratios (mean±S.D., n=3)

Chitosan concentration (%w/v)	CS/TPP (w/w)	Process yield (%)	Size (nm)	Zeta potential (mV)	Association Efficiency (A.E. %)	Loading Capacity (L.C. %)
0.1	3:1	50 ± 3	153 ± 11	+32.7 ± 2.1	63 ± 5	55 ± 4
	5:1	47 ± 5	165 ± 10	+34.2 ± 1.7	57 ± 7	37 ± 7
	7:1	41± 6	172 ± 14	+37.3 ± 3.6	48± 3	30 ± 5
0.2	3:1	46 ± 4	164 ± 21	+35.3 ± 2.7	57 ± 6	43 ± 3
	5:1	42 ± 7	177 ± 16	+37.5 ± 1.2	52 ± 2	32 ± 9
	7:1	39± 8	185 ± 18	+39.2 ± 3.6	44± 8	26 ± 5
0.3	3:1	40 ± 9	172± 14	+37.2± 1.8	52 ± 5	38 ± 4
	5:1	26± 5	184 ± 20	+40.6 ± 2.3	45 ± 3	32 ± 6
	7:1	22 ±4	240 ± 15	+41.2 ± 3.2	41 ± 4	21 ± 8

Results presented in Fig 9. indicated that the particle size increased with increasing the concentration of either chitosan and CS/TPP ratio. Fig. 10 and 11 show that association efficiency (A.E.) and loading capacity (L.C.) decreased from 63 to 52% and 55 to 38% respectively when the starting chitosan concentration increased from 0.1 to 0.3% w/w at CS/TPP = 3:1. The increase in solution viscosity with higher chitosan concentration could be a major contributor to the decrease. It has been reported (Vandenberg et al., 2001) that high viscosity associated with increased chitosan concentration hinders encapsulation of sCT by deterring sCT molecule movement around chitosan molecular chain. The effects of chitosan to TPP mass ratio on sCT association was studied at the mass ratios of 3, 5 and 7 at fixed chitosan and sCT concentration. It was found that sCT association efficiency and loading capacity decreased from 63 to 48% and 55 to 30% when chitosan to TPP mass ratios increased (prepared with 0.1% CS concentration). This reinforces the suggestion that a lower chitosan to TPP mass ratio favours protein association during the formation of the sCT loaded chitosan nanoparticles. One explanation is that high TPP mass at fix chitosan concentration may cause a rise in solution pH value, with a consequential effect on increased overall negative surface charge carried by the protein molecules, which enhanced electrostatic interactions between chitosan and sCT molecules (Alsarra et al., 2004).

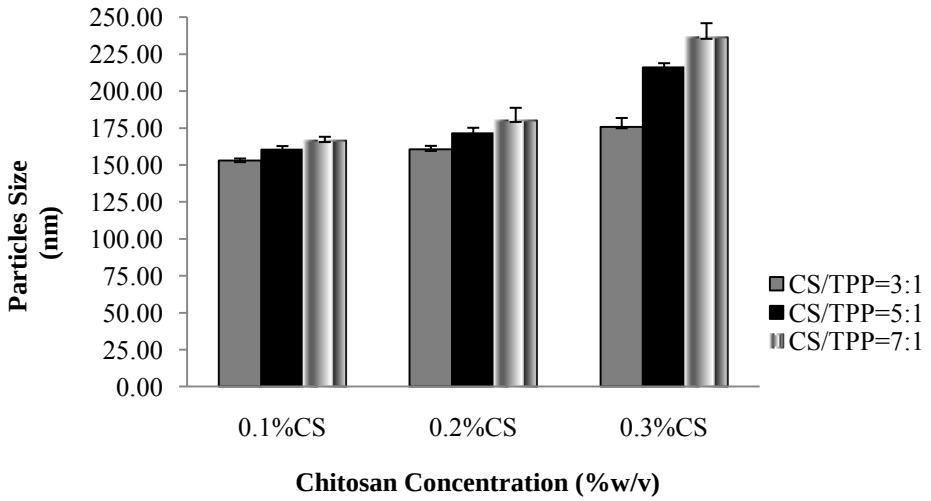

Figure 9. The influence of chitosan concentration and CS/TPP mass ratio on particles size; mean±S.D. (n=3)

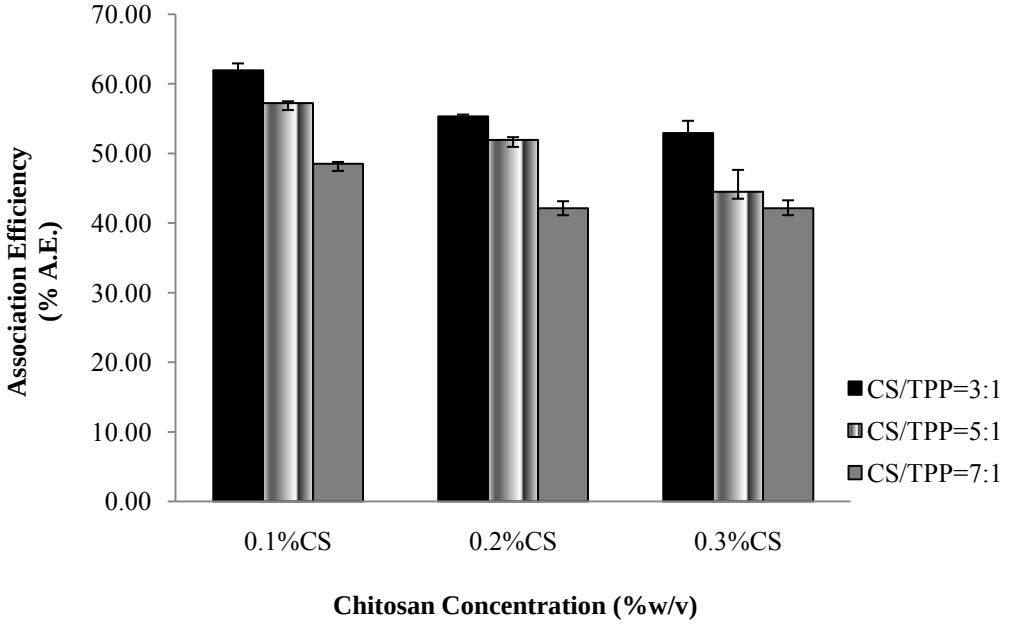

Figure 10. The influence of chitosan concentration and CS/TPP mass ratio on association efficiency (%A.E.); mean±S.D. (n=3)

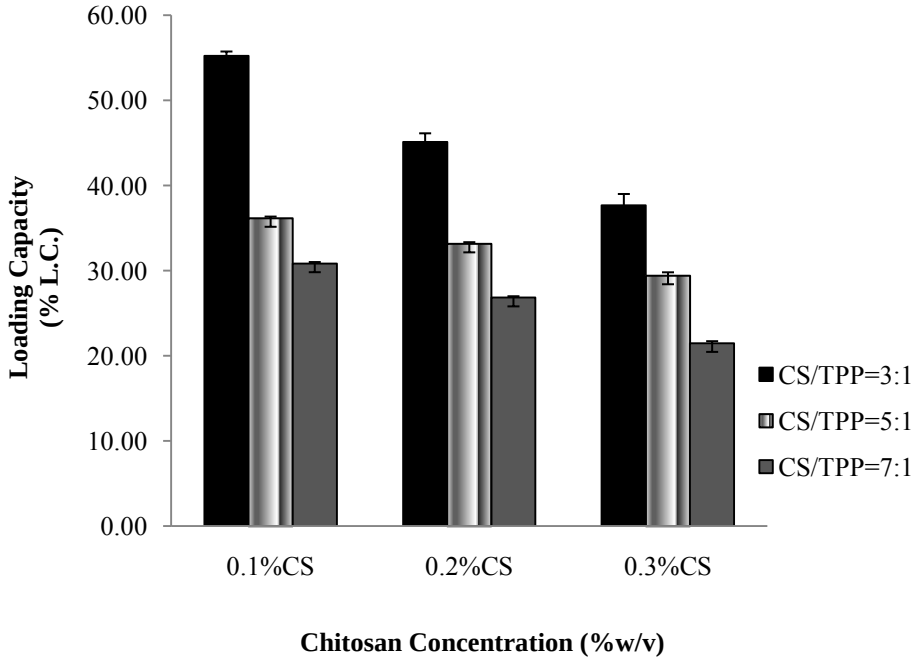

Figure 11. The influence of chitosan concentration and CS/TPP mass ratio on Loading capacity (%L.C.); mean±S.D. (n=3)

The release profile for sCT-loaded CS nanoparticles was observed in PBS pH 7.4, each experiment was done three times. As shown in Figure 12, 13, 14 and 15. In this study observed a burst release, maximum sCT release about 72%, 67% and 56% and reach to plateau within 3 h (Fig. 12, 13 and 14 respectively). The in vitro cumulative release profiles of salmon calcitonin from the CS/TPP nanoparticles with different weight ratios of CS to TPP (from 3:1, 5:1 and 7:1) prepared using 0.1, 0.2 and 0.3% (w/v) chitosan concentration are shown in Fig . 12, 13 and 14. The rapid releasing process was mainly due to the nanoparticles surface drugs could easily diffuse in the initial time. The second phase drug on the nanoparticles surface slowed release ranging from 30 to 90 min, which could be caused by the drugs diffused from the matrix. The third phase was a slower releasing process due to the polymer degradation. The cumulative percentage release of sCT from the compound nanoparticles was about 72% for 3 h. The release rate was higher in the case of formulations containing lower concentration of chitosan, and similarly, drug release was lower for formulations having a lower weight ratio of CS to TPP.

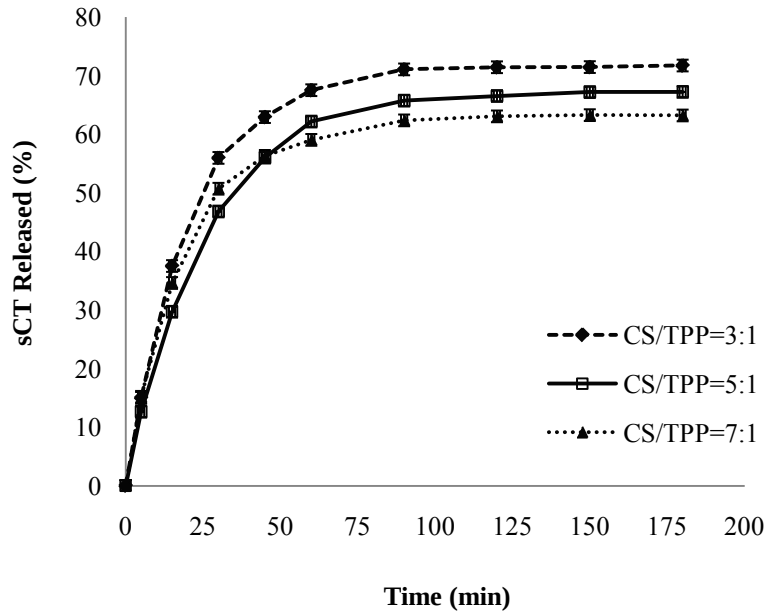

Figure 12. In vitro release of sCT from sCT-loaded CS nanoparticles with different weight ratio of CS to TPP prepared using 0.1% (w/v) chitosan concentration; mean ±S.D. (n = 3).

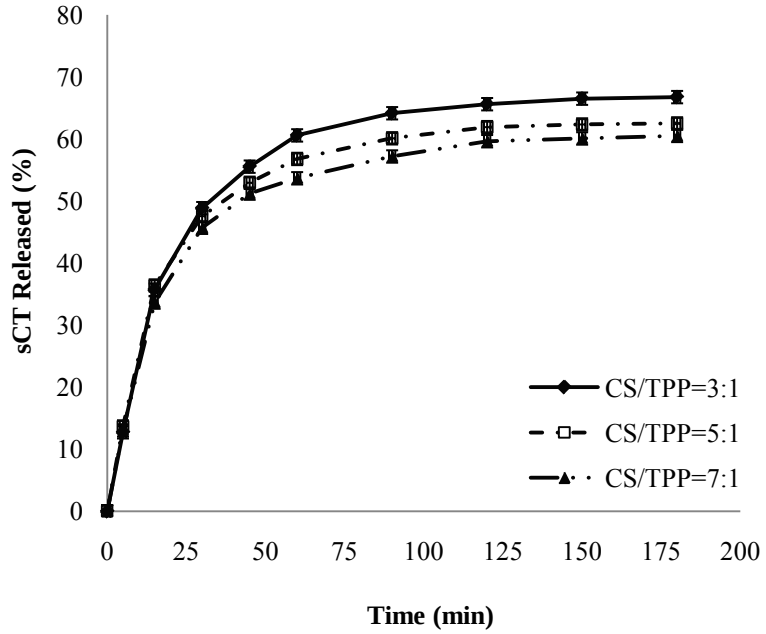

Figure 13. In vitro release of sCT from sCT-loaded CS nanoparticles with different weight ratio of CS to TPP prepared using 0.2% (w/v) chitosan concentration; mean ±S.D. (n = 3).

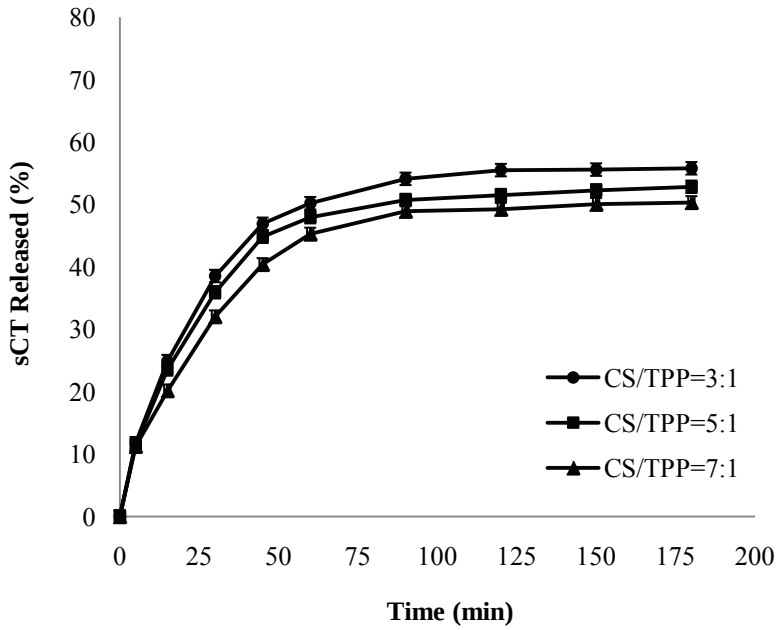

Figure 14. In vitro release of sCT from sCT-loaded CS nanoparticles with different weight ratio of CS to TPP prepared using 0.3% (w/v) chitosan concentration; mean ±S.D. (n = 3).

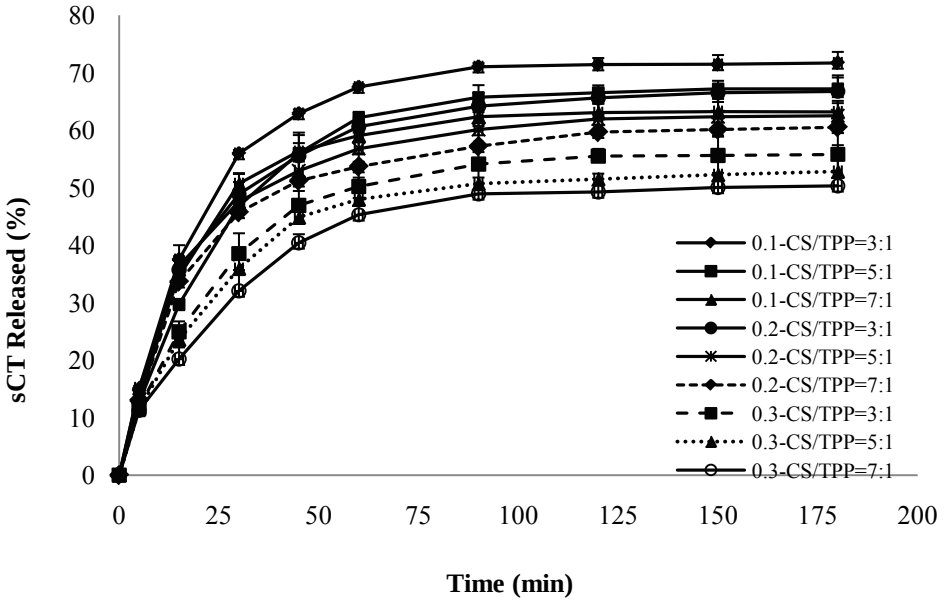

Figure 15. In vitro release of sCT from sCT-loaded CS nanoparticles with different chitosan concentration and weight ratio of CS to TPP; mean ±S.D. (n = 3).

Conformational changes assay

Conformational changes of protein may result in the changes in bioactivity. Thus, a fundamental understanding of the conformational behavior of protein during the process of ionic gelation for nanoparticles preparation. Circular dichroism (CD) and fluorescence spectroscopy were used to evaluate the conformational changes of salmon calcitonin after ionic gelation process in this study.

Circular dichroism

Further evidence of conformational changes of sCT upon the process of nanoparticles preparation was provided by CD spectra. CD is a sensitive technique to monitor the conformational changes in protein. The CD spectra of native sCT and sCT loaded chitosan nanoparticles are shown in Fig. 16. The native sCT showed two extreme valleys at 200 nm, characteristic of the α-helical structure of protein. The reasonable explanation is that the negative peaks is contributed to $n \rightarrow \pi^*$ transition for the peptide bond of α-helix.

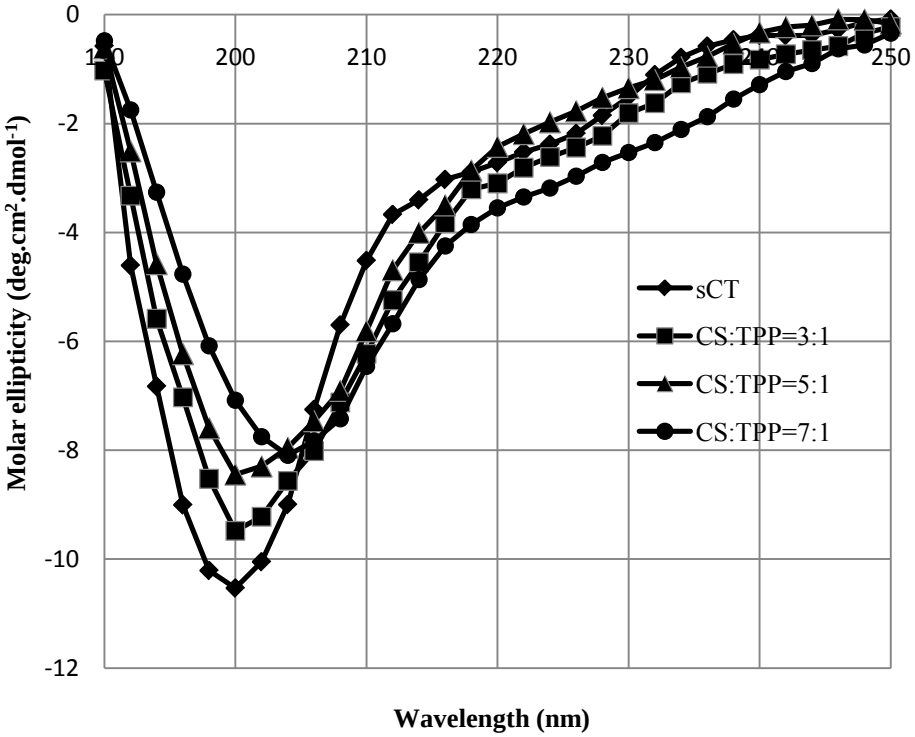

Figure 16. Effect of chitosan (0.1% w/v solution) on the sCT circular dichroism spectra in acetate buffer buffer pH4.4: (♦) native sCT; (■) CS:TPP=3:1; (▲) CS:TPP=5:1 and (●) CS:TPP=7:1.

The sCT loaded chitosan nanoparticles prepared at CS/TPP = 3:1 (w/w) caused only a decrease in band intensity without any significant shift of the peaks, clearly indicating that sCT loaded chitosan nanoparticles occurred a slight decrease in the α-helical structure compare to the native sCT, however, as for the sCT which prepared at CS/TPP = 5:1 and 7:1 (w/w), the bands became less negative and shift to 202 and 205 nm, indicating an decrease in the α-helical content of sCT at the expense of the coil region.

FTIR analysis

The secondary structure were studied by FTIR, it has been extensively used to study structural changes of protein in solid formulations (Dong et al., 1995; Carpenter et al., 1998). Fig. 17 depicts the FT-IR spectra of sCT, CS, TPP and sCT loaded CS nanoparticles. The results demonstrate the basic structural features of CS at 3434.5 cm^{-1} (–OH and $–NH_2$ stretching), 2920.3 cm^{-1} and 2878.6 cm^{-1} (–CH stretching), 1654.4 cm^{-1} ($–NH_2$ stretching; amide I), 1599 cm^{-1} (amide II), 1155.7 cm^{-1} (-PO), 1076 cm^{-1} (C–O–C stretching) and 601 cm^{-1} (pyranoside ring stretching vibration). The structural changes can be monitored conveniently in the amide I, II or III region, where amide I (1600–1700 cm^{-1}) is the most commonly exploited region. As illustrated in Fig. 17, sCT spectra displays two characteristic peaks at 1649.7 cm^{-1} and 1535.6 cm^{-1} assigned to the major α-helix structure were observed, implying that sCT was predominantly constructed by the higher content of helical structure (Souillac et al. 2002). No obvious structural changes of sCT were found when it was nanoparticles form, as compared with the FTIR spectra of native sCT. Only a slightly decrease in α-helical content of sCT was observed in the spectra of sCT-NPs and was reduced with the proportion of chitosan in nanoparticles being increased.

In this study, aggregate signal of protein was observed in the FTIR spectra of sCT-NPs prepared at CS/TPP = 7:1(w/w). The peak at 1649.7 cm^{-1} was gradually shifted to 1498 cm^{-1} due to the combination of α-helix and random coil. The results indicate that the sCT structure was in general, only slightly affected after association with the nanoparticles at CS/TPP = 3:1 and 5:1 (w/w). The α-helix band became wider after encapsulation, but visually it appeared to decrease in peak intensity. Ionic interactions that occur between opposite charges of the protein and the polymers could be responsible for small rearrangements of the protein structure and a simple subtraction of empty nanoparticles spectrum may not be complete because the protein also slightly affects the polymers through ionic interactions. However, the main peaks corresponding to β-sheet and especially α-helix remained almost unchanged, which indicates that the protein secondary structure was not significantly altered.

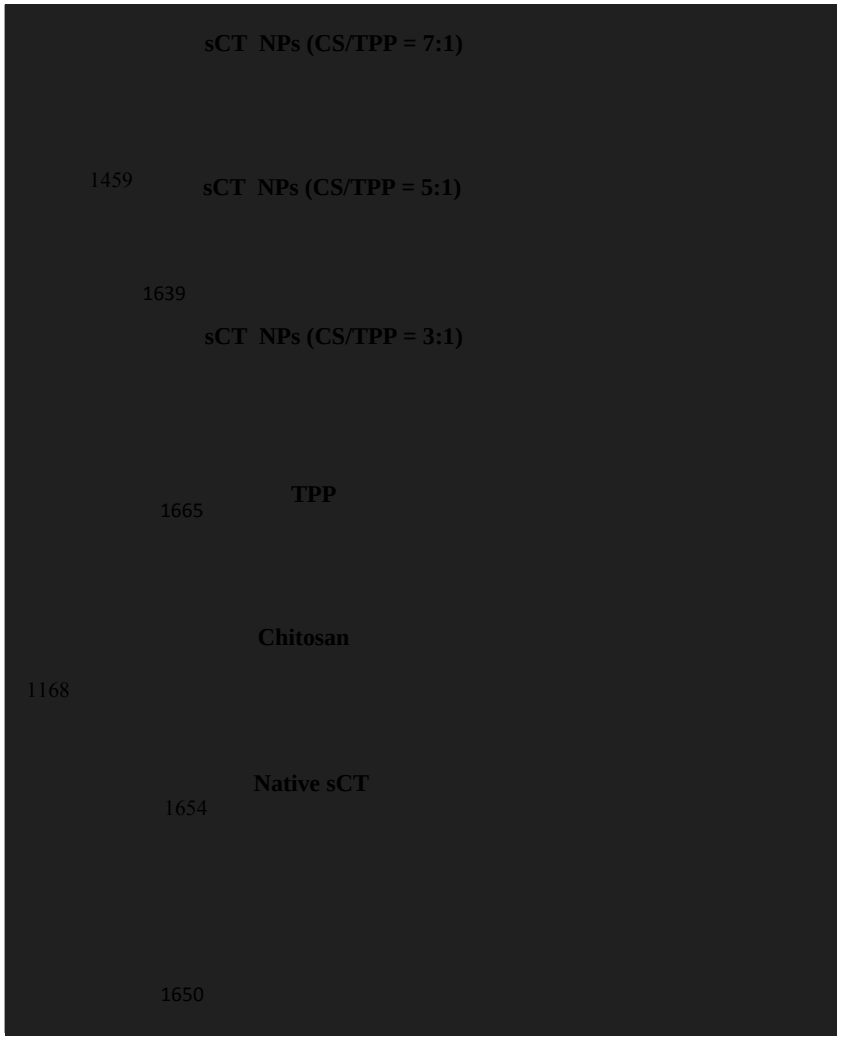

Figure 17. FTIR spectra of sCTs and sCTs-NP at CS:TPP = 3:1(w/w).

Nanoparticle stability study

As shown in Fig. 18, the particle size of nanoparticles displayed a tendency to decrese when the temperature was increased, while when the temperature was 4 °C and 25°C, the particle size was slightly decreased. The decrease in size of the nanoparticles at 40 °C was evident after only 10 day storage. This appears to be due to the decrease in molar mass of the chitosan, possibly due to hydrolysis causing scission of the polymer chains which results in a decrease in nanoparticle size and eventual disintegration (Gordon et al., 2011). In this study may have predicted that prolonged storage (3 months or more) at all the temperatures studied would have resulted in the decrease in size and eventual disappearance of nanoparticles and this is clearly not the case at 4 °C and 25 °C. It might be that the intrinsic viscosity of chitosan solution decreases linearly with increasing temperature.

This is because as temperature increases, the ratio of radius of gyration of chitosan is decreased and the hydrogen-bonded hydration water of chitosan is reduced, resulting in an increase in chitosan chain flexibility and a decrease in specific volume of chitosan molecule, respectively (Chen and Tsaih, 1998). At 4 and 25°C the size of nanoparticles remained similar to those of the freshly prepared samples. The nanoparticle shape has changed during storage and this may have some bearing on the apparent particle diameter. The results propose that chitosan nanoparticle the major cause of instability is the disintegration of the polymeric network (at higher temperatures). CS/TPP nanoparticles are susceptible to instability via the disintegration of the polymeric network through chemical means, resulting in the total breakdown of the nanoparticle when stored for 3 months or more at 40 °C. However size is one of the most important factors in determining the stability of nanoparticles.

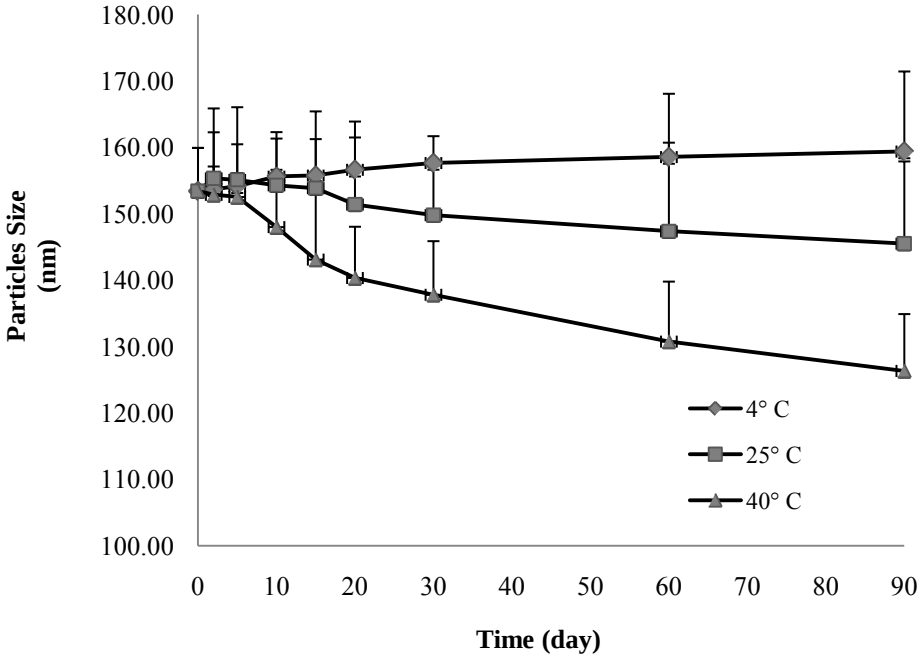

Figure 18. Effect of the temperature on the particle size of sCTs loaded CS-NP at 4 °C, 25°C and 40 °C; values are mean±S.D. (n = 3).

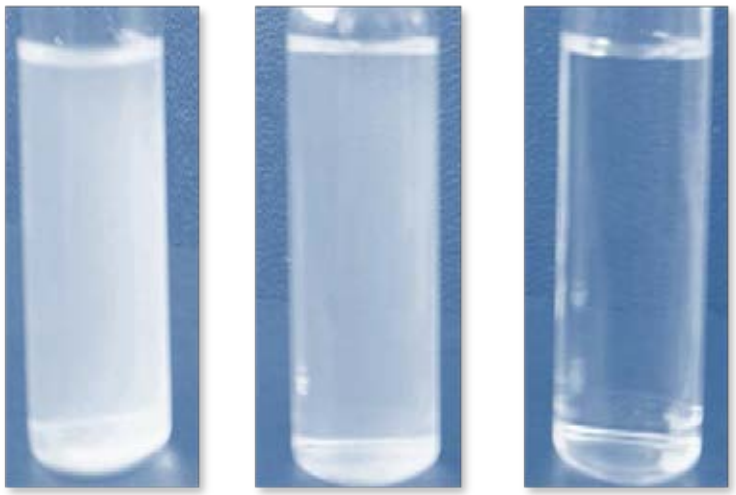

A. B. C.

Figure 19. sCT loaded CS-NPs suspensions prepared with 0.1% chitosan concentration, CS/TPP = 3:1 (w/w) after 3 months storage at: A.) 4 °C B.) 25° C and C.) 40°C.

The residual content of sCT in CS-NPs were examined, Fig. 20 shown that the sCT content changes at each storage temperature when compared with the initial content. For the first 30 days, sCT content of sCT loaded CS-NPs stored at 4 °C and25 °C were maintained up to more than 80% of initial content, whereas those of sCT loaded CS-NPs stored above room temperature (25 °C) decreased to about 60% level. On the other hand, almost all of of sCT loaded CS-NPs stored at 25 and 40°C lost the unique nanostructure after 30 days due probably to denaturation of protein conformation, compared to initial nanoparticles, in this study it was found that the nanoparticles are severely denatured as storage temperature increased. After 60 week storage at 40°C, sCT loaded CS-NPs lost their stability and sCT content decreased to the 40% level of initial fluorescence. Fig. 20 indicates that the storage temperature affected to particles size and content of sCT in CS-NPs. The nanoparticles are susceptible to instability when stored for 3 months and more at 25 and 40°C. The stability could potentially be improved by dry powder systems have many advantages including ease of drug administration, convenient portability, relatively simple formulation, low cost and inherently improved stability (Arakawa et al., 1993; Prime et al., 1997).

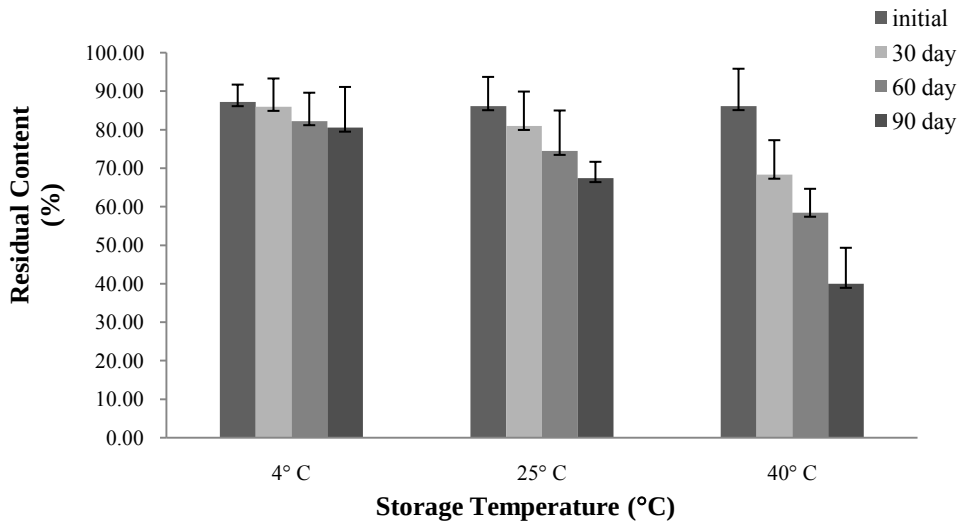

Figure 20. sCT residual content in NPs prepared with 0.1% CS (w/v); CS/TPP = 3:1 (w/w) at difference storage condition; mean±S.D.(n = 3).

Physicochemical properties and morphology of sCT loaded CS-NPs spray dried powder

The spray dried sCT loaded CS-NPs with excipients based formulation were prepared with different aerosol excipient such as lactose and mannitol. In this study the effect of excipients types, NPs/excipients weight ratio (w/w) and spray dry inlet temperature were investigated. The production of nanoparticle loaded microspheres was previously reported (Kawashima et al., 1998; Pohlmann et al., 2002; Tsapis et al., 2002; Sham et al., 2004) using both spray drying and freeze drying techniques, and materials of a different nature. The high temperature used, inherent to all the spray-drying processes, is known not to compromise the stability of the associated protein (Broadhead et al., 1992). Physicochemical characteristics of the resultant dry powder are shown in Fig. 21-23 and Table 3.

It was interesting to find in this study that the type of aerosol excipients, NPs/excipients ratios (w/w) and spray dry inlet temperature profoundly influenced the morphology of sCT loaded CS-NPs spray dried powders. As shown in Fig. 21, Dry powder produced using lactose, although morphologically adequate, were not feasible for this study. Due to their high hygroscopic properties, after recovering, the lactose powder it became sticky and handling was not easy especially for the spray dried powder produced from the NPs/lactose at ratio 10/90 (w/w). The addition of lactose (Fig. 22) resulted in smooth surface but oval and irregular shape, unlike lactose, the particles obtained from mannitol did not appear to be smooth, instead a pitted appearance and little aggregated with adequate morphology (Fig. 22). The differences in morphology between lactose and mannitol based formulations could be partially caused by the drying process. As can be seen the particle morphology was dependent on the formulation composition and spray dry inlet temperature. The particles formed were diverse in shape and size, with small primary particles (mostly <10 μm) that were agglomerated in bigger clusters (up to >10 μm). Anyhow, no differences were found between the particles made at different NPs/excipients (lactose and mannitol) ratios and spray dry inlet temperature. The SEM images suggest that the powders formed are amorphous in nature, as there were no obvious crystalline particles visible;

this was as expected, as powders generated through spray-drying solution formulations are known to be predominately amorphous in nature.

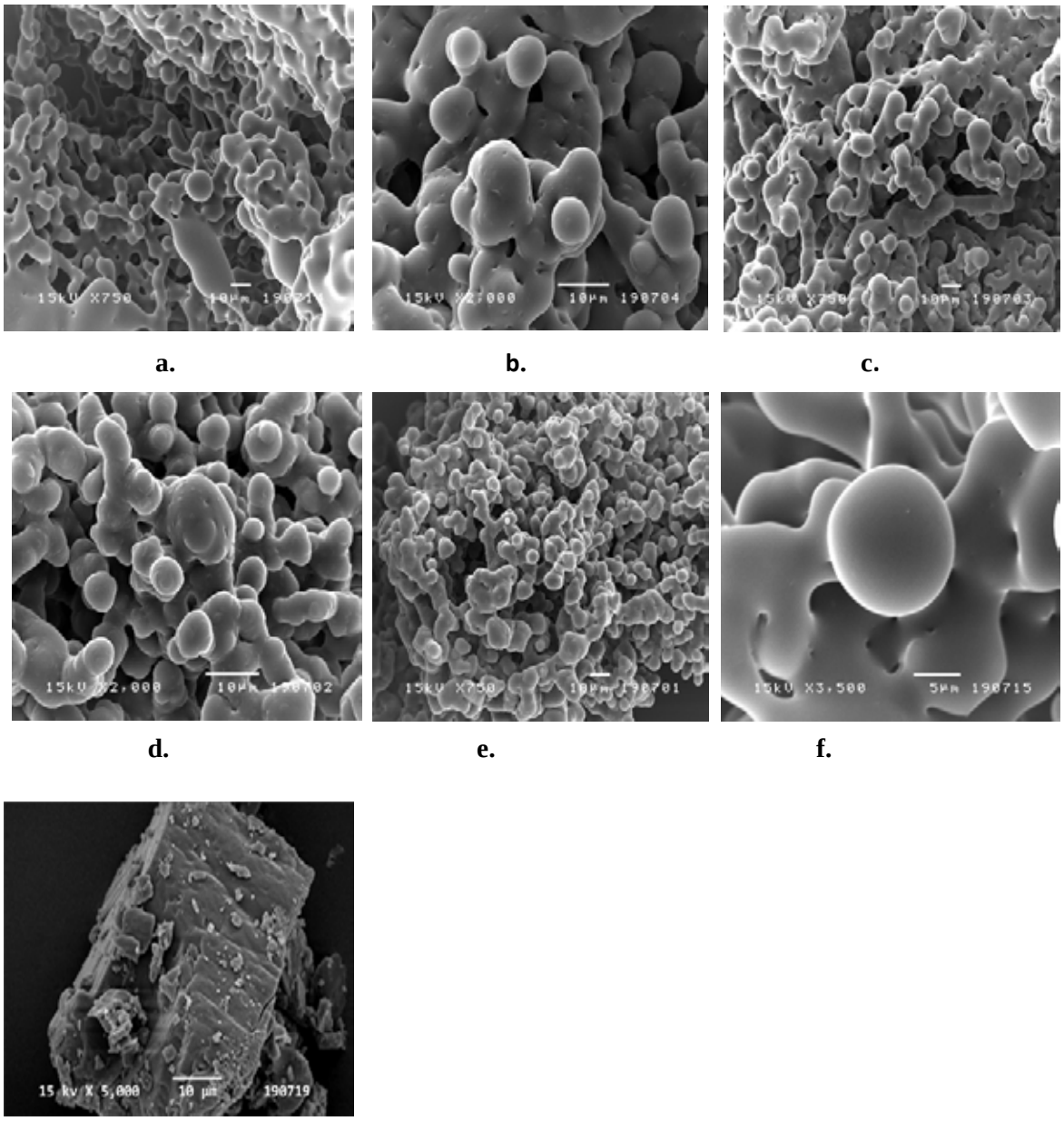

Figure 21. Scanning electron micrographs of sCT loaded CS-NPs spray dried powders**;** (a). NPs/L=10/90, (b). NPs/L=20/80, (c). NPs/L=30/70 at 130°c ; (d). NPs/L=10/90, (e). NPs/L=20/80, (f). NPs/L=30/70 at 150°c and (g). Lactose monohydrate powder

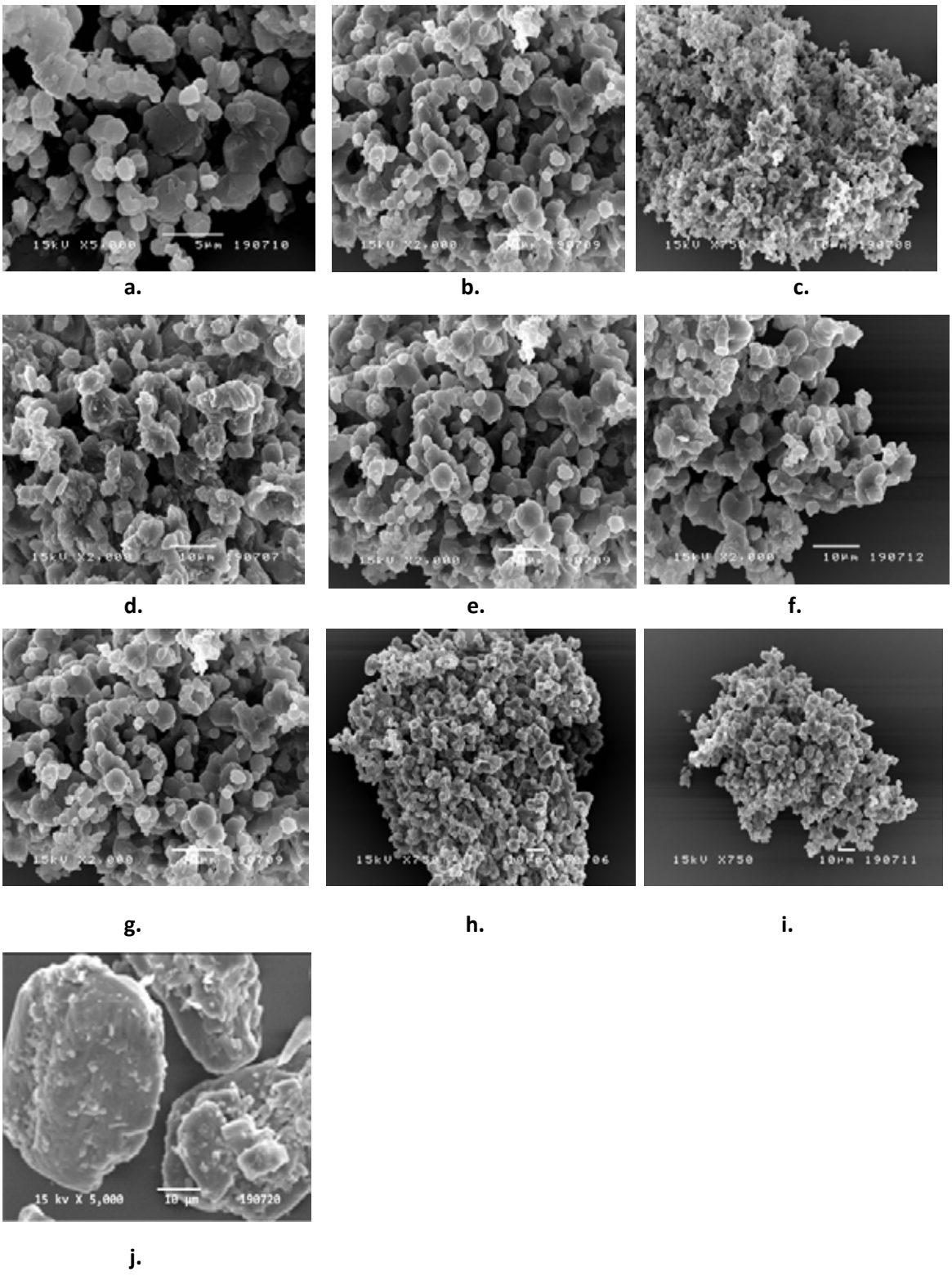

Figure 22. Scanning electron micrographs of sCT loaded CS-NPs spray dried powders**;** (a). NPs/M=10/90, (b). NPs/M=20/80, (c). NPs/M=30/70 at 110°c; (d). NPs/M=10/90, (e). NPs/M=20/80, (f). NPs/M=30/70 at 130°c; (g). NPs/M=10/90, (h). NPs/M=20/80 (i). NPs/M=30/70 at 150°c and (j). D-Mannitol powder

A total of spray-dried powders were investigated. The addition of the excipients caused considerable variation in the yield of dry powder between 25 to 68% as shown in Table 3. The formulations with using lactose as aerosol excipient showed an increase in powder yield when the weight ratio of NPs/lactose increased whereas the powder produced with mannitol as the excipient obtained higher process yield than lactose and the increasing of NPs/mannitol ratios, resulting in decrease of spray dried powder process yield. It was suggested that low spray dried powder yields are indicative of cohesive powders that demonstrate poor aerosolisation properties, and that the addition of formulation excipients may change the physicochemical characteristics of the resultant spray dried powders, resulting in an improved spray drying yield and potentially enhanced aerosolisation properties. Alternatively, low spray drying yields may be a reflection of highly adhesive particles resulting in adhesion of the powder to the walls of the spray drier. Laser diffraction data are presented in Fig. 23 and Table 3., the mean particle size of the resultant spray-dried powders was considerably less than 5 μm; excluding the spray-dried powders prepared with lactose, the average size was 7-18 μm, indicating that the powders were not suitable size for delivered to pulmonary. The higher temperature used, can improved the process yield and made the smaller size of spray-dried powders.

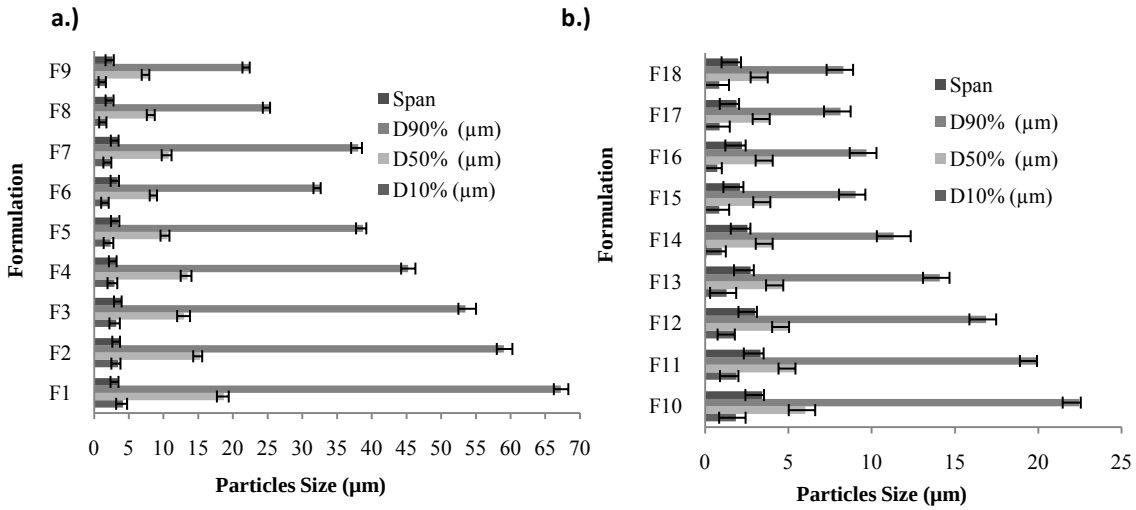

Figure 23. Particle size distributions of sCT loaded CS-NPs spray dried powder with (a.) lactose and (b.) mannitol based formulation prepared with different NPs/excipient ratios (w/w) and spray dry intet temperatures (mean±S.D., n=3).

Table 3. Effects of formulation and process parameters on particle size and yield percentage of sCT loaded CS-NPs spray dried powder (values are the mean±S.D., n = 3).

Formulation	Aerosol Excipient	NPs/Excipient (w/w)	Inlet temperature (°C)	Process Yield (%)	Particles Size ; $D_{(v, 50)}$ (μm)
F1	Lactose	10/90	110	25	18.71±2.61
F2	Lactose	20/80	110	28	15.29±1.92
F3	Lactose	30/70	110	27	12.97±1.31
F4	Lactose	10/90	130	32	13.48 ±1.74
F5	Lactose	20/80	130	35	10.58 ±2.02
F6	Lactose	30/70	130	38	9.02±1.82
F7	Lactose	10/90	150	37	10.75±1.04
F8	Lactose	20/80	150	41	8.63±2.63
F9	Lactose	30/70	150	43	7.87±1.28
F10	Mannitol	10/90	110	46	5.70±1.53
F11	Mannitol	20/80	110	41	5.42±2.34
F12	Mannitol	30/70	110	38	5.01±1.54
F13	Mannitol	10/90	130	57	4.67±2.12
F14	Mannitol	20/80	130	48	4.03±1.34
F15	Mannitol	30/70	130	42	3.89±1.48
F16	Mannitol	10/90	150	68	4.04 ±1.47
F17	Mannitol	20/80	150	57	3.86 ±2.05
F18	Mannitol	30/70	150	51	3.74±1.21

The particle size of a powder formulation intended for inhalation is together with the particle density, a prominent factor in the success of the formulation because it strongly influences the dispersion and sedimentation properties of the powder (Taylor andKellaway, 2001; Courrier et al., 2002). As previously mentioned, the aerodynamic diameter of particles for optimal lung administration should be of approximately 1–5µm (Bosquillon et al., 2001a). The physical and aerodynamic properties of the produced powders are depicted in Table 4. True densities were approximately 1.5 g/cm^3 and tap densities were low, ranging from 0.15 to 0.36 g/cm^3, which render aerodynamic diameters of 2.5–4.7 µm. Therefore, all the dry powders prepared with mannitol were theoretically suitable for administration to the deep lungs. The tendency was that the aerodynamic diameter increased with growing concentrations of mannitol, as has been clearly observed for all mannitol based formulations (Table 4) ($P < 0.05$). With respect to true densities, no statistically significant differences were found among the different powders containing nanoparticles, in contrast to what it was observed for the tapped densities ($P < 0.05$).

Table 4. Physical and aerodynamic properties of dry powders prepared with different nanoparticles/mannitol (NPs/M) ratios (mean±S.D.,*n*=3)

Formulation	True density (g/cm^3)	Tapped density (g/cm^3)	Carr's Index (%)	Aerodynamic diameter (µm)
F10	1.45±0.02	0.36±0.05	27.88±0.12	4.70±0.07
F11	1.46±0.04	0.32±0.02	25.71±0.08	4.12±0.04
F12	1.48±0.03	0.28±0.06	20.56±0.10	3.81±0.10
F13	1.49±0.06	0.35±0.03	24.85±0.06	4.37±0.09
F14	1.55±0.05	0.28±0.01	23.35±0.08	3.83±0.13
F15	1.59±0.03	0.25±0.04	19.58±0.13	2.89±0.06
F16	1.57±0.07	0.30±0.05	22.67±0.11	4.04±0.03
F17	1.59±0.02	0.23±0.07	20.57±0.07	3.76±0.11
F18	1.58±0.01	0.15±0.02	18.15±0.02	2.51±0.07

The tapped density of the spray dried powders was relatively low for all powders, and ranged between 0.15 g cm^{-3} and 0.36 g cm^{-3} (Table 4). These results had been suggested that lower powder tapped density is associated with better aerosolisation properties (Bosquillon et al., 2004). The Carr's Index value gives an indication of powder flow properties; a value less than 25% indicates a fluid flowing powder, whereas a value greater than 25% indicates cohesive powder characteristics that show the poor flowability (De Villiers, 2005). The Carr's Index values varied considerably in the spray dried powders, ranging from 18.1% to 27.8% that prepared with NPs/M=30/70 (w/w) at inlet temperature 150°C and NPs/M=10/90 (w/w) at inlet temperature 110°C, respectively. The addition of high concentration of mannitol appeared to produce powders with poor flowability, which had high Carr's Index of 27.8% in F10 indicating a cohesive powder with the worst flowability and F18 exhibited the best flow properties at 18.1% (Table 4). Physical characterisation of the spray-dried powders therefore demonstrated that each powder was appropriate dimensions for pulmonary administration. Despite these similarities, however, there was considerable variation in the flowability of the powders, as evidenced by the Carr's Index values.

Nanoparticles recovery from dry powders in aqueous medium

The fresh nanoparticles prepared with the ratio of CS/TPP at 3:1 (w/w) in 0.1%(w/v) CS solution and spray dried powder prepared with NPs/M=30/70 (w/w) at inlet temperature 150°C following incubation in PBS pH 7.4 were examined. It was observed that after incubating the powders in the aqueous medium under low stirring rate, mannitol was dissolved, resulting in a nanoparticle suspension. The TEM microphotographs as displayed in Fig. 24, the recovered nanoparticles present an aspect similar to that found in freshly prepared formulations. The slight enlargement and little change in spray dried powder prepared with NPs/M=10/90 (w/w) was form but still in the nanosize range. Fig. 24 and Table 5, represent the nanoparticles size and zeta potential after recovering with respect to fresh nanoparticles. The mean particle size before spray drying was about 400 nm and slightly increased after

nanoparticles recovering in the case of spray dried powder prepared with NPs/M=10/90 (w/w), in spite of the little change in zeta potential presented in some formulation. The increasing of particles size after spray drying was found in powders prepared with lactose and gelatin nanoparticles and was attributed to eventual changes in conformation due to the thermal conditions of the spray dry process (Sham et al., 2004). The results in this study could assume that when spray dried powder delivered to the lung, the particles are expected to be dissolved by the lung fluid and released the nanoparticles. The aerosol excipients are immediately dissolved in lung medium, and in vivo absorption of sCT loaded CS-NPs spray dried powder was investigated.

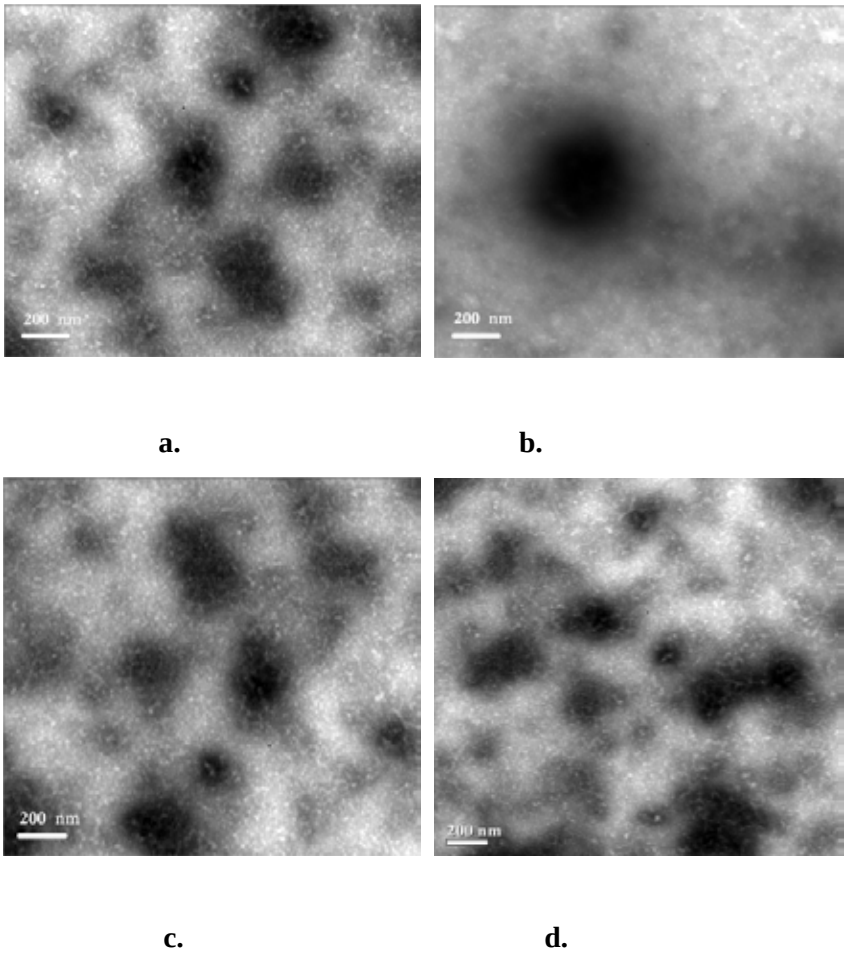

Figure 24. TEM microphotographs of: (a.) freshly prepared, (b.) recovered nanoparticles(NPs/M=10/90), (c.) recovered nanoparticles (NPs/M=20/80) and (d.) recovered nanoparticles (NPs/M=30/70); prepared at intet temperature 150°C.

Table 5. Nanoparticles size and zeta potential variations after recovering from spray dried powder prepared with different NPs/M theoretical ratios (mean±S.D., *n*=3).

NPs/Mannitol Ratio (w/w)	Size (nm)	Zeta potential (mV)
Fresh NPs	210±0.12	+24±0.08
NPs/M=10/90	398±0.09	+35±0.13
NPs/M=20/80	218±0.10	+31±0.11
NPs/M=30/70	215±0.15	+28±0.16

Evaluation of nanoparticles stability in the presence of lysozyme

The dry powder formulation containing NPs/M at ratio 30/70 (w/w) was chosen to study, the stability of the nanoparticles in lysozyme was investigated. The lysozyme concentration of 0.2 and 0.8 mg/ml were used (Konstan et al., 1981 and Grenha et al., 2005). Lysozyme was dissolved in PBS pH 7.4, which is close both to the lung pH and the optimal pH for lysozyme enzymatic activity (pH 6.4) (Calvo et al., 1997). The results in Fig. 25 showed that, fresh and recovered nanoparticles were affected by the lysozyme solution. The size decreasing with increasing the incubation time and the concentration of lysozyme, these results were expectable, considering the previous knowledge that lysozyme can attack CS, hydrolyzing the glycoside bonds between the acetylglucosamine units (Muzzarelli, 1997).

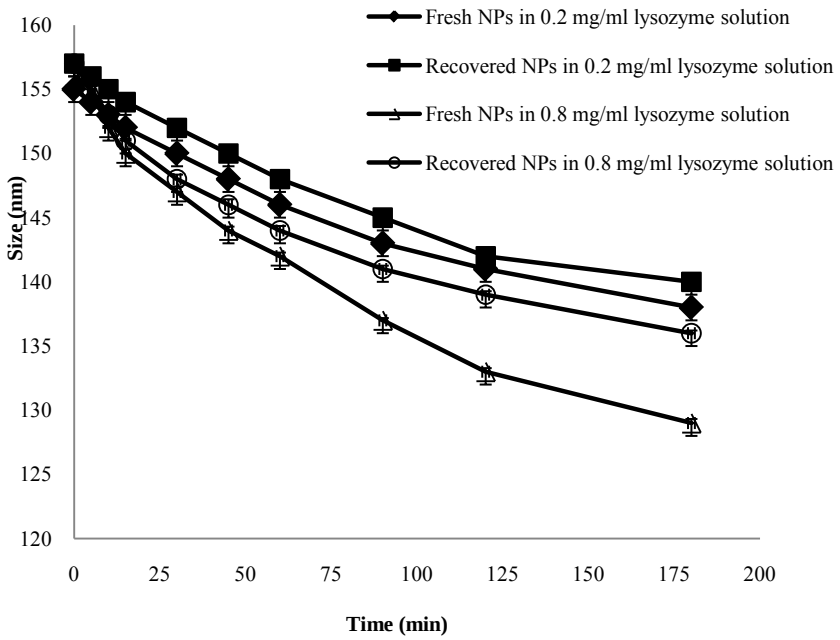

Figure 25. Effect of lysozme on the particles size of nanoparticles (CS/TPP=3:1) and recovered NPs from spray dried powder prepared with NPs/M=30/70 (w/w) (mean±S.D., n = 3).

Conformational changes assay by circular dichroism (CD)

In order to understand the structural changes of sCT during spray drying process, the CD analysis was performed in the "far-UV" region (190–240 nm) (Fig. 26-28). The sCT is composed of α-helix and random coil structure without β-sheet structure. The spectra depicted , when sCT loaded CS-NPs with mannitol based formulation were spray dried, the molar ellipticity was decreased in comparison to that of the bulk sCT. The addition of mannitol showed various effects on α-helix, depending on their composition. This observation indicated a clear decrease in molar ellipticity at 198 nm in all NPs/M ratios of mannitol based formulation. The important role of CS-NPs and mannitol on the conformational stability of spray dried sCT. Also, a slightly shift was observed with the content of CS-NPs increased. These results suggested that a change in secondary structure of sCT occurred depend on CS-NPs and mannitol ratios. The addition of mannitol decreased the protective effect of these

carrier on the structural integrity of sCT upon the process stresses. The CD spectra of the samples revealed the detrimental effect of CS-NPs to mannitol ratios and spray dried inlet temperature on control of α-helix content. The comparison of these spectra indicated that the optimal ratio of NPs/M (w/w) could preserve the α-helix content of sCT. As shown in Fig. 26-28, the presence of NPs/M at 30/70 (w/w) ratio with respect to sCT in the initial feed exhibited higher molar ellipticity, compared to the other ratios. The results in this study obtained the effect of NPs/M ratio and spray dry inlet temperatures on sCT dry powder stability, when the NPs content was decreased and the inlet temperature was increased the spectra show low molar ellipticity.

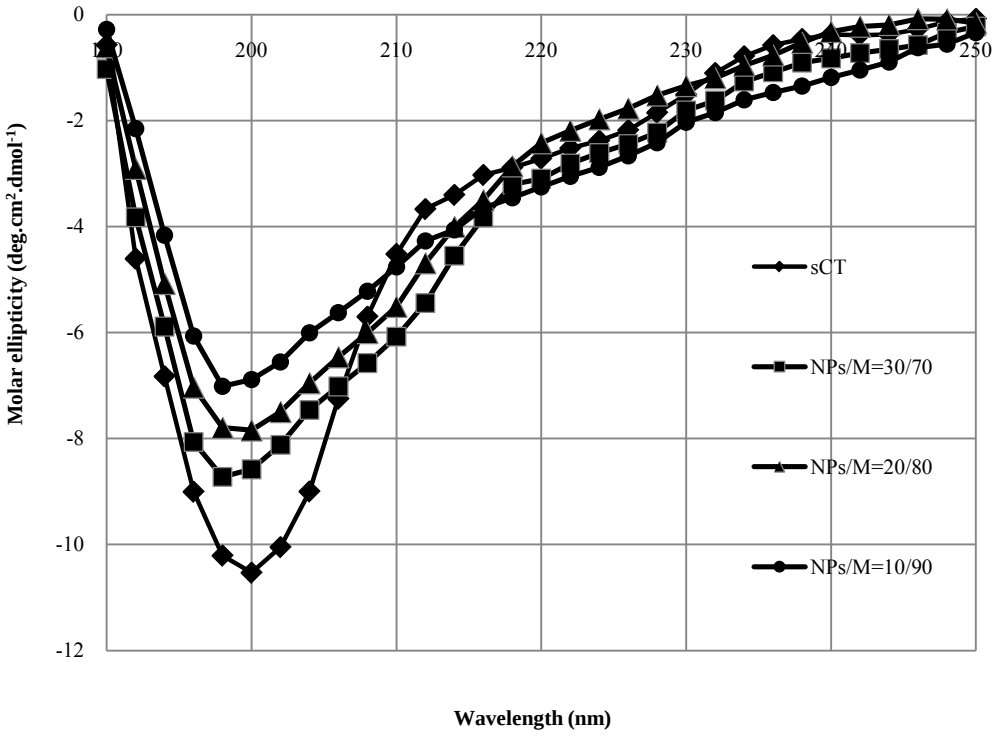

Figure 26. Effect of NPs/Mannitol ratios (NPs/M) on the sCT circular dichroism spectra in acetate buffer buffer pH4.4: (♦) native sCT; (■) NPs/M=30/70; (▲) NPs/M =20:80 and (●) NPs/M =10:90, prepared by spray drying at inlet temperature 110°C

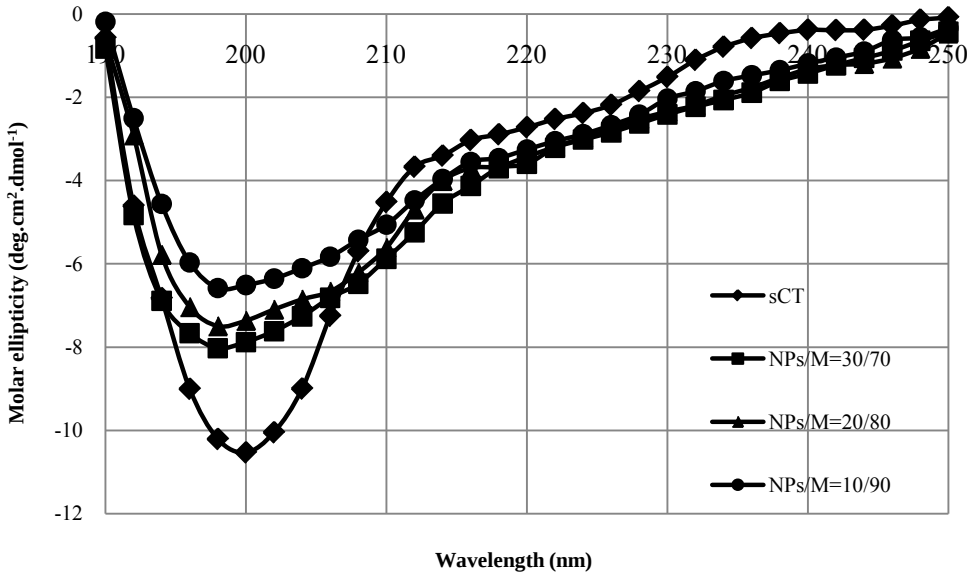

Figure 27. Effect of NPs/Mannitol ratios (NPs/M) on the sCT circular dichroism spectra in acetate buffer buffer pH4.4: (♦) native sCT; (■) NPs/M=30/70; (▲) NPs/M =20:80 and (●) NPs/M =10:90, prepared by spray drying at inlet temperature 130°C**.**

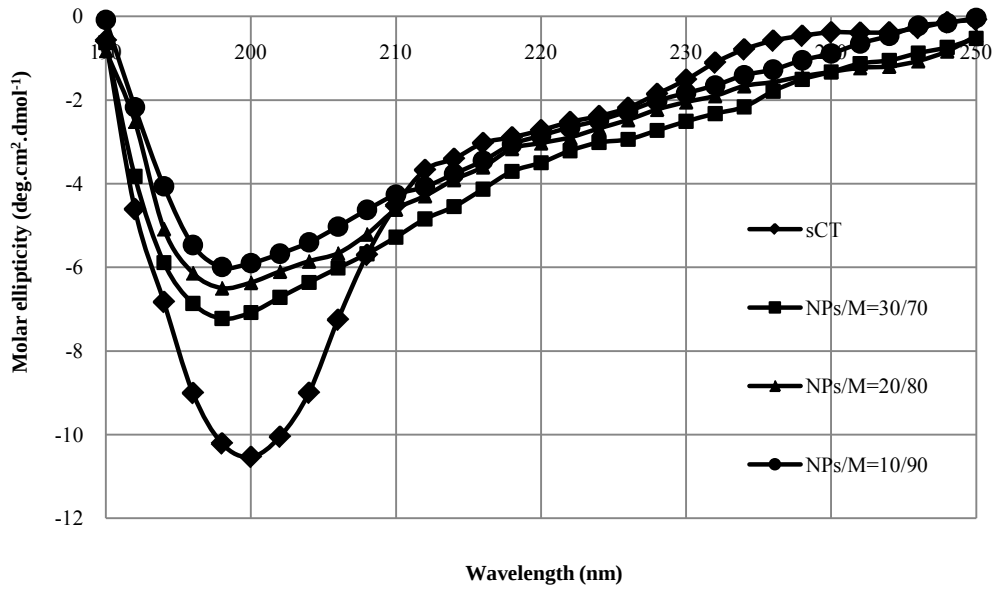

Figure 28. Effect of NPs/Mannitol ratios (NPs/M) on the sCT circular dichroism spectra in acetate buffer buffer pH4.4: (♦) native sCT; (■) NPs/M=30/70; (▲) NPs/M =20:80 and (●) NPs/M =10:90, prepared by spray drying at inlet temperature 150°C.

Conformational changes assay by Fourier transform infrared (FTIR) spectroscopy

The secondary structure of sCT in spray dried powders was studied by FTIR. FTIR has been extensively used to study structural changes of protein in solid formulation (Dong et al., 1995; Carpenter et al., 1998). The structural changes can be monitored conveniently in the amide I, II or III region, where amide I at 1600-1700 cm^{-1} is the most commonly exploited region. Fig. 29 shows the FTIR spectra of native sCT, mannitol and the sCTs loaded CS-NPs with excipient based dry powder. The FTIR spectrum of free sCT (Fig. 29a.) shows sharp distinguishing peak caused by stretching vibration of hydroxyl group (–OH) and protonated amine ($–NH_3^+$) around 3000–3500 cm^{-1} and 1540 cm^{-1}, respectively. Moreover, a strong absorption band caused by stretching vibration of amine groups ($–NH_2$) was found at 1650 cm^{-1}.

As illustrated in Fig. 29, displayed the structural changes of sCT were found as compared with the FTIR spectra of native sCT. The secondary structure of sCT in spray dried powders was studied by FTIR. FTIR has been extensively used to study structural changes of protein in solid formulation (Dong et al., 1995; Carpenter et al., 1998). The structural changes can be monitored conveniently in the amide I, II or III region, where amide I at 1600-1700 cm^{-1} is the most commonly exploited region. Fig. 29 shows the FTIR spectra of native sCT, mannitol and the sCTs loaded CS-NPs with excipient based dry powder. The FTIR spectrum of free sCT (Fig. 29a.) shows sharp distinguishing peak caused by stretching vibration of hydroxyl group (–OH) and protonated amine ($–NH_3^+$) around 3000–3500 cm^{-1} and 1540 cm^{-1}, respectively. Moreover, a strong absorption band caused by stretching vibration of amine groups ($–NH_2$) was found at 1650 cm^{-1}. As illustrated in Fig. 29, the structural changes of sCT were found as compared with the FTIR spectra of native sCT.

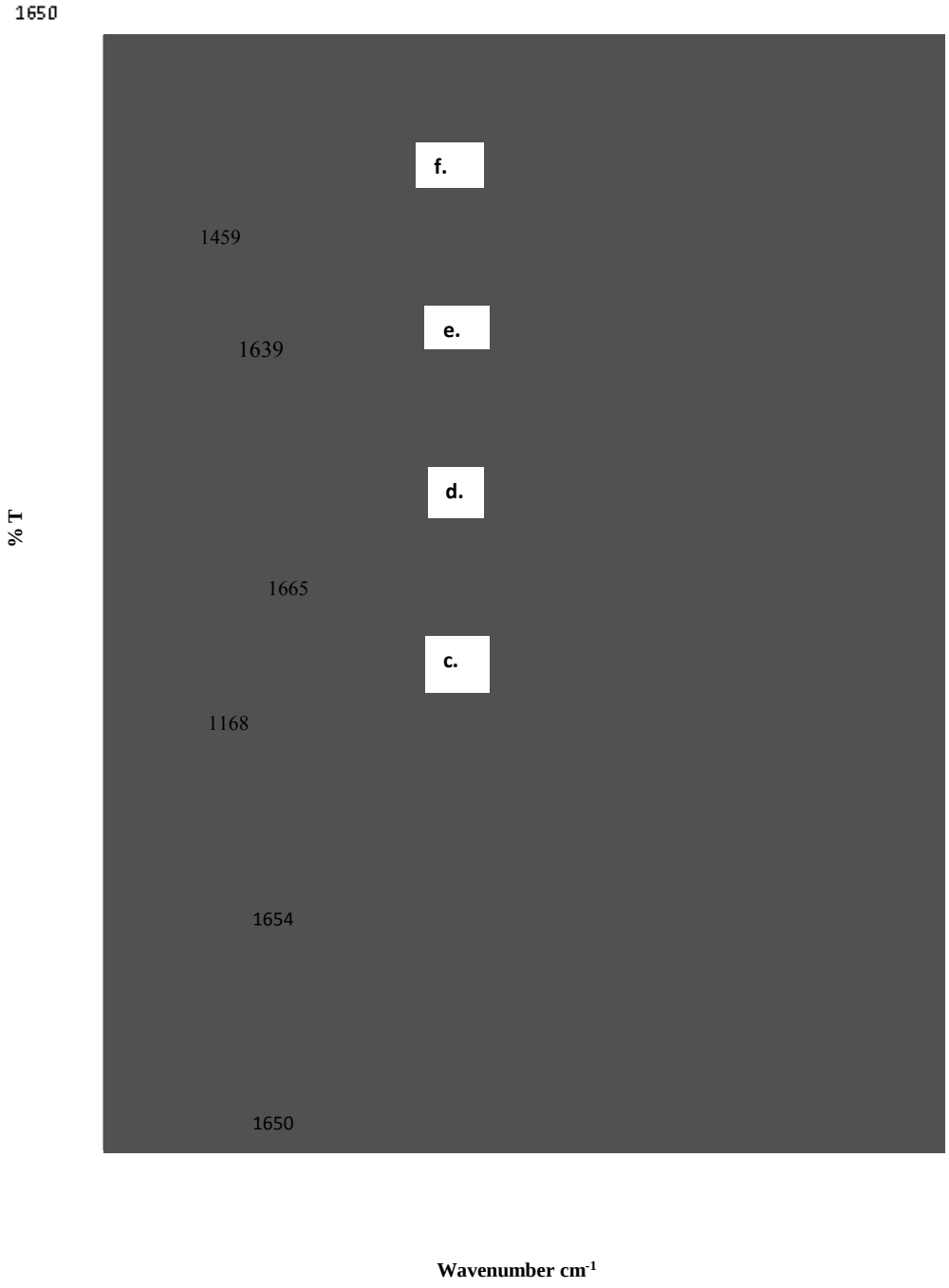

Figure 29. FTIR spectra of sCTs loaded CS-NPs with excipient based dry powder prepared by spray drying at inlet temperature 130°C; a). native sCT, b). CS, c). Mannitol, d). NPs/M=30/70, e). NPs/M=20/80 and f). NPs/M=10/90.

Integrity of encapsulated sCT

After drying process, the integrity of encapsulated sCT in chitosan nanoparticles spray dried powder, prepared at different NPs/M ratio and under different conditions, was confirmed by SDS-PAGE. Unprocessed sCT was also run as control. It was apparent that the spray drying process, especially at high inlet air temperature of 150 ^{o}C, did not deteriorate the integrity of sCT. As illustrated in Figure 30, all bands of sCT, recovered from chitosan microparticles with protein loading (Lanes 4-6), moved downwards the electrophoretic gel in a comparable distance to control (Lane 2and 3). No band was observed in either higher or lower molecular weight region, suggesting that neither aggregate formation nor peptide backbone clipping occurred. It was, therefore, conceivable that the spray drying process conditions used in this study, even at the supposedly high thermal stress, did not deteriorate the integrity of encapsulated sCT. The smear appeared on the lanes of sCT-loaded CS-NPs with mannitol based dry powder was believed to be the staining of chitosan (Lanes 4-6, Figure 30), since it was also found on the lane of blank chitosan microparticles (Lane 7).

Because all biological phenomena involve process of molecular recognition, it is essential that the delivery systems are able to release protein content in its native structure. Therefore, the structural conformation of sCT encapsulated in chitosan nanoparticles was studied with CD. Only investigation of secondary structure was then reported. sCT, which was recovered from spray dried sCT loading, yielded similar CD spectral shape to that of the unprocessed sCT (Figure 26-28). All three spectra exhibit a slightly decrease in molar ellipticity minima at *ca*. 198 nm, which were indicative of predominantly α-helical secondary structure (Pelton and McLean, 2000; Sreerama and Woody, 2000). It was noticed that the CD spectra of sCT recovered from spray dried protein with NPs/M =10:90, prepared at inlet temperature 150°C showed lower molar ellipticity in some degree than that of the unprocessed sCT. This might lead to the conclusion that encapsulation of sCT loaded chitosan microparticles into mannitol based by spray drying would have some detrimental

effect on secondary structure of protein. CD spectra of the recovered protein changed dramatically, in terms of both shape and molar ellipticity, from that of the unprocessed sCT. This indicated that α-helical secondary structure was lost in some extent, corresponding well with the degradation of protein found in SDS-PAGE.

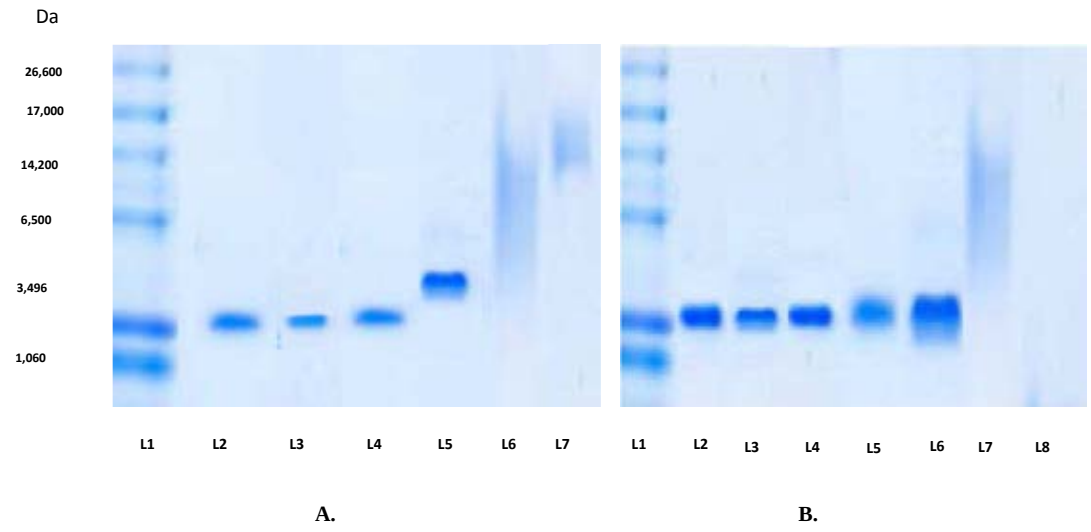

Figure 30. A.) SDS-PAGE analysis of Lanes 1: sCT standard marker, Lanes 2 and 3: unprocessed sCT, Lanes 4, 5 and 6: sCT recovered from sCT-loaded CS-NPs with mannitol based dry powder (NPs/M =30:70, NPs/M =20:80 and NPs/M =10:90 respectively), prepared at the inlet air temperature of 130 ^{o}C, Lanes 7: sample buffer and Lanes 8: blank chitosan microparticles; B.) SDS-PAGE analysis of Lanes 1: sCT standard marker, Lanes 2: unprocessed sCT, Lanes 3, 4 and 5: sCT recovered from sCT-loaded CS-NPs with mannitol based dry powder (NPs/M =30:70), prepared at the inlet air temperature of 110 ^{o}C, 130 ^{o}C and 150 ^{o}C, respectively, Lanes 6: blank chitosan microparticles and Lanes 7: sample buffer.

In vitro release studies of sCT from dry powders

sCT-loaded CS-NPs with mannitol based dry powder at different NPs/M ratios were subjected to *in vitro* release test at 37 ^{o}C in pH 7.4 phosphate buffered solution. The results are illustrated as a plot of percentage of sCT released against time in

Figure 31. Initially, at about 40% of sCT was burst released during 15 min and reach the plateau within 2 h finally, over 80% of sCT was completely released at 90 min. In vitro release profile suggested that the weakly interaction between CS-NPs and sCT, allowing the sCT release from the nanoparticles by a dissociation mechanism (Fern´andez-Urrusuno et al., 1999). The results can be observed that NPs/M ratio affect to the protein release profile, which is due to its high solubility in the aqueous release medium allowing the immediate nanoparticles delivery. It was noted that the lower NPs/M ratio could release more amount of the encapsulated sCT than the higher ratio.

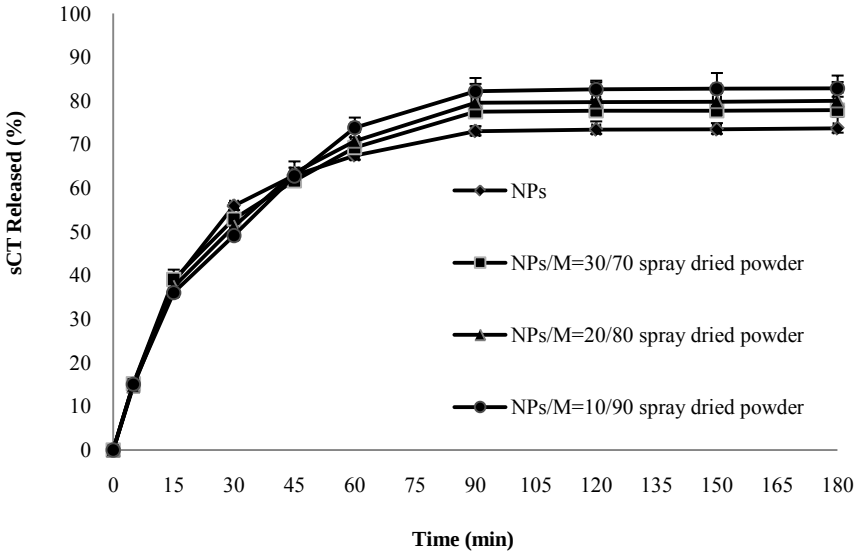

Figure 31. In vitro release profile of sCT from spray dried powder prepared with mannitol based at inlet temperature 130 °C; (mean±S.D.,n=3).

Evaluation of dry powder aerosolisation

The aerodynamic properties of the sCT loaded CS-NPs spray-dried powders were measured by inertial impaction (Fig. 32-34). From the particle distribution on the different impactor stages, the aerodynamic properties of the generated aerosols

could be calculated. The deposition data obtained from aerosolization of the sCT loaded CS-NPs with mannitol based spray dried powders are summarized in Table 6. A large number of mannitol also performed poorly aerosolisation properties during characterization. Table 6, shows the effect of mannitol on the spray dried powders. It was demonstrated that by increasing of NPs/M weight ratios from 10:90 (F10, F13 and F16) to 30:70 (F12, F15 and F18) the fine particles fraction percentage was increased from 46.09, 61.40 and 64.73 % to about 58.80, 63.50 and 72.05% respectively. The amounts of drug emitted from the glass device after aerosolization of the spray dried powder containing sCT loaded nanoparticles with mannitol based prepared at 150°C were significantly higher than the corresponding formulations prepared at 110°C with respect to the NPs/M weight ratios (Table 6).

The significant increase in emitted dose percentage of the drug aerosolized from powders containing NPs/M in comparison with the powder obtained from NPs alone showed that the addition of mannitol could improve the aerosol properties of the powders during this in vitro study. The comparison of these results obtained for spray dried powders produced in the presence of mannitol suggested that mannitol could present a positive effect on improvement of aerosolization properties of the sCT loaded nanoparticles with mannitol based powder. All mannitol based spray dried powder exhibited significantly higher deposition profiles compared to the sCT loaded nanoparticles alone. Therefore, it can be concluded that the addition of mannitol with respect to nanoparticle weights improves significantly the deposition profiles of the aerosolized spray dried powder. The highest FPF, ED and dispersibility of aerosolized powder in the presence of mannitol was observed for powders spray dried from aqueous solution containing 70% w/w mannitol with respect to NPs weight by spray drying at 150°c.

The lower in vitro deposition parameters of the drug aerosolized from spray dried powder with mannitol might be related to the surface properties of the particles. It is believed that Van der Waals forces could affect adhesion of particles with smooth

surfaces strongly. The effect of surface roughness on aerosolized properties of drug was reported by Chew and Chan, 2001. The FPF, ED and dispersibility were depended upon the NPs/M weight ratios and spray dry inlet temperature, they were significantly decreased (P<0.05) when amount of mannitol in the formulation was increased.

Table 6. Mass Median Aerodynamic Diameter (MMAD), Geometric Standard Deviation (GSD), Fine particle fraction (FPF), percentage emission (PE) and dispersibility of after aerosolization of the spray dried samples at 60 l/min; (mean±S.D., n=3)

Formulation	MMAD (μm)	Fine Particles Fraction Percentage (FPF%)	Emitted Dose Percentage (ED%)	Dispersibility (%)
Spray dried NPs	3.45	18.67	22.43	48.71
F10	4.69	46.09	55.64	62.83
F11	4.08	52.22	61.41	67.12
F12	3.83	58.80	68.62	71.12
F13	3.73	61.40	71.41	73.97
F14	3.21	62.28	72.15	75.10
F15	2.72	63.50	71.17	78.58
F16	2.01	64.73	72.40	80.23
F17	1.88	69.50	74.10	82.14
F18	1.51	72.05	77.32	80.97

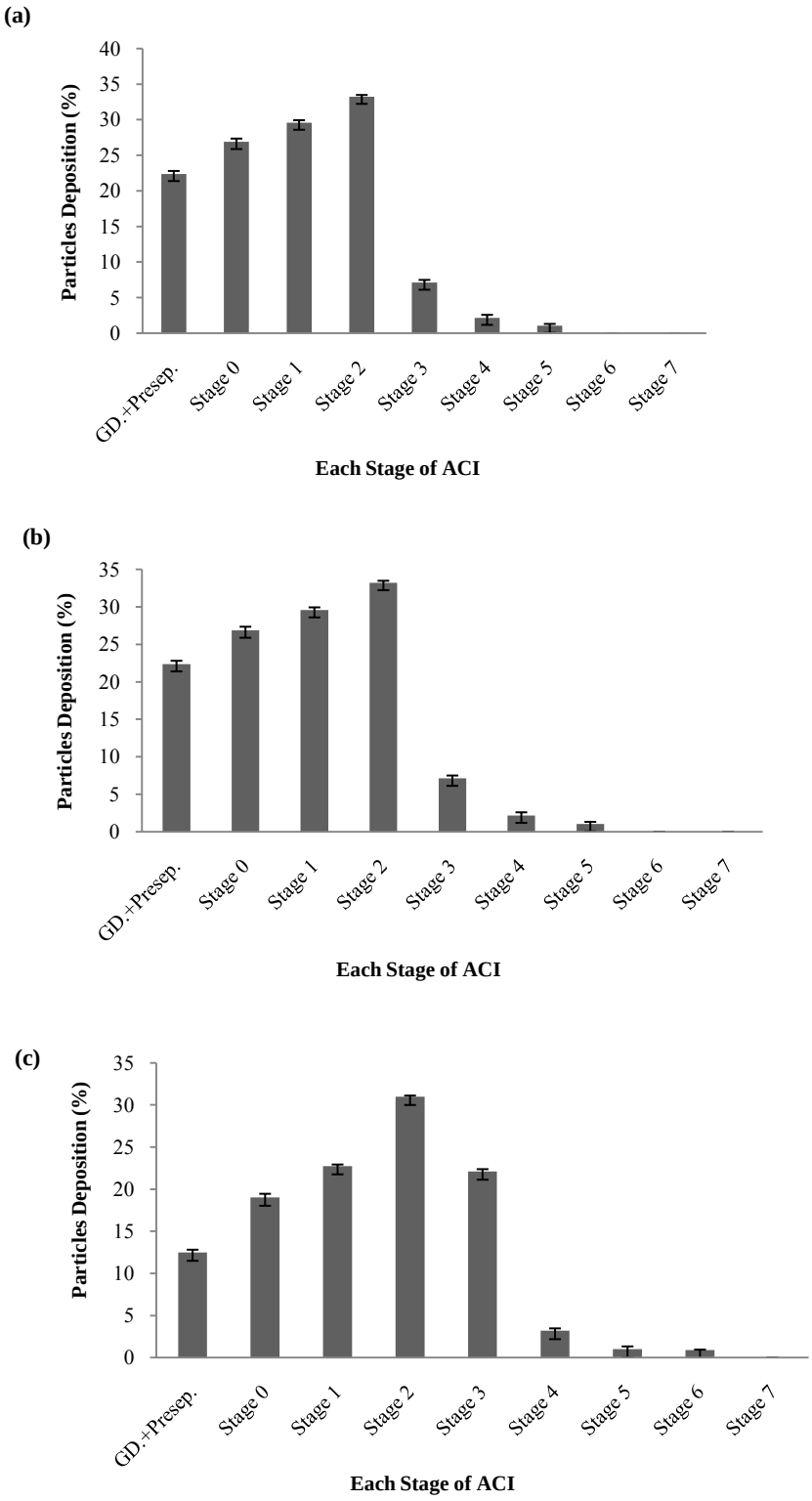

Figure. 32. Aerodynamic properties of spray-dried particles; distribution of (a); F_{10} (b); F_{11} and (c); F_{12} on the different stages of the Andeasen Cascade Impactor after aerosolization; values are presented as the mean±S.D. (n=3).

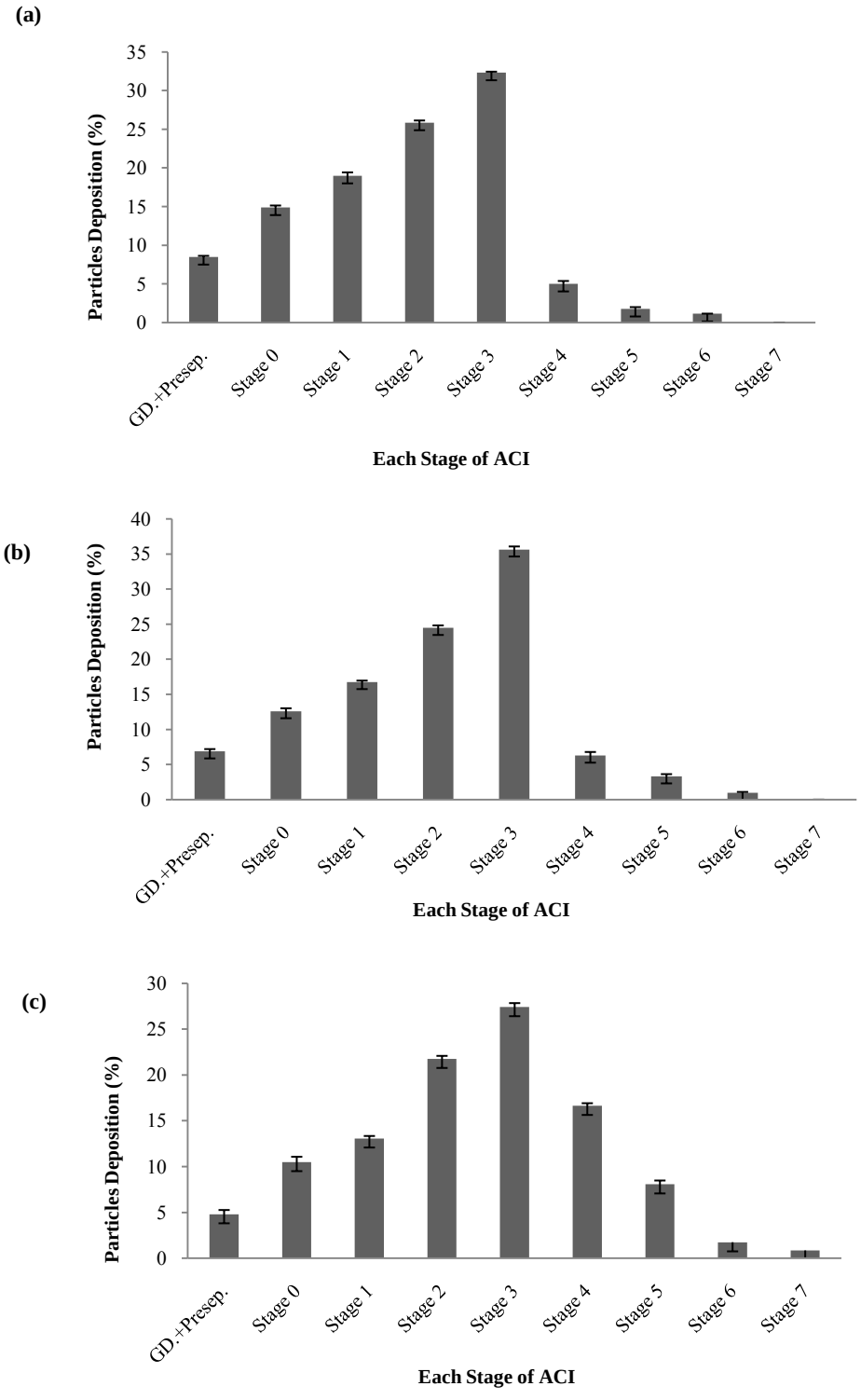

Figure. 33. Aerodynamic properties of spray-dried particles; distribution of (a); F_{13} (b); $F_{14}$and (c); F_{15} on the different stages of the Andeasen Cascade Impactor after aerosolization; values are presented as the mean±S.D. (n=3).

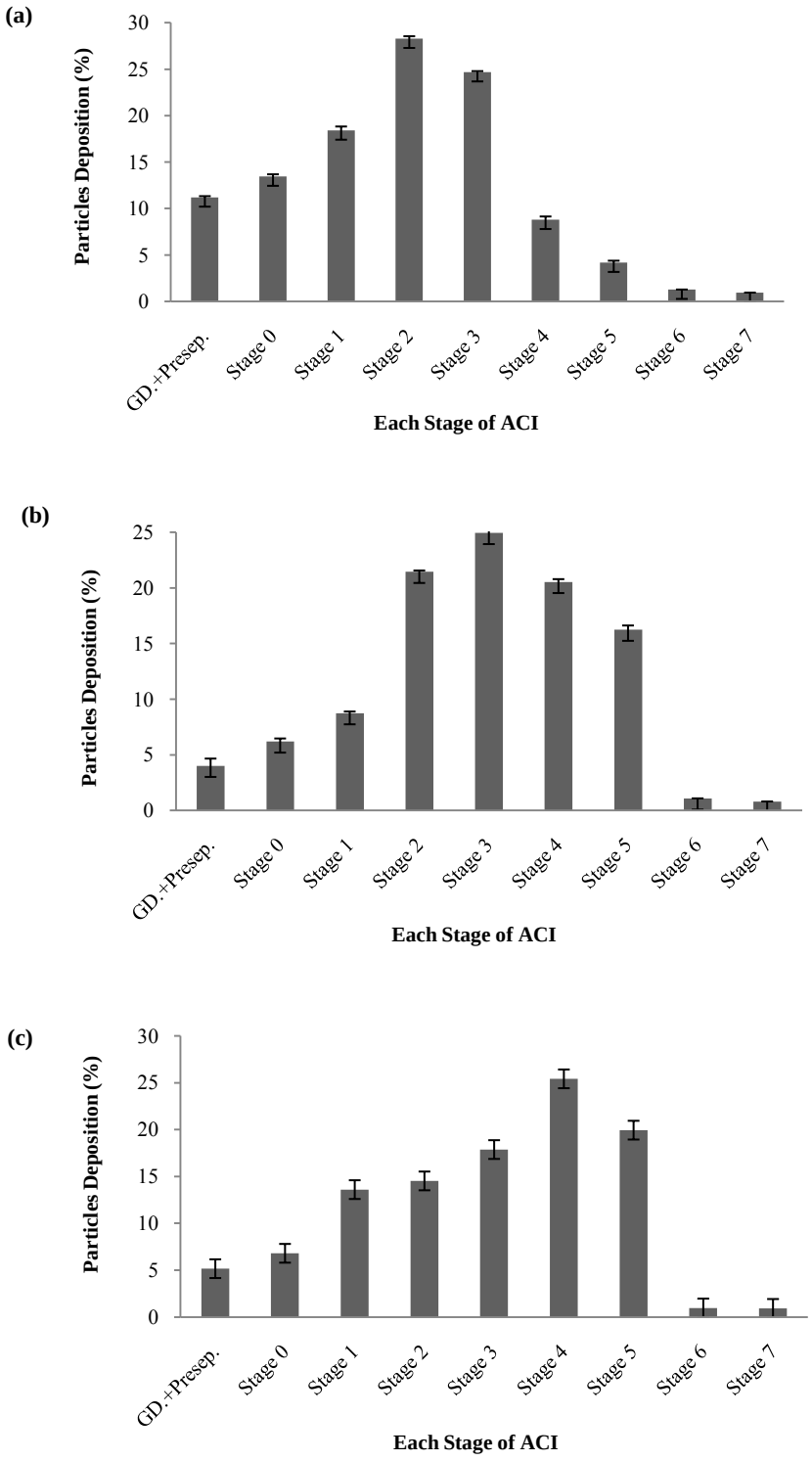

Figure 34. Aerodynamic properties of spray-dried particles; distribution of (a); F_{16} (b); $F_{17}$and (c); F_{18} on the different stages of the Andeasen Cascade Impactor after aerosolization; values are presented as the mean±S.D. (n=3).

In vivo absorption of sCT loaded CS-NPs spray dried powder

The sCT-loaded CS-NPs with mannitol based dry powder (NPs/M =30:70), prepared at the inlet air temperature of 130 ^{o}C was selected. The absorption in animal was performed with SD rats to evaluate the absorption of sCT. The serum sCT concentrations versus time profiles following insufflations of the sCT loaded CS-NPs spray dried powders, sCT loaded CS-NPs, native sCT, SC injection of sCT solution and blank spray dried powders were presented in Fig. 35. About 56% of sCT in spray dried powders was absorbed in 45 mins as compare to the other formulations, the result has shown that there were statistically significant differences between sCT loaded CS-NPs spray dried powders compared to free sCT (Fig. 35) ($P < 0.05$). The profiles show that the enhancement of pulmonary absorption of sCT was greater in the form of NPs and NPs with mannitol based spray dried powder than in the free form. After subcutaneous administration, plasma sCT concentration increased rapidly and reached to the peak concentration (C_{max}), of 68 pg.ml^{-1} in 30 min (T_{max}). Pharmacokinetic studies were included to assess potential differences in the pulmonary absorption, maximal plasma concentration (C_{max}), the time to peak (T_{max}), area under the curve (AUC_{0-360}) and the relative bioavailability (F_{rel}) were evaluated.

Pharmacokinetic parameters (Table 7) were obtained from the plasma concentration vs time profiles. In agreement with faster absorption, after the administration, C_{max} values of native sCT was lower than all of the samples. From these studies, it appeared that the sCT loaded NPs spray dried powder gave lower AUC_{0-360} than of subcutaneous injection and produced a higher potential of systemic absorption than sCT-NPs and native sCT powder.

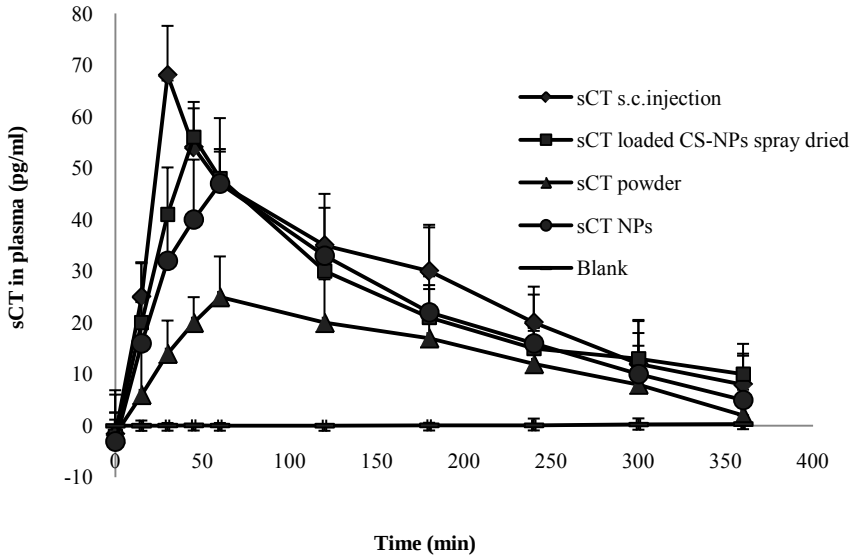

Figure 35. Plasma sCT concentration vs time profiles following intratracheal (i.t.) administration of sCT loaded CS-NPs spray dried powders, sCT loaded CS-NPs and native sCT, unloaded CS-NPs spray dried powders (blank) in comparison with subcutaneous (s.c.) administration to rats; mean±S.D. (n=3).

Table 7 Pharmacokinetic parameters

Sample	C_{max} ($pg.ml^{-1}$)	T_{max} (min)	AUC_{0-360} ($min.pg.ml^{-1}$)	Relative Bioavailability (F_{rel})
s.c. injection	68±5.14	30	10,014.60±125.47	2.00
Native sCT powder	25±3.03	60	5,004.60±87.64	1.00
sCT-NPs	47±4.45	60	8,068.80±105.18	1.61
sCT loaded NPs-SD	56±4.56	45	8,578.80±98.63	1.71
NPs-SD	0.34±1.23	360	0.697±24.38	0.0083

CHAPTER V

CONCLUSIONS

This study demonstrates the preparation of salmon calcitonin loaded chitosan/TPP nanoparticles by ionic gelation method. The particles size, zeta potential and association efficiency of nanoparticles were highly dependent on the ratio of CS:TPP and concentration of chitosan solution used. The smaller size and positive zeta potential for sCT loaded CS-NPs indicate their potential to provide mucoadhesion in pulmonary. FTIR and CD analysis of NPs demonstrated the evidence of crosslinking between positively charged amino group and negatively charged phosphate group. The sCT loaded particles demonstrated enhanced hydrogen bonding due to interaction of sCT with unreacted amino groups of CS. The CS-NPs had shown an excellent capacity for entrapment of sCT and clear evidence that chitosan concentration and weight ratios of CS/TPP solution is crucial for the association efficiency, loading capacity and yield.

All sCT loaded nanoparticles can be successfully incorporated in microspheres by co-spray drying of nanoparticles with lactose or mannitol provide aerosol excipients for pulmonary delivery. The spray-dried powders can be prepared to an appropriate particle diameter range for the pulmonary delivery of therapeutically peptides. The inlet temperatures and NPs/mannitol ratios significantly affects the dry powder properties. However, the resulting have shown that mannitol made them more suitable for aerosolization and increased the pulmonary deposition parameters of the aerosolized drug significantly.

The increasing weight ratios of nanoparticles:mannitol in the spray dries powder led to an decrease in the particles aerodynamic diameter. The reduction of interactions between the resulting particles leading to enhanced dispersibility and functional in vitro pulmonary deposition. It has also been suggested by scanning electron microscopy, the pitted surface of the mannitol based spray dried powders may present fewer sites for interparticulate cohesion. It was facilitated the dispersion of individual particles during aerosolisation and making mannitol an effective aerosol

excipient in spray dried powders for pulmonary drug delivery of both local and systemically proteins/peptides. Recovering of nanoparticles from spray dries powder is efficiently conducted in vitro after incubation in an aqueous medium pH 7.4. The present study indicated that, after sCT loaded CS-NPs spray dried powder contact with the lung aqueous environment, the dry powder are expected to release the nanoparticles and, as a consequence, the therapeutic peptides.

The formulations composed of nanoparticles were produced in order to form easily dispersible and reproducible microparticles size agglomerates of dry powder particles. The spray dried powders, with a NPs/mannitol at ratio 30:70, present high deposition properties for delivered to pulmonary. The observed difference in aerosolisation properties of sCT loaded CS-NPs spray dried powder must be related to the differences in NPs/mannitol weight ratios and processing inlet temperature, their effect on the particle characteristics of the spray dried powder. The study revealed that chitosan did not affect the secondary conformation of sCT in aqueous solution.

The conformational structure of sCT was found to be less altered after spray drying, the high NPs/mannitol ratio at 30:70 w/w had the greatest stabilization effect for the spray dried sCT. It was able to obtain good aerodynamic features for the different formulations, with fine good FPF, ED and dispersibility values. The presence of CS-NPs and mannitol did significantly affect the aerodynamic behavior and might improve the long term stability of the protein formulations. Following intratracheal administration to the rats, the quantitative analyses of sCT and pharmacokinetic parameter have demonstrated that this system is able to deliver sCT loaded CS-NPs spray dried powder into the deep lungs and transport the released sCT to the systemic circulation. This effect was more pronounced for the sCT loaded CS-NPs spray dried powder compared to the native sCT and sCT loaded CS-NPs. The dry powder system holds great promise for pulmonary delivery of peptides.

The future plans should be as follows:

1. To evaluate the pulmonary toxicity of sCT loaded CS-NPs spray dried powder.
2. To investigate long term stability of sCT loaded CS-NPs spray dried powder.
3. To develope a new drug delivery system such as complexes formed between chitosan/tripolyphosphate nanoparticles and phospholipids or sCT–TPP ionic complex for promote the peptide absorption.

REFERENCES

Agu, R.U., Ugwoke, M.I., Armand, M., Kinget, R. and Verbeke, N. 2001. The lung as a route for systemic delivery of therapeutic proteins and peptides. Respir. Res. 2: 198-209.

Aktas, Y., Andrieux, K., Alonso, M.J., Calvo, P., Gürsoy, R.N., Couvreur, P., et al. 2005. Preparation and in vitro evaluation of chitosan nanoparticles containing a caspase inhibitor. Int. J. Pharm. 298: 378-383.

Alle´mann, E., Gurny, R. and Doekler, E. 1993. Drug-loaded nanoparticles preparation methods and drug targeting issues. Eur. J. Pharm.Biopharm. 39: 173-191.

Alle´mann, E., Leroux, J.C. and Gurny, R. 1998. Polymeric nano- and microparticles for the oral delivery of peptides and peptidomimetics. Adv. Drug. Deliv. Rev. 34: 171-189.

Arakawa, T., Pretrelski, S.J., Kenney, W.C. and Carpenter, J.F. 1993. Factors affecting short-term and long-term stabilities of proteins. Adv. Drug. Deliv. Rev. 10: 1-28.

Aydın, Z. and Akbuga, Z. 1996. Chitosan beads for the delivery of salmon calcitonin: preparation and release characteristics. Int. J. Pharm. 131: 101-103.

Azarmi, S., Roa, W.H. and Löbenberg, R. 2008. Targeted delivery of NPs for the treatment of lung diseases. Adv. Drug. Deliv. Rev. 60: 863-875.

Azria, M., Copp, D.H. and Zanelli, J.M. 1995. 25 years of salmon calcitonin: from synthesis to therapeutic use. Calcif. Tissue. Int. 57: 405-408.

Bai, J.P.F., Chang, L.L. and Guo, J.H. 1996. Effects of poly(acrylic) polymers on the degradation of insulin and peptide drugs by chymotrypsin and trypsin. J. Pharm. Pharmaco. 48: 17-21.

Bi, R., Shao, W., Wang, Q. and Zhang, N.V. 2009. Solid lipid NPs as insulin inhalation carriers for enhanced pulmonary delivery. J. Biomed. Nanotechnol. 5: 84-92.

Bridges, P.A. and Taylor, K.M. 1998. Nebulizers for the generation of liposomal aerosols. Int. J. Pharm. 173: 117-122.

Brunner, A., Maeder, K. and Goepferich, A. 1999. pH and osmotic pressure inside biodegradable microspheres during erosion. Pharm. Res. 16: 847-853.

Calvo, P., Remuñán-López, C., Vila-Jato, J.L. and Alonso, M.J. 1997. Chitosan and chitosan/ethylene oxide-propylene oxide block copolymer nanoparticles as novel carriers for protein and vaccines. Pharm. Res. 14: 1431-1436.

Chew N.Y.K. and Chan H.K. 2001. Use of solid corrugated particles to enhance powder aerosol performance. Pharm. Res. 18: 1570-1577.

Chae, S.Y., Jang, M.K. and Nah, J.W. 2005. Influence of molecular weight on oral absorption of water soluble chitosans. J. Contr. Rel. 102: 383-394.

Chow, A.H., Tong, H.H., Chattopadhyay, P. and Shekunov, B.Y. 2007. Particle engineering for pulmonary drug delivery. Pharm. Res. 24: 411-417.

Corrigan, D.O., Healy, A.M. and Corrigan, O.I. 2006. Preparation and release of salbutamol from chitosan and chitosan co-spray dried compacts and multiparticulates. Eur. J. Pharm. Biopharm. 62: 295-305.

Couvreur, P., Duberne,t C. and Puisieux, F. 1995. Controlled drug delivery with nanoparticles: current possibilities and future trends. Eur. J. Pharm. Biopharm. 41: 2-13.

Dailey, L.A, Schmehl, T., Gessler, T., Wittma,r M., Grimminger, F. and Seeger, W. 2003. Nebulization of biodegradable nanoparticles: impact of nebulizer technology and nanoparticle characteristics on aerosol features. J. Control. Release. 86: 131-144.

Dellamary, L.A., Tarara, T.E., Smith, D.J., Woelk, C.H., Adractas, A., Costello, M.L., Gill, H. and Weers, J.G. 2000. Hollow porous particles in metered dose inhalers. Pharm. Res. 601: 168-174.

Felt, O., Buri, P. and Gurny, R. 1998. Chitosan: a unique polysaccharide for drug delivery. Drug Dev. Ind. Pharm. 24: 979-993.

Fernández-Urrusuno, R., Calvo, P., Remuñán-lópez, C., Vila-Jato, J.L. and Alonso, M.J. 1999. Enhacement of nasal absorption of insulin using chitosan nanoparticles. Pharm. Res. 16: 1576-1581.

Garcia-Fuentes, M., Torres, D. and Alonso, M.J. 2005. New surface-modified lipid anoparticles as delivery vehicles for salmon calcitonin. Int. J. Pharm. 296: 122-132.

Geller, D., Thipphawong, J., Otulana, B., Caplan, D., Ericson, D., Milgram, L., Okikawa, J., Quan, J. and Bowman, C.M. 2003. Bolus inhalation of rhDNase with the AERx system in subjects with cystic fibrosis. J. Aerosol Med. 16: 175-182.

Grainger, C.I., Alcock, R., Gard, T.G., Quirk, A.V., Amerongen, van G., Swart, de R.L. and Hardy, J.G. 2004. Administration of an insulin powder to the lungs of cynomolgus monkeys using a Penn Century insufflators. Int. J. Pharm. 269: 523-527.

Grenha, A., Seijo, B. and Remuñán-López, C. 2005. Microencapsulated chitosan nanoparticles for lung protein delivery. Eur. J. Pharm. Sci. 25: 427-437.

Grenha, A., Seijo, B., Serra, C. and Remuñán-lópez, C. 2007. Chitosan nanoparticle-loaded mannitol microspheres: structure and surface characterization. Biomacromolecules. 8: 2072-2079.

Glover, W., Chan, H.K., Eberl, S., Daviskas, E. and Verschuer, J. 2008. Effect of particle size of dry powder mannitol on the lung deposition in healthy volunteers. Int. J. Pharm. 349: 314-322.

Harvey, S.C. and Withrow, C.D. 1985. Hormones. In: Gennaro, A.R., Chase, G.D., Gibson, M.R., Granberg, C.B., Harvey, S.C. (Eds.). Remington's Pharmaceutical Sciences. Mack Printing Company, Pennsylvania. 951-1001.

Hattersley, G. and Chambers, T.J. 1989. Calcitonin receptors as markers for osteoclastic differentiation: Correlation between generation of bone resorptive cells and cells that express calcitonin receptors in mouse bone marrow cultures. Endocrinology. 125: 1606-1612.

Illum, L. 1998. Chitosan and its use as a pharmaceutical excipient. Pharm. Res. 15: 1326-1331.

Issa, M., Köping-Höggård, M. and Artursson, P. 2005. Chitosan and the mucosal delivery of biotechnology drugs. Drug. Discov. Today. Technol. 2: 1-6.

Jalaliour, M., Najafabadi, R., Gilani, K., Esmail, Y.H. and Tajerzadeh, H. 2008. Effect of dimethylbeta-cyclodextrin concentrations on the pulmonary delivery of recombinant human growth hormone dry powder in rats. J. Pharm. Sci. 97: 5176-5185.

James, J., Crean, B., Davies, M., Toon, R., Jinks, P. and Roberts, C.J. 2008. The surface characterisation and comparison of two potential sub-micron, sugar bulking excipients for use in low-dose, suspension formulations in metered dose inhalers. Int. J. Pharm. 361: 209-221.

Jaspart, S., Bertholet, P. and Piel G. 2007. Solid lipid microparticles as a sustained release system for pulmonary drug delivery. Eur. J. Pharm. Biopharm. 65: 47-56.

Jung, T., Breitenbach, A. and Kissel, T. 2000. Sulfobutylated poly(vinyl alcohol)-graft-poly(lactide-co-glycolide)s facilitate the preparation of small negatively charged biodegradable nanospheres. J. Control. Release. 67: 157-169.

Kawashima, Y., Yamamoto, H., Takeuchi, H. and Kuno, Y. 2000. Mucoadhesive d,l-lactide/glycolide copolymer nanospheres coated with chitosan to improve oral delivery of calcitonin. Pharm. Dev. Technol. 5: 77 - 85.

Kobayashi, S., Kondo, S. and Juni, K. 1996. Pulmonary delivery of salmon calcitonin dry powders containing absorption enhancers in rats. Pharm. Res. 13: 80-83.

Konstan, M.W., Chen, P.W., Sherman, J.M., Thomassen, M.J., Woodm, R.E. and Boat, T.F. 1981. Human lung lysozyme: sources and properties. Am. Rev. Respir. *Dis*.123: 120-124.

Lauweryns, J.M. and Baert, J.H. 1977. Alveolar clearance and the role of the pulmonary lymphatics. Am. Rev. Respir. Dis.115: 625-683.

Lee, K.C., Soltis, E.E. and Newman, P.S. 1991. In vivo assessment of salmon calcitonin sustained release from biodegradable microspheres. J. Control. Rel. 17: 199-206.

Lee, S.L., Adams, W.P., Li, B.V., Conner, D.P., Chowdhury, B.A. and Yu, L.X. 2009. In vitro considerations to support bioequivalence of locally acting drugs in dry powder inhalers for lung diseases. AAPS. J. 11: 414-423.

Lee, W.A., Ennis, R.D., Longenecker, J.P. and Bengtsson, P. 1994. The bioavailability of intranasal salmon calcitonin in healthy volunteers with and without a permeation enhancer. Pharm. Res. 11: 747-750.

Lee, Y.H. and Sinko, P.J. 2000. Oral delivery of salmon calcitonin. Adv. Drug Deliv. Rev. 42: 225-238.

Leung, K.K.M., Bridges, P.A. and Taylor, K.M.G. 1996. The stability of liposomes to ultrasonic nebulization. Int. J. Pharm. 145: 95-102.

Lowe, P.J. and Temple, C.S. 1994. Calcitonin and insulin in isobutylcyanoacrylate nanocapsules: protection against proteases and effect on intestinal absorption in rats. J. Pharm. Pharmacol. 46: 547-552.

Li, H.Y. and Birchall, J. 2006. Chitosan-modified dry powder formulations for pulmonary gene delivery. Pharm. Res. 23: 941-950.

Li, Y.P., Pei Y.Y., Zhang X.Y., Gu Z.H., Zhou Z.H. and Yuan W.F. 2001. PEGylated PLGA nanoparticles as protein carriers: synthesis, preparation and biodistribution in rats. J. Control. Release. 71: 203-211.

Mansouri, S., Lavigne, P., Corsi, K., Benderdour, M., Beaumont, E. and Fernandes, J.C. 2004. Chitosan-DNA nanoparticles as non-viral vectors in gene therapy: strategies to improve transfection efficacy. Eur. J. Pharm. Biopharm. 57: 1-8.

Mehta, R.C., Jeyanthi, R. and Calıs, S. 1994. Biodegradable microspheres as depot for parenteral delivery of peptide drugs. J. Control. Rel. 29: 375-384.

McCallion, O.N., Taylor, K.M., Thomas, M. and Taylor, A.J. 1995. Nebulization of fluids of different physicochemical properties with air-jet and ultrasonic nebulizers. Pharm. Res. 12: 1682-1688.

Muzzarelli, R.A.A. 1997. Human enzymatic activities related to the therapeutic administration of chitin derivatives. Cell. Mol. Life. Sci. 53: 131-140.

Nyambura, B.K., Kellaway, I.W. and Taylor, K.M.G. 2009. The processing of

nanoparticles containing protein for suspension in hydrofluoroalkane propellants. Int. J.Pharm. 372: 140-146.

Panyam, J. and Labhasetwar, V. 2003. Biodegradable nanoparticles for drug and gene delivery to cells and tissue. Adv. Drug Deliv. Rev. 55: 329-347.

Patton, J.S. 1996. Mechanisms of macromolecule absorption by the lungs. Adv. Drug. Deliv. Rev. 19: 3-36.

Patton, J.S. 2000. Pulmonary delivery of drugs for bone disorders. Adv. Drug. Deliv. Rev. 42: 239-248.

PDR. 2011. Physicians' Desk Reference Network. Montvale, NJ. 3250.

Prime, D., Atkins, P.J., Slater, A. and Sumby, B. 1997. Review of dry powder inhalers. Adv. Drug Deliv. Rev. 26: 51-58.

Rooijen, N. and Sanders, A. 1998. The macrophage as target or obstacle in liposome-based targeting strategies. Int. J. Pharm. 162: 45-50.

Sakagami, M. 2006. In vivo, in vitro and ex vivo models to assess pulmonary absorption and disposition of inhaled therapeutics for systemic delivery. Adv. Drug. Deliv. Rev. 58: 1030-1060.

Sakuma, S., Suzuki, N., Kikuchi, H., Hiwatari, K. and Akashi, M. 1997. Oral peptide delivery using nanoparticles composed of novel graft copolymers having hydrophobic backbone and hydrophilic branches. Int. J. Pharm. 149: 93-106.

Schneyer, C.R. 1991. Calcitonin and the treatment of osteoporosis. Md. Med. J. 40: 469-473.

Scheuch, G., Kohlhaeufl, M.J., Brand, P. and Siekmeier, R. 2006. Clinical perspectives on pulmonary systemic and macromolecular delivery. Adv. Drug. Deliv. Rev. 58: 996-1008.

Serres, A., Baudys, M. and Wankim, S. 1996. Temperature and pH-sensitive polymers for human calcitonin delivery. Pharm. Res. 13: 196-201.

Sham, J.O., Zhang, Y., Finlay, W.H., Roa, W.H. and Löebernberg, R. 2004. Formulation and characterization of spray-dried powders containing nanoparticles for aerosol delivery to the lung. Int. J. Pharm. 269: 457-467.

Shi, L., Plumley, C.J. and Berkland, C. 2007. Biodegradable nanoparticle flocculates for dry owder aerosol formulation. Langmuir. 23: 10897-10901.

Shin, B.S., Jung, J.H., Lee, K.C. and Yoo, S.D. 2004. Nasal absorption and pharmacokinetic disposition of salmon calcitonin modified with low molecular weight polyethylene glycol. Chem. Pharm. Bull. 52: 957-960.

Shoyele, S.A. and Cawthorne, S. 2006. Particle engineering techniques for inhaled biopharmaceuticals. Adv. Drug. Deliv. Rev. 58: 1009-1029.

Siekmeier, R. and Scheuch, G. 2009. Treatment of systemic diseases by inhalation of biomolecule aerosols. J. Physiol. Pharmacol. 60: 15-26.

Soppimath, K.S., Aminabhavi, T.M., Kulkarni, A.R. and Rudzinski, W.E. 2001. Biodegradable polymeric nanoparticles as drug delivery devices. J. Control. Release. 70: 1-20.

Sung, J.C., Pulliam, B.L. and Edwards, D.A. 2007. Nanoparticles for drug delivery to the lungs. Trends Biotechnol. 25: 563 -70.

Torres-Lugo, M. and Peppas, N.A. 2000. Transmucosal delivery systems for calcitonin: a review. Biomaterials. 21: 1191-1196.

Ugwoke, M.I., Verbeke, N. and Kinget, R., 2001. The biopharmaceutical aspects of nasal mucoadhesive drug delivery. J. Pharm. Pharmacol. 53: 3-22.

Villiers, De M.M. 2005. Powder flow and compressibility, in: Ghosh, T.K., Jasti, B.R. (Eds.). Theory and Practice of Contemporary Pharmaceutics. CRC Press, Boca Raton, Florida, USA: 298-299.

Vyas, S.P. and Khatri, K. 2007. Liposome-based drug delivery to alveolar macrophages. Expert. Opin. Drug. Deliv. 4: 95-99.

Williams, R.O., Barron, M.K., Alonso, J.M. and Remuñán-López, C. 1998. Investigation of a pMDI system containing chitosan microspheres P134a. Int. J. Pharm. 174: 209-222.

Yang, W., Peters, J.I. and Williams III, R.O. 2008. Inhaled nanoparticles-a current review. Int. J. Pharm. 356: 239-247.

Youn, Y.S., Jung, J.Y., Oh, S.H., Yoo, S.D. and Lee, K.C. 2006. Improved intestinal delivery of salmon calcitonin by Lys18-amine specific PEGylation, stability, permeability, pharmacokinetic behavior and in vivo hypocalcemic efficacy. J. Control. Release. 114: 334-342.

Yu, S.Y., Ju, Y.J., Seung, H.O., Sun, D.Y. and Kang, C.L. 2006. Improved intestinal delivery of salmon calcitonin by Lys18-amine specific PEGylation: Stability, permeability, pharmacokinetic behavior and in vivo hypocalcemic efficacy. J. Control. Release. 114: 334-342.